

# Towards Quantifying the Hessian Structure of Neural Networks

Zhaorui Dong<sup>\*1</sup>, Yushun Zhang<sup>\*12</sup>, Zhi-Quan Luo<sup>12</sup>, Jianfeng Yao<sup>†1</sup>, Ruoyu Sun<sup>†12</sup>

<sup>1</sup>The Chinese University of Hong Kong, Shenzhen, China

<sup>2</sup>Shenzhen Research Institute of Big Data

{zhaoruidong, yushunzhang}@link.cuhk.edu.cn

luozq, jeffyyao, sunruoyu@cuhk.edu.cn

## Abstract

Empirical studies reported that the Hessian matrix of neural networks (NNs) exhibits a near-block-diagonal structure, yet its theoretical foundation remains unclear. In this work, we reveal two forces that shape the Hessian structure: a “static force” rooted in the architecture design, and a “dynamic force” arisen from training. We then provide a rigorous theoretical analysis of “static force” at random initialization. We study linear models and 1-hidden-layer networks with the mean-square (MSE) loss and the Cross-Entropy (CE) loss for classification tasks. By leveraging random matrix theory, we compare the limit distributions of the diagonal and off-diagonal Hessian blocks and find that the block-diagonal structure arises as  $C \rightarrow \infty$ , where  $C$  denotes the number of classes. Our findings reveal that  $C$  is a primary driver of the near-block-diagonal structure. These results may shed new light on the Hessian structure of large language models (LLMs), which typically operate with a large  $C$  exceeding  $10^4$  or  $10^5$ .<sup>1</sup>

**Keywords:** Hessian, Neural Networks, Random Matrix Theory

## 1 Introduction

The Hessian matrix of neural networks (NNs) is crucial for understanding training dynamics, as well as motivating better algorithm designs. A classical work [Collobert, 2004] first empirically reported that the Hessian of NNs is highly structured: the Hessian is observed to be *near-block-diagonal*. We reproduce this result in Figure 1. Unfortunately, no rigorous theory has been established in the past two decades to explain this phenomenon.

Very recently, the near-block diagonal structure of Hessian has drawn renewed attention in the machine learning community as it helps understanding the training of large language models (LLMs) [Zhang et al., 2024a,b, Kunstner et al., 2024]. Again, these works primarily focus on empirical observations, and there is no rigorous theoretical results on the underlying source of the special structure. The following fundamental question remains largely open:

*When and why does the Hessian of NNs exhibit near-block-diagonal structure?*

Before delving into this question, we first list some of its important implications.

---

\*: Equal contribution. Alphabetically ordered.

†: Correspondence author: Ruoyu Sun. Email: sunruoyu@cuhk.edu.cn. Correspondence may also be addressed to Jianfeng Yao. Email: jeffyyao@cuhk.edu.cn.

<sup>1</sup>Our code is available at <https://github.com/zyushun/Hessian-structure>.

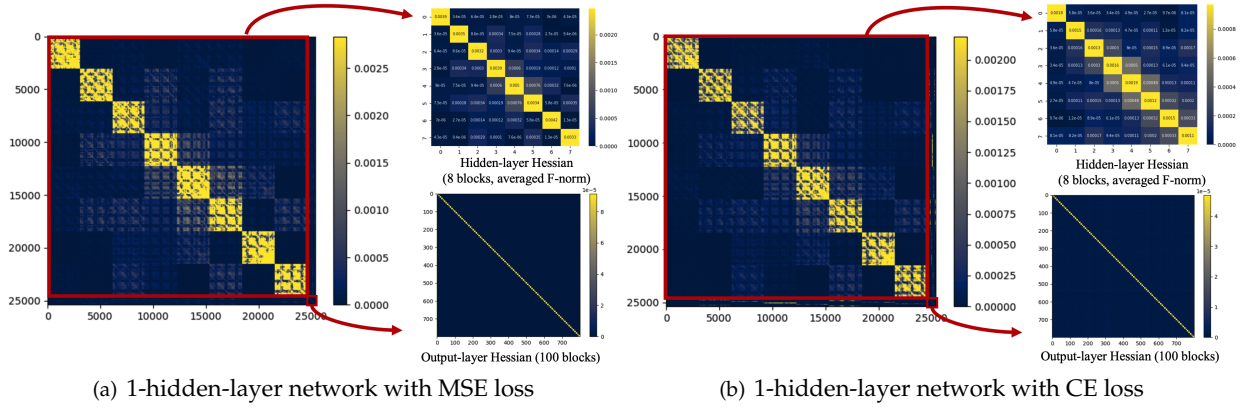


Figure 1: **(a, b)**: The Hessian matrix of a 1-hidden-layer network with 8 hidden neurons at random initialization on CIFAR-100 dataset (# hidden neuron  $m = 8$  and # classes or output neuron  $C = 100$ ). For clearer visualization, we report the absolute value of each Hessian entry, and this applies to all Hessian matrices reported in this work. We observe near-block-diagonal structures under both MSE and CE loss with  $m + C = 108$  blocks in total.

- **I.** Understanding Hessian structure can help understand NN training. For instance, the effectiveness of diagonal preconditioned methods such as Adam [Kingma and Ba, 2014] is usually strongly related to the Hessian structure; see, e.g., Sun and Ye [2021], Qu et al. [2022], Das et al. [2024]. Recently, the near-block-diagonal Hessian is observed along the training process and such structure is shown to be related to the effectiveness of Adam on LLMs [Zhang et al., 2024a, Kunstner et al., 2024]. Besides Adam, the near-block-diagonal Hessian structure may play a crucial role in the effectiveness of block-diagonal preconditioned methods (e.g., [Martens and Grosse, 2015, Gupta et al., 2018, Goldfarb et al., 2020, Jordan et al., 2024]). Among these methods, Shampoo [Gupta et al., 2018] is recently used for training Gemini 1.5 Flash [Team et al., 2024]; and Muon optimizer [Jordan et al., 2024] is used for training Moonlight [Liu et al., 2025] very recently.
- **II.** Understanding Hessian structure can help design new training methods for NNs. For instance, Adam-mini [Zhang et al., 2024b], a recently proposed optimizer, utilizes the near-block-diagonal Hessian structure to cut down 50% memory consumption in Adam. We believe the special Hessian structure can inspire more new optimizers.
- **III.** The near-block-diagonal Hessian structure can offer a new class of problems for the optimization community to study. For the optimization community, it is rare to analyze (near-) block-diagonal Hessian structure since typical problems do *not* have such structure. For instance, in the classical non-linear programming dataset [Lavezzi et al., 2022], all problems have non-block-diagonal Hessians. Understanding the special Hessian structure of NN can draw attention from the optimization community, motivating further study into this specialized class of problems.

In this work, we first numerically reveal two forces that shape the Hessian structure: a “static force” rooted in the architecture design, and a “dynamic force” arisen from training. Then, we provide a rigorous theoretical analysis of “static force” at random initialization. We focus on linear models and 1-hidden-layer networks at random initialization. We consider standard classification problems with  $C$  classes under the mean-square (MSE) loss and the Cross-Entropy (CE) loss. Leveraging tools from random matrix theory, we characterize the limit distributions of diagonal and off-diagonal Hessian blocks as the sample size  $N$  and input dimension  $d$  grow proportionally to infinity. Our theory shows that the off-diagonal blocks will be pushed to 0 as the number of classes  $C$  increases, and this happens for both MSE and CE loss. These findings highlight that  $C$  is a primary driver of the near-block-diagonal Hessian structure. Our theory may shed new light on the Hessian structures of LLMs since they usually have large  $C$  (more than  $10^4$  or  $10^5$ )<sup>2</sup>.

Our findings challenge the conventional wisdom of [Collobert, 2004], which argues that CE loss is the primary determining factor. Later, we will analyze why [Collobert, 2004] had misattributed the emergence of the near-block diagonal structure to CE loss.

Our main contributions are summarized as follows.

<sup>2</sup> $C = 32k$  in Llama 2 [Touvron et al., 2023] and  $C = 128k$  in many recent models such as DeepSeek-V3 [Liu et al., 2024].

- We numerically investigate the source of the near-block-diagonal Hessian structure. We reveal two forces that shape such structure: a “static force” rooted in the architecture, and a “dynamic force” arisen from training. In particular, the “dynamic force” compresses cross-layer Hessian components during training; and the “static force” compresses the cross-neuron component in each layer for both initialization stage and training stage.
- We provide rigorous theory on the Hessian of linear models at random initialization. As the sample size  $N$  and input dimension  $d$  grow proportionally to infinity, we calculate the limit distribution for the Frobenious norm of the diagonal and off-diagonal blocks of Hessian. Specifically, the diagonal blocks correspond to the Hessian of weights associated with the same class, while the off-diagonal blocks represent the Hessian of weights from different classes. We find that: the ratio between the off-diagonal and diagonal blocks decays to zero at the rate of  $O(1/C)$ , where  $C$  is the number of classes. This demonstrates that the Hessian becomes block-diagonal as  $C \rightarrow \infty$ , and the number of blocks equals  $C$ .
- We extend the above analysis to 1-hidden-layer networks. We primarily focus on two sub-matrices in Hessian: the hidden-layer Hessian and the output-layer Hessian, which are highlighted with red boxes in Figure 1. For the hidden-layer Hessian, the ratios between their off-diagonal and diagonal blocks decay to zero at the rate of  $O(1/\sqrt{C})$ . For the output-layer Hessian, the decay rate is  $O(1/C)$ . This demonstrates that these sub-matrices will become block-diagonal as  $C \rightarrow \infty$ . In this case, the total number of blocks in these sub-matrices equals  $(m + C)$ , where  $m$  denotes the number of hidden neurons.
- We highlight some key technical contributions in our proof. The major challenge lies in characterizing the limit distribution of *non-independent* random matrix products, which in general is a difficult problem in random matrix theory. For the Hessian of NNs, we find that such dependency arises from ReLU activation and CE loss, and the dependency diminishes as  $d \rightarrow \infty$ . Subsequently, we propose a systematic procedure to address this type of “diminishing dependencies” caused by ReLU activation and CE loss. Our approach implements the *Lindeberg interpolation principle*, which is originally proposed to prove the Central Limit Theorem (CLT).

**Notations.** For a matrix  $X \in \mathbb{R}^{m \times n}$ , we denote  $X^\top$  as the transpose of  $X$ . We use  $I_{n \times n}$  and  $0_{n \times n}$  to denote the identity matrix and the zero matrix of size  $n \times n$ . We denote  $\|X\|_F$  as the Frobenious norm of  $X$ . We denote  $[n]$  as the index set  $\{1, \dots, n\}$ . We say  $x \stackrel{d}{=} y$  if the random variable (r.v.)  $x$  and  $y$  share the same distribution. We denote the Dirac measure at  $x$  by  $\delta_x$ . We denote the support of measure  $\mu$  by  $\text{supp}(\mu)$  and the expectation of  $x$  by  $\mathbb{E}[x]$ . We use  $\mathcal{N}(\mu, \sigma^2)$  and  $\mathcal{X}^2(\mu, \sigma^2)$  to denote Gaussian and chi-square distribution with mean  $\mu$  and variance  $\sigma^2$ . We use  $\Im(z)$  to denote the image part of a complex number  $z \in \mathbb{C}$ . We denote  $\mathbb{C}^+ = \{z \in \mathbb{C} | \Im(z) > 0\}$ . In this paper, we will intermittently employ the notations  $H_{ww}$ ,  $H_{vv}$ , and  $H_{wv}$  to denote the hidden-layer, output-layer, and cross-layer Hessian, respectively, of a 1-hidden-layer network.

## 2 Related works

**Hessian spectrum analysis.** Most studies on Hessian of NNs focus on Hessian eigenvalue distribution, a.k.a., the spectrum. LeCun et al. [2002], Dauphin et al. [2014], Sagun et al. [2016, 2017], Chaudhari et al. [2019], Ghorbani et al. [2019], Granziol et al. [2019], Yao et al. [2020] reported that the Hessian spectra of NNs consist of a “bulk” together with a few “outliers”. Pennington and Bahri [2017], Fort and Ganguli [2019], Pappayan [2020], Wu et al. [2020], Liao and Mahoney [2021], Singh et al. [2021] studied the shape of the Hessian spectrum and Hessian rank in theory. Pappayan [2018, 2019], Sankar et al. [2021] numerically studied the relation between the spectrum of Hessian and that of Gauss-Newton matrix. Keskar et al. [2016], Yao et al. [2018], Zhang et al. [2019], Granziol et al. [2022] studied the connection between the Hessian spectrum of NNs and some training phenomena such as the effect of batch sizes. Ghorbani et al. [2019], Yao et al. [2020] explained the effectiveness of training techniques such as BatchNorm via the shape of Hessian spectrum. Zhang et al. [2024a] numerically studied the blockwise Hessian spectrum of CNNs and Transformers. They further connect the blockwise spectra to the effectiveness of Adam. Another line of works studied the interplay between Hessian extreme eigenvalues and the trajectories of gradient methods (e.g., [Wu et al.,

2017, Draxler et al., 2018, Gur-Ari et al., 2018, Jastrzebski et al., 2018, Chaudhari et al., 2019, Jiang et al., 2019, He et al., 2019, Alain et al., 2019, Wei and Schwab, 2019, Li et al., 2020b, Jastrzebski et al., 2020, Cohen et al., 2021, 2022, Arora et al., 2022, Wang et al., 2022, Lyu et al., 2022, Park and Kim, 2022]).

Different from all these works, we study the macroscopic structure of the Hessian rather than its spectrum. Note that these two topics are rather orthogonal: it is possible to change the matrix structure without changing its eigenvalues, and vice versa. Specifically, we focus on the ratio between diagonal Hessian blocks and off-diagonal ones, which is not covered in the spectrum analysis.

**Hessian structure analysis.** Collobert [2004] empirically observed the following phenomenon: when using a neural network to solve a binary classification problem under CE loss, the Hessian is near-block-diagonal. They also reported that the near-block-diagonal structure disappears when changing to MSE loss. Collobert [2004] thereby conjectured that the near-block-diagonal Hessian stems from CE loss, and they provided an one-line informal explanation (re-stated later in Section 3.2). The near-block-diagonal structure was also reported recently under CE loss for various models including 1-hidden-layer network [Zhang et al., 2024a], 1-hidden-layer Transformers [Zhang et al., 2024b], and linear models [Kunstner et al., 2024]. Similar Hessian structure is later numerically reported on more practical models including GPT-2 [Maes et al., 2024], and OPT-125M [Malinovskii et al., 2024]. These results show that the near-block-diagonal structure appeared in a wide range of architectures. We point out that these works primarily focus on empirical observations, and the rigorous theoretical analysis is still missing.

Very recently, Ormaniec et al. [2024] employed matrix calculus to derive the Hessian expression of a 1-hidden-layer Transformer to understand the difficulties in training Transformers. While deriving the Hessian expression is non-trivial and valuable due to the complicated design of Transformers, the subsequent analysis of Hessian structure is rather simplified: e.g., they view the weights and data as constant matrices and did not incorporate their random distributions. Consequently, the exact distribution of each Hessian block has not been characterized yet, and the origin of the near-block-diagonal structure remains unexplored.

Different from the aforementioned work, we establish the first rigorous theory on the Hessian structure of linear and 1-hidden-layer network via random matrix theory. Our theory reveals that the number of classes  $C$  is one major cause of the near-block-diagonal structure.

**Algorithm design.** Multiple algorithm designs are proposed by approximating Hessian (or other curvature matrices) by block-diagonal matrices (e.g., [Roux et al., 2007, Martens and Grosse, 2015, Desjardins et al., 2015, Zhang et al., 2017, Gupta et al., 2018, George et al., 2018, Goldfarb et al., 2020, Dangel et al., 2020, Jordan et al., 2024, An et al., 2025]). Our theory can explain why these methods work. The special Hessian structure also has strong connections to diagonal preconditioned methods (e.g., [Kingma and Ba, 2014, Liu et al., 2023]).

## 3 Empirical Observations and Existing Wisdom

### 3.1 Two Forces Shaping the Hessian Structure

Now we conduct more fine-grained empirical studies on Hessian structures of NNs. In particular, we explore the Hessian structure of a 1-hidden-layer network on a Gaussian synthetic dataset. The detailed experimental setups are presented in Appendix B.5.

We emphasize that these experiments can reveal more Hessian properties not shown in the CIFAR-100 experiments in Figure 1. We highlight the new changes as follows.

- We change the input dimension  $d$  and # classes  $C$  to amplify the effect of cross-layer Hessian components  $H_{wv}$ . In the CIFAR-100 example in Figure 1, the proportions of the Hessian of hidden layer and output layer, which we abbreviate as  $H_{ww}$  and  $H_{vv}$ , are largely imbalanced. In particular,  $H_{ww}$  occupied the vast majority of the entries, while  $H_{vv}$  only accounted for a small portion. This imbalanced distribution would cause the cross-layer components, which we abbreviate as  $H_{wv}$ , to occupy only a minor fraction of the whole Hessian matrix, making them easily overlooked. To better illustrate the pattern of the entire Hessian, we change  $(d, C) = (3072, 100)$  to  $(d, C) = (500, 500)$  so that  $H_{ww}$ ,  $H_{vv}$ , and  $H_{wv}$  are proportionally balanced within the Hessian.



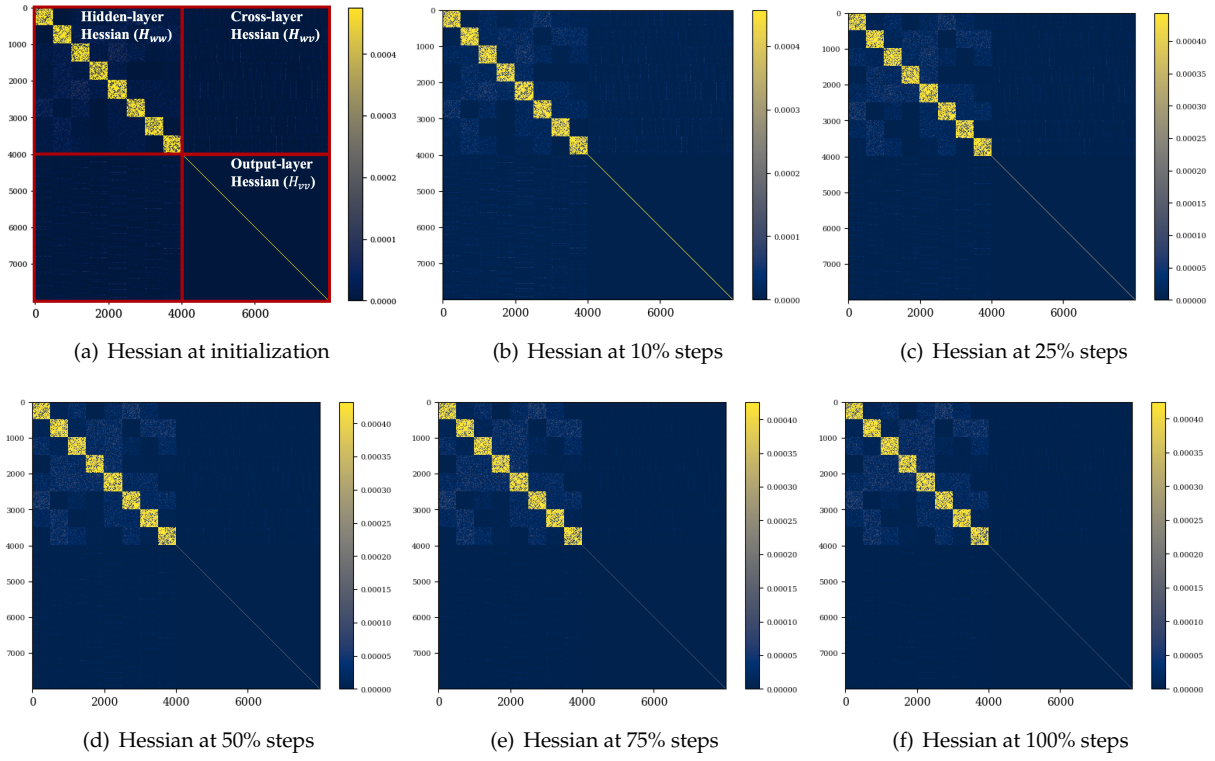


Figure 2: (a-f): The Hessian of a 1-hidden-layer network on Gaussian synthetic data under MSE loss. We notice the near-block-diagonal patterns in  $H_{ww}$  and  $H_{vv}$  with  $m + C = 508$  blocks in total, and they maintain along training.

- We change the dataset from CIFAR-100 to Gaussian synthetic dataset. Such change suggests that the Hessian structure might be inherently general and is not overfitted to one specific dataset like CIFAR-100.
- In addition to the Hessian at random initialization, we present the Hessian along training until convergence. We present the loss curves in Appendix B.5.

The results are shown in Figure 2 and 3. We summarize two findings.

- **Finding 1:** For both MSE loss and CE loss, we observe near-block-diagonal structures in  $H_{ww}$  and  $H_{vv}$  and such structures maintains along training.
- **Finding 2:** For CE loss, we observe new special structures in  $H_{wv}$  at random initialization:  $H_{wv}$  exhibits a “block-circulant” pattern with periodic stripes. Note that such structure is not observed for MSE loss. When using CE loss, the full Hessian matrix appears to be a combination of “block-circulant” matrix (for  $H_{wv}$ ) and block-diagonal matrix (for  $H_{ww}$  and  $H_{vv}$ ). We refer to it as “block-circulant-block-diagonal matrix”. We observe that the “block-circulant” pattern in  $H_{wv}$  vanishes as training goes on, while the near-block-diagonal patterns in  $H_{ww}$  and  $H_{vv}$  remain obvious.

**Main Takeaways and insights from the experiments.** Based on the findings from Figure 2 and 3, we find that there are at least two forces shaping the Hessian structure.

- (1) A “static force” rooted in the architecture design. For both MSE and CE loss, this force compresses the cross-neuron components in  $H_{ww}$  and  $H_{vv}$ . This force is effective in both initialization stage and the training stage. For MSE loss, we conjecture it also compresses the cross-layer component  $H_{wv}$ .
- (2) A “dynamic force” arisen from training. When using CE loss, this force gradually erases the initial “block-circulant” pattern in the cross-layer component  $H_{wv}$  along training.

In the sequel, we study how both forces shape the Hessian structure. We will primarily focus on the effect of “static force” at random initialization, particularly, how the architecture shapes the Hessian structure for  $H_{ww}$  and  $H_{vv}$  for both CE loss and MSE loss. As for “how the ‘dynamic force’ eliminates the block-circulant pattern in  $H_{wv}$  along training”, we find that it can be explained directly from Hessian expressions. We provide an initial analysis in Appendix A and leave more fine-grained analysis as future direction.

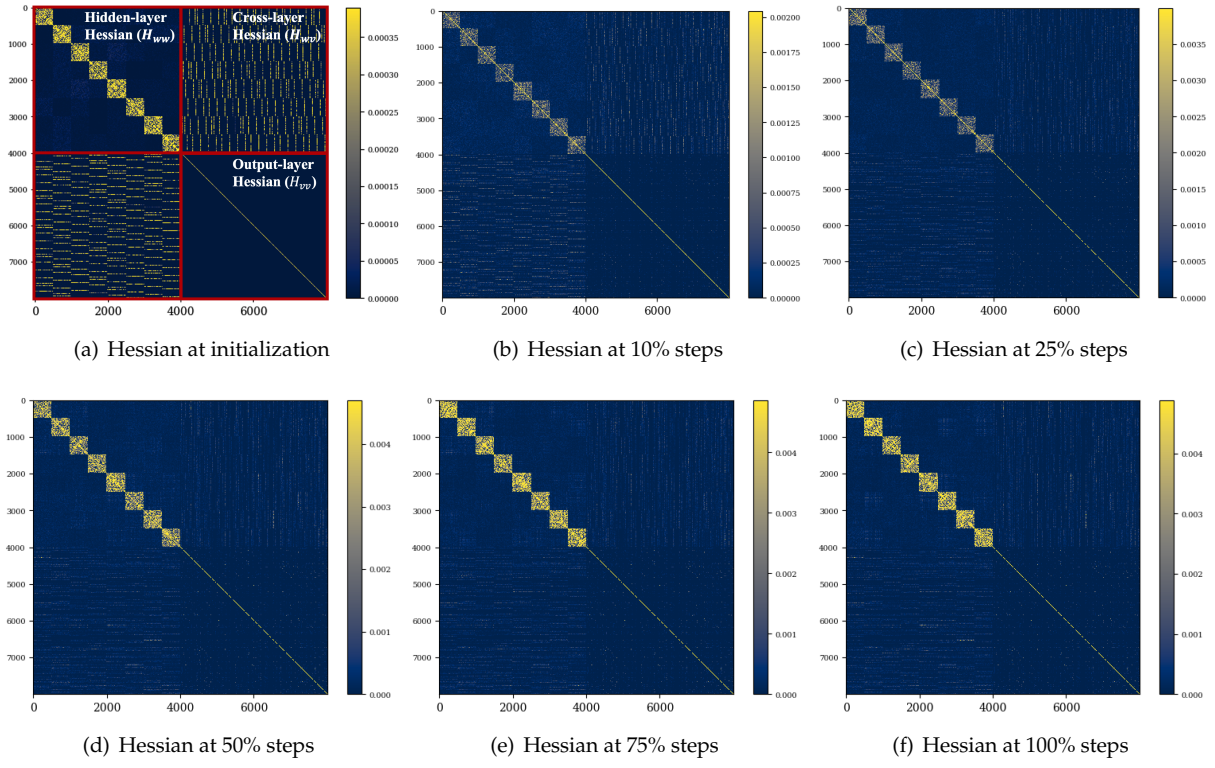


Figure 3: **(a-f)**: The Hessian of a 1-hidden-layer network on Gaussian synthetic data under CE loss. At initialization, we observe the “block-circulant” pattern in  $H_{wv}$ , and the near-block-diagonal structure in  $H_{ww}$  and  $H_{vv}$  (with  $m + C = 508$  blocks in total). We refer to it as “*block-circulant-block-diagonal matrix*”. We notice that the “block-circulant” pattern in  $H_{wv}$  vanishes along training, while the near-block-diagonal patterns in  $H_{ww}$  and  $H_{vv}$  are preserved.

### 3.2 Existing Wisdom

Here, we revisit the results in [Collobert, 2004], which has remained for two-decades the dominating understanding of the near-block-diagonal Hessian structure. The author attributes the near-block-diagonal structure to CE loss. We will point out that this perspective might not be accurate.

Collobert [2004] considered the binary classification problem: minimizing  $\ell_{\text{CE}}(f(\theta; x), y)$  where  $\ell_{\text{CE}}(\cdot, \cdot)$  is CE loss,  $f(\theta; x) = \sum_{i=1}^n v_i \sigma(w_i^\top x) \in \mathbb{R}$  is an single-output-1-hidden-layer neural network with input  $x \in \mathbb{R}^d$ , weight  $w_i \in \mathbb{R}^d$ ,  $v_i \in \mathbb{R}$ , and label  $y \in \{0, 1\}$ . The author focused on the hidden-layer Hessian  $H_{ww}$ , and they point out that off-diagonal-blocks in  $H_{ww}$  would contain

$$\frac{\partial^2 \ell_{\text{CE}}(f(\theta; x), y)}{\partial w_i \partial w_j^\top} = p(1-p) v_i v_j \sigma'(w_i^\top x) \sigma'(w_j^\top x) x x^\top \quad \text{for } i \neq j, \quad (1)$$

where  $p = 1/(1 + \exp(-yf(\theta, x)))$  denotes the probability of correct prediction, and  $\sigma'(\cdot)$  is the derivative of  $\sigma(\cdot)$ . Collobert [2004] argued that CE loss is the key factor for the near-block-diagonal structure. The author provided a one-line intuitive explanation: since the training objective is to maximize  $p$ , the term  $p(1-p)$  will decay to zero, which pushes the off-diagonal blocks to zero. Numerically, Collobert [2004] reported that CE loss brings the near-block-diagonal Hessian structure, while MSE loss does not (their Figure 7.3 & 7.5, also restated in Figure 5 in Appendix B.1). The author argued that this is because MSE loss does not produce the term  $p(1-p)$ .

We point out that the arguments in [Collobert, 2004] might not be accurate. In particular:

1. For binary classification, the term  $p(1-p)$  occurs for both diagonal and off-diagonal blocks. This can be easily inferred in our latter analysis in **Case 1** with  $C = 2$ . Therefore, it cannot serve as a distinguishing factor between the diagonal and off-diagonal blocks. For CE loss, the observed block-diagonal structure might be due to other properties.
2. Our numerical results in Figure 1 show that the near-block-diagonal Hessian structure occurs not only during the training, but also at initialization. As such, the special structure is not the result of “maximizing  $p$ ” or “minimizing  $(1-p)$ ”.

In the subsequent analysis, we will show that the number of classes  $C$ , instead of the CE loss, is one key factor. Specifically, the near-block-diagonal Hessian structure arises as  $C \rightarrow \infty$  for *both* the MSE and the CE loss. [Collobert, 2004] did not observe the special structure under the MSE loss because binary classification with  $C = 2$  was considered.

We emphasize that we do not claim “large  $C$ ” as the *only* cause for the near-block-diagonal Hessian structure, but just that it is a sufficient condition. It is also possible that the special structure arises with small  $C$  (Figure 7.3 in [Collobert, 2004]) due to other reasons, which we have not explored yet.

## 4 Preliminaries and Intuitive Understanding

**Our settings.** We consider a general setting of multi-class classification problems. Given a classification dataset with  $n$  samples  $\{(x_n, y_n)\}_{n=1}^N$ , where  $x_n \in \mathbb{R}^d$  is the input data,  $y_n \in \{1, \dots, C\}$  is the label, and  $C$  is the number of classes. This setting is quite general: it covers simple logistic regressions, as well as the most advanced LLMs. we consider the following four cases.

**Case 1: linear models with MSE loss.** Consider the linear model  $f(V; x) = Vx \in \mathbb{R}^C$ , where  $V = (v_1^\top; \dots; v_C^\top) \in \mathbb{R}^{C \times d}$  is the weight matrix, and  $v_i \in \mathbb{R}^d$  is the weight associated with the  $i$ -th class (or output neuron). Consider minimizing the MSE loss as follows:

$$\min_V \ell_{\text{MSE}}(V) := \frac{1}{N} \sum_{n=1}^N \|Vx_n - \mathcal{Y}_n\|_2^2, \quad (2)$$

where  $\mathcal{Y}_n \in \{0, 1\}^C$  is a  $C$ -dimensional one-hot vector with 1 at the index for the class of  $y_n$  and 0 elsewhere. The Hessian matrix is, for  $i, j \in [C]$ :

$$\begin{cases} \frac{\partial^2 \ell_{\text{MSE}}(V)}{\partial v_i \partial v_i^\top} = \frac{1}{N} \sum_{n=1}^N x_n x_n^\top \\ \frac{\partial^2 \ell_{\text{MSE}}(V)}{\partial v_i \partial v_j^\top} = 0_{d \times d}. \end{cases} \quad (3)$$

The Hessian matrix is always block-diagonal with  $C$  blocks in this case. Note that the Hessian expression in (3) also holds for general real-valued vector  $\mathcal{Y}_n \in \mathbb{R}^C$ , so the same Hessian structure arises in the regression tasks as well.

**Case 2: linear models with CE loss.** Consider the same linear model as in **Case 1**. We now change the loss function to the CE loss.

$$\min_V \ell_{\text{CE}}(V) := -\frac{1}{N} \sum_{n=1}^N \log \left( \frac{\exp(v_{y_n}^\top x_n)}{\sum_{c=1}^C \exp(v_c^\top x_n)} \right). \quad (4)$$

Define  $p_{n,i} := \exp(v_i^\top x_n) / (\sum_{c=1}^C \exp(v_c^\top x_n))$ . The Hessian matrix is, for  $i, j \in [C]$ .

$$\begin{cases} \frac{\partial^2 \ell_{\text{CE}}(V)}{\partial v_i \partial v_i^\top} = \frac{1}{N} \sum_{n=1}^N p_{n,i} (1 - p_{n,i}) x_n x_n^\top \\ \frac{\partial^2 \ell_{\text{CE}}(V)}{\partial v_i \partial v_j^\top} = -\frac{1}{N} \sum_{n=1}^N p_{n,i} p_{n,j} x_n x_n^\top. \end{cases} \quad (5)$$

**Intuitive understanding:** at random initialization, suppose each entry in  $V$  follows i.i.d. zero-mean Gaussian distribution, we have  $p_{n,i} \approx \frac{1}{C}$  for all  $n \in [N], i \in [C]$ . As such:

$$\frac{\left\| \frac{\partial^2 \ell_{\text{CE}}(V)}{\partial v_i \partial v_j^\top} \right\|_F}{\left\| \frac{\partial^2 \ell_{\text{CE}}(V)}{\partial v_i \partial v_i^\top} \right\|_F} \approx \frac{\sum_{n=1}^N p_{n,i} p_{n,j}}{\sum_{n=1}^N p_{n,i} (1 - p_{n,i})} \approx \frac{\frac{1}{C^2}}{\frac{1}{C} \left(1 - \frac{1}{C}\right)} = \frac{1}{C-1}, \quad (6)$$

which pushes the Hessian to become block-diagonal as  $C \rightarrow \infty$ .

**Case 3: 1-hidden-layer networks with MSE loss.** We now consider the 1-hidden-layer network with  $m$  hidden neurons:  $f(W, V; x) = V\sigma(Wx) \in \mathbb{R}^C$ , where  $W \in (w_1^\top; \dots; w_m^\top) \in \mathbb{R}^{m \times d}$ ;  $\sigma(z) = \max\{0, z\}$  is the ReLU activation and is applied elementwise to  $Wx$ ;  $V = (v_1^\top; \dots; v_C^\top) \in \mathbb{R}^{C \times m}$ . Consider the MSE loss as follows.

$$\min_{W, V} \ell_{\text{MSE}}(W, V) := \frac{1}{N} \sum_{n=1}^N \|V\sigma(Wx_n) - \mathcal{Y}_n\|_2^2, \quad (7)$$

The hidden-layer Hessian  $H_{ww}$  is: for  $i, j \in [m]$ ,

$$\begin{cases} \frac{\partial^2 \ell_{\text{MSE}}(W, V)}{\partial w_i \partial w_i^\top} = \frac{1}{N} \left( \sum_{c=1}^C v_{c,i}^2 \right) \left( \sum_{n=1}^N \mathbf{1}(w_i^\top x_n > 0) x_n x_n^\top \right) \\ \frac{\partial^2 \ell_{\text{MSE}}(W, V)}{\partial w_i \partial w_j^\top} = \frac{1}{N} \left( \sum_{c=1}^C v_{c,i} v_{c,j} \right) \left( \sum_{n=1}^N \mathbf{1}(w_i^\top x_n > 0) \mathbf{1}(w_j^\top x_n > 0) x_n x_n^\top \right). \end{cases} \quad (8)$$

The output-layer Hessian  $H_{vv}$  is: for  $i, j \in [C]$ ,

$$\begin{cases} \frac{\partial^2 \ell_{\text{MSE}}(W, V)}{\partial v_i \partial v_i^\top} = \frac{1}{N} \sum_{n=1}^N \sigma(Wx_n) \sigma(Wx_n)^\top \\ \frac{\partial^2 \ell_{\text{MSE}}(W, V)}{\partial v_i \partial v_j^\top} = 0_{d \times d}, \end{cases} \quad (9)$$

The output-layer Hessian is block-diagonal. We now discuss the hidden-layer Hessian.

**Intuitive understanding:** at random initialization, suppose entries in  $v_i \in \mathbb{R}^d$  follow an i.i.d. zero-mean Gaussian distribution, then

$$\frac{\left\| \frac{\partial^2 \ell_{\text{MSE}}(W, V)}{\partial w_i \partial w_j^\top} \right\|_F}{\left\| \frac{\partial^2 \ell_{\text{MSE}}(W, V)}{\partial w_i \partial w_i^\top} \right\|_F} \approx \frac{\left( \sum_{c=1}^C v_{c,i} v_{c,j} \right)}{\left( \sum_{c=1}^C v_{c,i}^2 \right)} \xrightarrow{C \rightarrow \infty} \frac{\text{Cov}(v_{i,i}, v_{i,j})}{\text{Var}(v_{i,i})}. \quad (10)$$

As  $v_{i,i}, v_{i,j}$  are independent,  $\text{Cov}(v_{i,i}, v_{i,j}) = 0$  and thus the block-diagonal structure in  $H_{ww}$  occurs as  $C \rightarrow \infty$ .

**Case 4: 1-hidden-layer networks with CE loss.** We now consider 1-hidden-layer networks with CE loss.

$$\min_{W, V} \ell_{\text{CE}}(W, V) := -\frac{1}{N} \sum_{n=1}^N \log \left( \frac{\exp(v_{y_n}^\top \sigma(Wx_n))}{\sum_{c=1}^C \exp(v_c^\top \sigma(Wx_n))} \right). \quad (11)$$

The hidden-layer Hessian  $H_{ww}$  is: for  $i, j \in [m]$ ,

$$\begin{cases} \frac{\partial^2 \ell_{\text{CE}}(W, V)}{\partial w_i \partial w_i^\top} = \frac{1}{N} \sum_{n=1}^N \left( \sum_{c=1}^C p_{n,c} v_{c,i}^2 - \left( \sum_{c=1}^C p_{n,c} v_{c,i} \right)^2 \right) \mathbf{1}(w_i^\top x_n > 0) x_n x_n^\top \\ \frac{\partial^2 \ell_{\text{CE}}(W, V)}{\partial w_i \partial w_j^\top} = \frac{1}{N} \sum_{n=1}^N \left( \sum_{c=1}^C p_{n,c} v_{c,i} v_{c,j} - \left( \sum_{c=1}^C p_{n,c} v_{c,i} \right) \left( \sum_{c=1}^C p_{n,c} v_{c,j} \right) \right) \mathbf{1}(w_i^\top x_n > 0) \mathbf{1}(w_j^\top x_n > 0) x_n x_n^\top \end{cases} \quad (12)$$

The output-layer Hessian  $H_{vv}$  is: for  $i, j \in [C]$ ,

$$\begin{cases} \frac{\partial^2 \ell_{\text{CE}}(W, V)}{\partial v_i \partial v_i^\top} = \frac{1}{N} \sum_{n=1}^N p_{n,i} (1 - p_{n,i}) \sigma(Wx_n) \sigma(Wx_n)^\top \\ \frac{\partial^2 \ell_{\text{CE}}(W, V)}{\partial v_i \partial v_j^\top} = -\frac{1}{N} \sum_{n=1}^N p_{n,i} p_{n,j} \sigma(Wx_n) \sigma(Wx_n)^\top. \end{cases} \quad (13)$$

**Intuitive understanding:** at random initialization, suppose entries in  $W, V$  follows i.i.d. zero-mean Gaussian distribution, we have  $p_{n,i} \approx \frac{1}{C}$  for all  $n \in [N], i \in [C]$ . As such:

$$\frac{\left\| \frac{\partial^2 \ell_{\text{CE}}(W, V)}{\partial w_i \partial w_j^\top} \right\|_F}{\left\| \frac{\partial^2 \ell_{\text{CE}}(W, V)}{\partial w_i \partial w_i^\top} \right\|_F} \approx \frac{\left( \sum_{c=1}^C v_{c,i} v_{c,j} - \left( \sum_{c=1}^C v_{c,i} \right) \left( \sum_{c=1}^C v_{c,j} \right) \right) / C}{\left( \sum_{c=1}^C v_{c,i}^2 - \left( \sum_{c=1}^C v_{c,i} \right)^2 \right) / C} \xrightarrow{C \rightarrow \infty} \frac{\text{Cov}(v_{i,i}, v_{i,j})}{\text{Var}(v_{i,i})}. \quad (14)$$

Since  $v_{i,i}, v_{i,j}$  are independent,  $\text{Cov}(v_{i,i}, v_{i,j}) = 0$  and thus the block-diagonal structure in  $H_{ww}$  occurs as  $C \rightarrow \infty$ . Similarly, we have

$$\frac{\left\| \frac{\partial^2 \ell_{\text{CE}}(W, V)}{\partial v_i \partial v_j^\top} \right\|_F}{\left\| \frac{\partial^2 \ell_{\text{CE}}(W, V)}{\partial v_i \partial v_i^\top} \right\|_F} \approx \frac{\sum_{n=1}^N p_{n,i} p_{n,j}}{\sum_{n=1}^N p_{n,i} (1 - p_{n,i})} \approx \frac{\frac{1}{C^2}}{\frac{1}{C} \left(1 - \frac{1}{C}\right)} = \frac{1}{C-1}, \quad (15)$$

and thus the block-diagonal structure in  $H_{vv}$  arises as  $C \rightarrow \infty$ .

## 5 Main Results

We now formalize the above informal analysis into rigorous statements. Since the Frobenious norm of Hessian blocks involves the 2nd-order moments of eigenvalues of random matrices, we will resort to the tools from random matrix theory. We first state some standard assumptions.

**Assumption 1.** The entries of the data matrix  $X_N = (x_1, \dots, x_N) \in \mathbb{R}^{d \times N}$  are i.i.d.  $\mathcal{N}(0, 1)$ .

**Assumption 2.** The model weights in  $W$  and  $V$  are initialized by LeCun initialization. That is: for the linear model,  $V_{i,j} \stackrel{\text{i.i.d.}}{\sim} \mathcal{N}(0, \frac{1}{d})$ ,  $i \in [C], j \in [d]$ ; for 1-hidden-layer network,  $W_{i,j} \stackrel{\text{i.i.d.}}{\sim} \mathcal{N}(0, \frac{1}{d})$ ,  $i \in [m], j \in [d]$ ,  $V_{i,j} \stackrel{\text{i.i.d.}}{\sim} \mathcal{N}(0, \frac{1}{m})$ ,  $i \in [C], j \in [m]$ .

Note that Assumption 1 on data distribution is standard in random matrix theory [Pastur, 2020]. It is possible to extend the Gaussian distribution to, e.g., Gaussian orthogonal ensembles and more general i.i.d. distribution. However, such generalization is non-trivial and each case may require an independent paper (e.g. Pastur [2022], Pastur and Slavin [2023]). We now state our results for linear models and 1-hidden-layer networks under Assumptions 1 and 2.

**Theorem 1. (Linear models.)** Consider the Hessian expressions in (5) and assume Assumptions 1 and 2 hold. Suppose  $d, N \rightarrow \infty$ ,  $\frac{d}{N} \rightarrow \gamma \in (0, +\infty)$ , then for fixed  $C \geq 2$ , it holds almost surely that

$$\lim_{d, N \rightarrow \infty} \frac{1}{d} \left\| \frac{\partial^2 \ell_{\text{CE}}(V)}{\partial v_i \partial v_i^\top} \right\|_F = g_{ii}(\gamma, C), \quad \forall i \in [C], \quad (16)$$

$$\lim_{d, N \rightarrow \infty} \frac{1}{d} \left\| \frac{\partial^2 \ell_{\text{CE}}(V)}{\partial v_i \partial v_j^\top} \right\|_F = g_{ij}(\gamma, C), \quad \forall i, j \in [C], i \neq j, \quad (17)$$

where functions  $g_{ii}, g_{ij}$  are given in Appendix C. Furthermore,

$$\lim_{C \rightarrow \infty} C^2 g_{ii}(\gamma, C) = \gamma e + 1, \quad (18)$$

$$\lim_{C \rightarrow \infty} C^4 g_{ij}(\gamma, C) = \gamma e^2 + 1. \quad (19)$$

Theorem 1 implies that we have the following relation between the diagonal and off-diagonal blocks:

$$\lim_{d, N \rightarrow \infty} \frac{\left\| \frac{\partial^2 \ell_{\text{CE}}(V)}{\partial v_i \partial v_j^\top} \right\|_F^2}{\left\| \frac{\partial^2 \ell_{\text{CE}}(V)}{\partial v_i \partial v_i^\top} \right\|_F^2} = \frac{g_{ij}(\gamma, C)}{g_{ii}(\gamma, C)}, \quad \lim_{C \rightarrow \infty} \frac{C^2 g_{ij}(\gamma, C)}{g_{ii}(\gamma, C)} = \frac{\gamma e^2 + 1}{\gamma e + 1}. \quad (20)$$

When  $C \rightarrow \infty$ , the ratio vanishes at the rate  $\mathcal{O}(1/C^2)$ , and the block-diagonal structure emerges.

The next theorem presents a similar result for 1-hidden-layer networks.



**Theorem 2. (1-hidden-layer networks.)** Consider the Hessian expressions in (8) to (13), and assume Assumptions 1 and 2 hold. Then for any fixed  $m \geq 3$ , suppose  $d, N \rightarrow \infty$ ,  $\frac{d}{N} \rightarrow \gamma \in (0, +\infty)$ , it holds that

$$\lim_{d, N \rightarrow \infty} \frac{1}{d} \mathbf{E} \left[ \left\| \frac{\partial^2 \ell_{CE}(W, V)}{\partial w_i \partial w_i^\top} \right\|_F^2 \right] = h_{ii}(\gamma, C), \quad \lim_{d, N \rightarrow \infty} \frac{1}{d} \mathbf{E} \left[ \left\| \frac{\partial^2 \ell_{CE}(W, V)}{\partial w_i \partial w_j^\top} \right\|_F^2 \right] = h_{ij}(\gamma, C), \quad (21)$$

$$\lim_{d, N \rightarrow \infty} \frac{1}{d} \mathbf{E} \left[ \left\| \frac{\partial^2 \ell_{MSE}(W, V)}{\partial w_i \partial w_i^\top} \right\|_F^2 \right] = u_{ii}(\gamma, C), \quad \lim_{d, N \rightarrow \infty} \frac{1}{d} \mathbf{E} \left[ \left\| \frac{\partial^2 \ell_{MSE}(W, V)}{\partial w_i \partial w_j^\top} \right\|_F^2 \right] = u_{ij}(\gamma, C), \quad (22)$$

$$\lim_{d, N \rightarrow \infty} \mathbf{E} \left[ \left\| \frac{\partial^2 \ell_{CE}(W, V)}{\partial v_i \partial v_i^\top} \right\|_F^2 \right] = q_{ii}(\gamma, C), \quad \lim_{d, N \rightarrow \infty} \mathbf{E} \left[ \left\| \frac{\partial^2 \ell_{CE}(W, V)}{\partial v_i \partial v_j^\top} \right\|_F^2 \right] = q_{ij}(\gamma, C), \quad (23)$$

where functions  $h_{ii}, h_{ij}, u_{ii}, u_{ij}, q_{ii}, q_{ij}$  given in Appendix D. Furthermore, we have

$$\lim_{C \rightarrow \infty} h_{ii}(\gamma, C) = \frac{1+2\gamma}{4m^2}, \quad \lim_{C \rightarrow \infty} C h_{ij}(\gamma, C) = \frac{\gamma(m-1)^2}{2^m(m-2)^3 m} \left( \sqrt{\frac{m}{m-2}} + 1 \right)^{m-2}, \quad (24)$$

$$\lim_{C \rightarrow \infty} \frac{u_{ii}(\gamma, C)}{C^2} = \frac{1+2\gamma}{4m^2}, \quad \lim_{C \rightarrow \infty} \frac{u_{ij}(\gamma, C)}{C} = \frac{1+4\gamma}{16m^2}, \quad (25)$$

$$\lim_{C \rightarrow \infty} C^2 q_{ii}(\gamma, C) = m a_{12} b_1^{m-1} + m(m-1) a_{11}^2 b_1^{m-2} \quad (26)$$

$$\lim_{C \rightarrow \infty} C^4 q_{ij}(\gamma, C) = m a_{22} b_2^{m-1} + m(m-1) a_{21}^2 b_2^{m-1}, \quad (27)$$

where the constant terms  $a_{11}, a_{12}, a_{21}, a_{22}, b_1, b_2$  are presented in (62) in Appendix D.

Similar to the implication of Theorem 1 in (20), Theorem 2 implies that the ratios

$$\lim_{d, N \rightarrow \infty} \frac{\mathbf{E} \left[ \left\| \frac{\partial^2 \ell_{CE}(W, V)}{\partial w_i \partial w_j^\top} \right\|_F^2 \right]}{\mathbf{E} \left[ \left\| \frac{\partial^2 \ell_{CE}(W, V)}{\partial w_i \partial w_i^\top} \right\|_F^2 \right]}, \quad \lim_{d, N \rightarrow \infty} \frac{\mathbf{E} \left[ \left\| \frac{\partial^2 \ell_{MSE}(W, V)}{\partial w_i \partial w_j^\top} \right\|_F^2 \right]}{\mathbf{E} \left[ \left\| \frac{\partial^2 \ell_{MSE}(W, V)}{\partial w_i \partial w_i^\top} \right\|_F^2 \right]}, \quad \lim_{d, N \rightarrow \infty} \frac{\mathbf{E} \left[ \left\| \frac{\partial^2 \ell_{CE}(W, V)}{\partial v_i \partial v_j^\top} \right\|_F^2 \right]}{\mathbf{E} \left[ \left\| \frac{\partial^2 \ell_{CE}(W, V)}{\partial v_i \partial v_i^\top} \right\|_F^2 \right]} \quad (28)$$

vanish at the rate  $\mathcal{O}(1/C)$ ,  $\mathcal{O}(1/C)$ ,  $\mathcal{O}(1/C^2)$ , respectively, and the block-diagonal structure in  $H_{ww}$  and  $H_{vv}$  also emerges as  $C$  increases.

## 6 Key Challenges and Proof Sketches

Now we explain the major technical challenges and the main ideas in our proofs. We primarily introduce the proof procedure for Theorem 1, i.e., linear models with CE loss (**Case 2**). Despite the simple form of linear models, we find that it is rather non-trivial to characterize its Hessian structure, and the classical random matrix approaches *cannot* be directly applied. After introducing the proof for Theorem 1, we will discuss how to extend our analysis to Theorem 2 (**Case 3 and 4**). **Since the complete proof of Theorem 1 and 2 are rather long and technical, we present them in Appendix C and D, respectively.**

**Challenges for proving Theorem 1.** We first rewrite the Hessian expression in **Case 2** as follows, and then we discuss why the classical random matrix approaches cannot be directly applied here. Due to the limited space, we only discuss the diagonal blocks  $\frac{\partial^2 \ell_{CE}(V)}{\partial v_i \partial v_i^\top}$ . The same challenges and solutions also apply to the off-diagonal blocks  $\frac{\partial^2 \ell_{CE}(V)}{\partial v_i \partial v_j^\top}$ , which we omit here.

$$\frac{\partial^2 \ell_{CE}(V)}{\partial v_i \partial v_i^\top} \stackrel{(5)}{=} \frac{1}{N} \sum_{n=1}^N p_{n,i} (1 - p_{n,i}) x_n x_n^\top := \frac{1}{N} X_N \Lambda_N X_N^\top \in \mathbb{R}^{d \times d}, \quad (29)$$

where  $X_N = (x_1, \dots, x_N) \in \mathbb{R}^{d \times N}$ ,  $\Lambda_N = \text{diag}(p_{1,i}(1 - p_{1,i}), \dots, p_{N,i}(1 - p_{N,i})) \in \mathbb{R}^{N \times N}$ , and  $p_{n,i} := \exp(v_i^\top x_n) / \left( \sum_{c=1}^C \exp(v_c^\top x_n) \right)$ . Note that both  $X_N$  and  $\Lambda_N$  are random matrices. How to characterize  $\|\frac{1}{N} X_N \Lambda_N X_N^\top\|_F$ ? We first recall some classical results in random matrix theory.

**Classical results from random matrix theory and why they cannot be directly applied.** We first introduce some basic concepts in random matrix theory.

- **Eigenvalue distribution and weak convergence of probability measures.** For a symmetric matrix  $A \in \mathbb{R}^{d \times d}$ , we define  $\mu_A = \frac{1}{d} \sum_{i=1}^d \delta_{\lambda_i(A)}$  as the empirical eigenvalue distribution of  $A$ .  $\mu_A$  is a probability measure on  $\mathbb{R}$  that assigns equal probability  $\frac{1}{d}$  to each eigenvalue. Note that when  $A$  is a random matrix,  $\mu_A$  is a random measure. For a sequence of random matrices  $(A_n)_{n=1}^\infty$ , we will consider the weak convergence of its eigenvalue distribution  $(\mu_{A_n})_{n=1}^\infty$ .
- **Stieltjes transform.** For a probability measure  $\nu$  on  $\mathbb{R}$ , The Stieltjes transform of  $\nu$  is defined as

$$s_\nu(z) = \int_{\mathbb{R}} \frac{1}{x - z} d\nu(x), \quad z \in \mathbb{C}^+ \setminus \text{supp}(\nu).$$

A probability measure is uniquely characterized by its Stieltjes transform. For a symmetric matrix  $A$ , we write  $s_{\mu_A}(z)$  as  $s_A(z)$  for short. A sequence of eigenvalue distributions  $(\mu_{A_n})_{n=1}^\infty$  converges weakly to a probability measure  $\mu$  if and only if  $s_{A_n}(z) \rightarrow s_\mu(z)$ ,  $\forall z \in \mathbb{C}^+$ .

Now we notice that  $\|A\|_F^2$  is nothing but the 2nd-order moment of  $\mu_A$ . Moreover, we can retrieve the moments of  $\mu_A$  from  $s_A(z)$  by

$$s_A(z) = -\frac{1}{z} - \frac{m_1}{z^2} - \frac{m_2}{z^3} - \dots, \quad z \rightarrow \infty, \quad (30)$$

where  $m_k = \int_{\mathbb{R}} t^k d\mu_A(t)$  denotes the  $k$ -th order moment. Therefore, the calculation of  $\|A\|_F^2$  can be achieved by finding the limiting eigenvalue distribution of  $A$  as the matrix size  $d \rightarrow \infty$ , which is a classical topic in random matrix theory. Typically, the random matrices of the type  $X_N \Lambda_N X_N^\top$  are closely related to the sample covariance matrices. The case that  $\Lambda_N$  is deterministic or independent of  $X_N$  has already been deeply studied (e.g., Yao et al. [2015], Bai and Silverstein [2010], Bai and Zhou [2008], Marčenko and Pastur [1967]). For the limiting eigenvalue distribution, we have the following classical result, the generalized Marcenko-Pastur theorem.

**Theorem 3.** [Marčenko and Pastur, 1967] Consider random matrices  $X_N \in \mathbb{R}^{d \times N}$  with entries i.i.d. with mean 0 and variance 1; and  $\Lambda_N \in \mathbb{R}^{N \times N}$  which is either deterministic or independent of  $X_N$ . Suppose that the eigenvalue distribution of  $\Lambda_N$  converges weakly almost surely to a deterministic probability measure  $\nu$ . Let  $A_N = \frac{1}{d} X_N \Lambda_N X_N^\top$ , then as  $N, d \rightarrow \infty, d/N \rightarrow \gamma \in (0, +\infty)$ ,  $\mu_{A_N}$  converges weakly almost surely to a deterministic probability measure  $\mu$ . Here  $\mu$  is uniquely specified by a functional equation of its Stieltjes transform  $s(z)$ :

$$s_\mu(z) = \frac{1}{\frac{1}{\gamma} \int_{\mathbb{R}} \frac{td\nu(t)}{1 + ts_\mu(z)} - z}, \quad \forall z \in \mathbb{C}^+. \quad (31)$$

Unfortunately, Theorem 3 can not be directly applied to our case. This is because Theorem 3 requires  $\Lambda_N$  and  $X_N$  to be independent, while  $\Lambda_N$  and  $X_N$  in (29) are clearly dependent.

**Key observation: asymptotic independence.** For our matrix of interests (29), although  $\Lambda_N \in \mathbb{R}^{N \times N}$  and  $X_N \in \mathbb{R}^{d \times N}$  are not independent for any fixed  $d$ , we observe that they are *asymptotically independent* as  $d \rightarrow \infty$ . This is because:

- Recall  $v_i \sim \mathcal{N}(0, \frac{1}{d})$  and denote  $z = v_i^\top x_n$ , then  $z|x \sim \mathcal{N}(0, \frac{\|x\|_2^2}{d})$ . Further, since  $x \sim \mathcal{N}(0, 1)$ , we have  $\frac{\|x\|_2^2}{d} \sim \chi^2(1, \frac{2}{d})$ , which concentrates to 1 as  $d \rightarrow \infty$ .

- As such,  $z$  asymptotically follows  $\mathcal{N}(0, 1)$  and thus is independent of  $x$ . Therefore,  $\Lambda_N$  and  $X_N$  are asymptotically independent.

Therefore, as  $d, N \rightarrow \infty$ , it seems possible to obtain the same limiting eigenvalue distribution as in Theorem 3 for our matrix (29). The remaining question is how to prove it rigorously. One possible path is from free probability theory [Mingo and Speicher, 2017], proving the asymptotic freeness between  $\Lambda_N$  and  $X_N X_N^\top$  [Collins and Hayase, 2023].

**Our solutions.** In this work, we use a rather classical decoupling technique, motivated by the *Lindeberg interpolation principle*. The Lindeberg principle is originally an elegant proof for the Central Limit Theorem (CLT) [Lindeberg, 1922], by replacing the random variables with Gaussian ones incrementally and proving the impact is negligible under certain conditions. The Lindeberg principle is also applicable for random matrices [Götze et al., 2015, Pastur, 2020, Chatterjee, 2006]. We find that such methods are useful for handling asymptotic independence in our case.

We now illustrate our proof strategy. The idea is to first decouple and then apply Theorem 3.

- **Step 1.** For our matrix (29) (denoted as  $H_{ii}^{\text{CE}}$ ), we introduce the decoupled matrix

$$\tilde{H}_{ii}^{\text{CE}} = \frac{1}{N} \sum_{n=1}^N \tilde{p}_{n,i} (1 - \tilde{p}_{n,i}) x_n x_n^\top, \quad \tilde{p}_{n,i} := \frac{\exp(v_i^\top \tilde{x}_n)}{\sum_{c=1}^C \exp(v_c^\top \tilde{x}_n)}, \quad (32)$$

where  $\tilde{X}_N = (\tilde{x}_1, \dots, \tilde{x}_N) \in \mathbb{R}^{d \times n}$  is an independent copy of  $X_N$ . The goal is to prove that

$$\lim_{N \rightarrow \infty} (s_{H_{ii}^{\text{CE}}}(z) - s_{\tilde{H}_{ii}^{\text{CE}}}(z)) = 0, \quad \text{a.s.} \quad \forall z \in \mathbb{C}^+.$$

From standard measure concentration results,  $s_{H_{ii}^{\text{CE}}}(z), s_{\tilde{H}_{ii}^{\text{CE}}}(z)$  concentrates around their means as  $N \rightarrow \infty$ .

Therefore, it suffices to prove that  $\lim_{N \rightarrow \infty} (\mathbf{E}[s_{H_{ii}^{\text{CE}}}(z)] - \mathbf{E}[s_{\tilde{H}_{ii}^{\text{CE}}}(z)]) = 0$ .

- **Step 2.** Following the Lindeberg principle, we define the matrix interpolation process

$$X_N(t) = \sqrt{t} X_N + \sqrt{1-t} \tilde{X}_N, \quad t \in [0, 1].$$

Note that  $X_N(0) = X_N$  and  $X_N(1) = \tilde{X}_N$ . We then define

$$H_{ii}^{\text{CE}}(t) = \frac{1}{N} \sum_{n=1}^N p_{n,i}(t) (1 - p_{n,i}(t)) x_n x_n^\top, \quad \text{where } p_{n,i}(t) := \frac{\exp(v_i^\top x_n(t))}{\sum_{c=1}^C \exp(v_c^\top x_n(t))}.$$

Using basic matrix calculus, we arrive at the following equation:

$$\mathbf{E}[s_{H_{ii}^{\text{CE}}}(z)] - \mathbf{E}[s_{\tilde{H}_{ii}^{\text{CE}}}(z)] = \int_0^1 \mathbf{E} \left[ \frac{d}{dt} s_{H_{ii}^{\text{CE}}(t)} \right] dt. \quad (33)$$

- **Step 3.** We notice that the r.h.s. of (33) can be bounded in the form of  $\mathbf{E}[Zf(Z)]$ . We then bound it using Stein's Lemma: for  $Z \sim \mathcal{N}(0, 1)$  and differentiable function  $f : \mathbb{R} \rightarrow \mathbb{C}$  with sub-exponential decay at infinity, we have:

$$\mathbf{E}[Zf(Z)] = \mathbf{E}[f'(Z)]. \quad (34)$$

We then prove that the r.h.s. of (34) decays to zero at rate  $\mathcal{O}(1/\sqrt{N})$ , and thus  $H_{ii}^{\text{CE}}$  shares the same limit distribution as  $\tilde{H}_{ii}^{\text{CE}}$ . Note that Stein's Lemma requires Gaussian data  $X_N$  in Assumption 1. We refer to Appendix A.6 of [Talagrand, 2003] for the proof of Stein's Lemma.

- **Step 4.** Apply Theorem 3. The decoupled matrix  $\tilde{H}_{ii}^{\text{CE}}$  has the type  $X_N \tilde{\Lambda}_N X_N^\top$  where  $\tilde{\Lambda}_N$  is independent of  $X_N$ . Then Theorem 3 is applicable to obtain the limiting eigenvalue distribution of  $\tilde{H}_{ii}^{\text{CE}}$ . Then we apply the expansion (30) in the functional equation (31) to get the limiting second moment of  $\mu_{\tilde{H}_{ii}^{\text{CE}}}$ , which is also the limit of  $\|H_{ii}^{\text{CE}}\|_{\text{F}}^2$ . This concludes the proof.

**Challenges for the hidden-layer Hessian in 1-hidden-layer networks.** Now we extend our analysis on linear models to 1-hidden-layer networks. Similar as before, We primarily discuss the diagonal blocks of the Hessian. The same challenges and solutions also apply to the off-diagonal blocks, which we omit here. We first discuss the hidden-layer Hessian.

$$\frac{\partial^2 \ell_{\text{CE}}(W, V)}{\partial w_i \partial w_i^\top} = \frac{1}{N} \sum_{n=1}^N \underbrace{\left( \sum_{c=1}^C p_{n,c} v_{c,i}^2 - \left( \sum_{c=1}^C p_{n,c} v_{c,i} \right)^2 \right)}_{(a)} \underbrace{\mathbf{1}(w_i^\top x_n > 0)}_{(b)} x_n x_n^\top := \frac{1}{N} X_N \Lambda_N X_N^\top, \quad (35)$$

Before applying the same decoupling technique as in linear models, we first show that  $X_N$  and  $\Lambda_N$  are also asymptotic independent as  $d \rightarrow \infty$ . We present the following reasons:

- We start with (b) first. Recall  $w_i \sim \mathcal{N}(0, \frac{1}{d})$  and denote  $z_{n,i} = w_i^\top x_n$ . Following the same argument as in the linear model case, we have  $z_{n,i} | x_n \sim \mathcal{N}(0, 1)$  as  $d \rightarrow \infty$ . So  $z_{n,i}$  is asymptotically independent of  $x_n$ , and thus  $\mathbf{1}(z_{n,i} > 0)$  is also asymptotically independent of  $x_n$ ,  $\forall n \in [N]$ . Therefore, (b) and  $X_N$  are asymptotically independent.
- Now we discuss (a). Denote  $y_{n,c} = (z_{n,1}, \dots, z_{n,m})^\top v_c$ . Since  $(z_{n,1}, \dots, z_{n,m})^\top$  is independent of  $x_n$  as  $d \rightarrow \infty$ , so do  $y_{n,c}$  and  $p_{n,c}$ . As such, (a) and  $X_N$  are asymptotically independent.

As such, (a) and (b) are asymptotically independent of  $X_N$ , thus it is reasonable that we can apply our previous decoupling technique here. A similar procedure also applies to the hidden weights with MSE loss. We present the detailed proof in Appendix D.1 and D.2, respectively.

**Challenges for the output-layer Hessian in 1-hidden-layer networks.** Now we discuss the new challenges for the output-layer Hessian. We rewrite  $\frac{\partial^2 \ell_{\text{CE}}(W, V)}{\partial v_i \partial v_i^\top}$  as follows.

$$\frac{\partial^2 \ell_{\text{CE}}(W, V)}{\partial v_i \partial v_i^\top} = \frac{1}{N} \sum_{n=1}^N p_{n,i} (1 - p_{n,i}) \sigma(W x_n) \sigma(W x_n)^\top := \frac{1}{N} F_N \Lambda_N F_N^\top, \quad (36)$$

where  $F_N = (\sigma(W x_1), \dots, \sigma(W x_N)) \in \mathbb{R}^{m \times N}$ . We highlight two major difference with the  $X_N \Lambda_N X_N^\top$  in linear models (29) and the hidden weights in 1-hidden-layer networks in (35).

- **First**, in the previous cases (29) and (35), the matrices have growing dimension. Now the matrix in (36) has fixed dimension  $m$ , which is away from the standard setting of random matrix theory.
- **Second**, the matrices  $F_N$  and  $\Lambda_N$  have more complicated dependence structure. The dependence between  $Z_N$  and  $\Lambda_N$  is caused by both  $W$  and  $X_N$ , which means that we need to decouple  $\Lambda_N$  with  $\{W, X_N\}$  at the same time. Meanwhile, in previous cases (29) and (35), we only need to decouple  $\Lambda_N$  with  $X_N$ .

To tackle the above challenges, we choose to handle (36) using a largely different approach from above. We consider fixed  $m$  and conduct the following steps. Since the complete proof is rather long and technical, we relegate it to Appendix D.3.

- **Step 1.** Replace  $W X_N$  with  $Z_N$ , where  $Z_N \in \mathbb{R}^{m \times N}$  has i.i.d.  $N(0, 1)$  entries. This can be done by letting  $d \rightarrow \infty$  and applying the Lindeberg principle. This step decouples  $\Lambda_N$  with  $H_N$ .
- **Step 2.** Calculate the expectation of the entry-wise second moment of the Hessian matrices. Note that the decoupling in Step 1 is essential, otherwise, the calculation in Step 2 would be complicated.

## 7 Numerical Results

We now provide some numerical evidence to support our theory. Due to the limited space, here we only discuss **Case 2: linear models with CE loss.** We relegate **Case 1**, **Case 3**, and **Case 4** to Appendix B.2. We

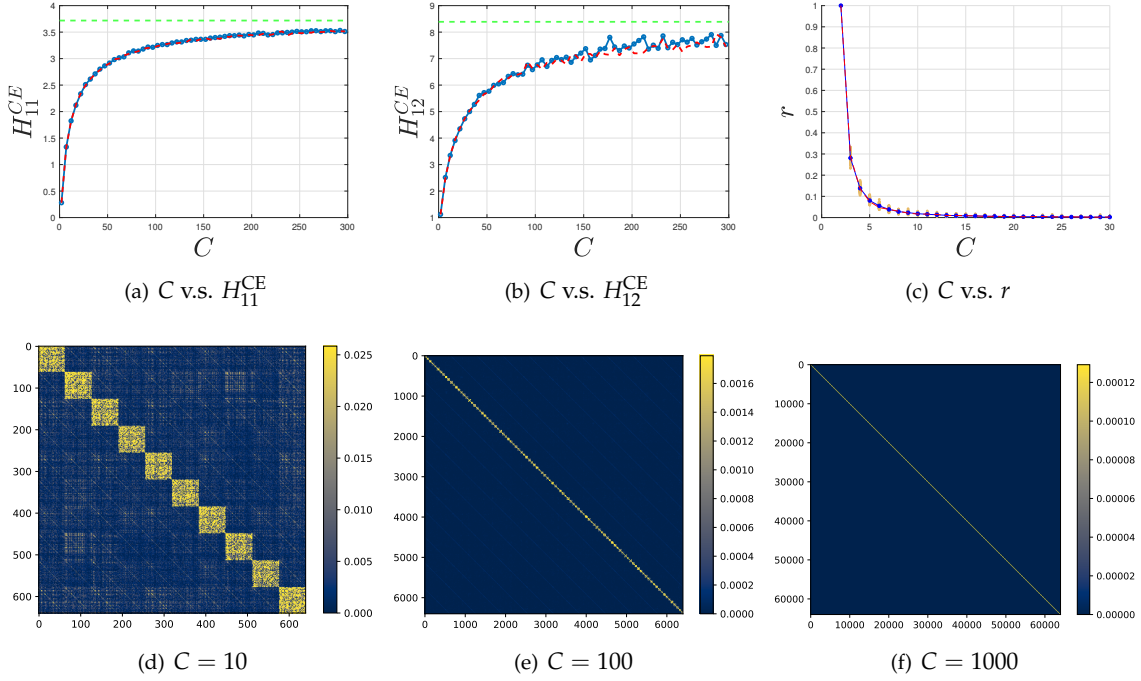


Figure 4: **(a, b, c)**: The evolution of  $H_{11}^{CE}$ ,  $H_{12}^{CE}$ , and  $r$  as  $C$  increases. For each  $C$ , the realizations of  $H_{11}^{CE}$  and  $H_{12}^{CE}$  concentrate around the red curves, which are their theoretical means in (16) and (17) in Proposition 2 (shown later in Appendix C). As  $C \rightarrow \infty$ ,  $H_{11}^{CE}$  and  $H_{12}^{CE}$  approach the green lines, which are their theoretical limits in Theorem 1. Further,  $r$  vanishes to 0 as  $C$  increases, and the decay rate matches Theorem 1. This means that off-diagonal blocks become relatively negligible as  $C$  increases. **(e, f, g)**: The Hessian of **Case 2: linear models with CE loss**. We use random initialization and Gaussian synthetic data. The block-diagonal structure becomes clear when  $C$  increases.

will investigate the following quantities, which appeared in Theorem 1:

$$H_{11}^{CE} := \frac{C^2}{d} \left\| \frac{\partial^2 \ell_{CE}(V)}{\partial v_1 \partial v_1^\top} \right\|_F^2, \quad H_{12}^{CE} := \frac{C^4}{d} \left\| \frac{\partial^2 \ell_{CE}(V)}{\partial v_1 \partial v_2^\top} \right\|_F^2, \quad r := \left\| \frac{\partial^2 \ell_{CE}(V)}{\partial v_1 \partial v_2^\top} \right\|_F^2 / \left\| \frac{\partial^2 \ell_{CE}(V)}{\partial v_1 \partial v_1^\top} \right\|_F^2.$$

We consider the same Gaussian synthetic dataset as in Section 3.1 (which follows Assumption 1) and try different  $C$ . For each  $C$ , we simulate 1000  $H_{11}^{CE}$  and  $H_{12}^{CE}$  with LeCun initialization (Assumption 2), and track their changes with  $C$ . The results are shown in Figure 4. We make the following four observations. These observations match our theoretical prediction.

- **First**, for each  $C$ , the realizations of  $H_{11}^{CE}$  and  $H_{12}^{CE}$  concentrate around the red curves, which are their theoretical means in (16) and (17) in Proposition 2 (shown later in Appendix C).
- **Second**, as  $C \rightarrow \infty$ , we find that the  $H_{11}$  and  $H_{12}$  approach the green lines, which are their theoretical limits in Theorem 1. These results justify the results in Theorem 1.
- **Third**, as  $C \rightarrow \infty$ , we have  $r \rightarrow 0$ , and the decay rate matches our theoretical prediction. This means that off-diagonal blocks become relatively negligible as  $C$  increases.
- **Forth**, as shown in Figure 4 (e-g), the block-diagonal Hessian structure becomes clear when  $C$  increases.

## 8 Conclusions

In this work, we reveal two forces that shape the near-block-diagonal Hessian structure of NNs: a “static force” rooted in the architecture design, and a “dynamic force” arisen from training. We then provide a rigorous theoretical analysis of “static force” of linear and 1-hidden-layer NNs at random initialization. It is intriguing to extend our study beyond initialization and simple models. We provide more discussions of future directions in Appendix A



## Acknowledgement

Yushun Zhang would like to thank Weronika Ormaniec, Sidak Pal Singh, Jeremy Cohen, Prof. Yinyu Ye, and Prof. Madeleine Udell for the valuable discussion.

## References

- G. Alain, N. L. Roux, and P.-A. Manzagol. Negative eigenvalues of the hessian in deep neural networks. *arXiv preprint arXiv:1902.02366*, 2019.
- K. An, Y. Liu, R. Pan, S. Ma, D. Goldfarb, and T. Zhang. Asgo: Adaptive structured gradient optimization. *arXiv preprint arXiv:2503.20762*, 2025.
- S. Arora, Z. Li, and A. Panigrahi. Understanding gradient descent on the edge of stability in deep learning. In *International Conference on Machine Learning*, pages 948–1024. PMLR, 2022.
- Z. Bai and J. W. Silverstein. *Spectral analysis of large dimensional random matrices*. Springer New York, 2010.
- Z. Bai and W. Zhou. Large sample covariance matrices without independence structures in columns. *Statistica Sinica*, 18(2):425–442, 2008.
- S. Chatterjee. A generalization of the lindeberg principle. *Annals of Probability*, 34(6):2061 – 2076, 2006.
- P. Chaudhari, A. Choromanska, S. Soatto, Y. LeCun, C. Baldassi, C. Borgs, J. Chayes, L. Sagun, and R. Zecchina. Entropy-sgd: Biasing gradient descent into wide valleys. *Journal of Statistical Mechanics: Theory and Experiment*, 2019(12):124018, 2019.
- J. M. Cohen, S. Kaur, Y. Li, J. Z. Kolter, and A. Talwalkar. Gradient descent on neural networks typically occurs at the edge of stability. *arXiv preprint arXiv:2103.00065*, 2021.
- J. M. Cohen, B. Ghorbani, S. Krishnan, N. Agarwal, S. Medapati, M. Badura, D. Suo, D. Cardoze, Z. Nado, G. E. Dahl, et al. Adaptive gradient methods at the edge of stability. *arXiv preprint arXiv:2207.14484*, 2022.
- B. Collins and T. Hayase. Asymptotic freeness of layerwise jacobians caused by invariance of multilayer perceptron: The haar orthogonal case. *Communications in Mathematical Physics*, 397(1):85 – 109, 2023.
- R. Collobert. Large scale machine learning. Technical report, Université de Paris VI, 2004.
- F. Dangel, S. Harmeling, and P. Hennig. Modular block-diagonal curvature approximations for feedforward architectures. In *International Conference on Artificial Intelligence and Statistics*, pages 799–808. PMLR, 2020.
- R. Das, N. Agarwal, S. Sanghavi, and I. S. Dhillon. Towards quantifying the preconditioning effect of adam. *arXiv preprint arXiv:2402.07114*, 2024.
- Y. N. Dauphin, R. Pascanu, C. Gulcehre, K. Cho, S. Ganguli, and Y. Bengio. Identifying and attacking the saddle point problem in high-dimensional non-convex optimization. *Advances in neural information processing systems*, 27, 2014.
- G. Desjardins, K. Simonyan, R. Pascanu, et al. Natural neural networks. *Advances in neural information processing systems*, 28, 2015.
- F. Draxler, K. Veschgini, M. Salmhofer, and F. Hamprecht. Essentially no barriers in neural network energy landscape. In *International conference on machine learning*, pages 1309–1318. PMLR, 2018.
- S. Fort and S. Ganguli. Emergent properties of the local geometry of neural loss landscapes. *arXiv preprint arXiv:1910.05929*, 2019.

- T. George, C. Laurent, X. Bouthillier, N. Ballas, and P. Vincent. Fast approximate natural gradient descent in a kronecker factored eigenbasis. *Advances in neural information processing systems*, 31, 2018.
- B. Ghorbani, S. Krishnan, and Y. Xiao. An investigation into neural net optimization via hessian eigenvalue density. In *International Conference on Machine Learning*, pages 2232–2241. PMLR, 2019.
- D. Goldfarb, Y. Ren, and A. Bahamou. Practical quasi-newton methods for training deep neural networks. *Advances in Neural Information Processing Systems*, 33:2386–2396, 2020.
- F. Götze, H. Kösters, and A. Tikhomirov. Asymptotic spectra of matrix-valued functions of independent random matrices and free probability. *Random Matrices: Theory and Applications*, 4(02):1550005, 2015.
- D. Granziol, T. Garipov, D. Vetrov, S. Zohren, S. Roberts, and A. G. Wilson. Towards understanding the true loss surface of deep neural networks using random matrix theory and iterative spectral methods. 2019.
- D. Granziol, S. Zohren, and S. Roberts. Learning rates as a function of batch size: A random matrix theory approach to neural network training. *Journal of Machine Learning Research*, 23(173):1–65, 2022.
- V. Gupta, T. Koren, and Y. Singer. Shampoo: Preconditioned stochastic tensor optimization. In *International Conference on Machine Learning*, pages 1842–1850. PMLR, 2018.
- G. Gur-Ari, D. A. Roberts, and E. Dyer. Gradient descent happens in a tiny subspace. *arXiv preprint arXiv:1812.04754*, 2018.
- B. Hanin and M. Nica. Products of many large random matrices and gradients in deep neural networks. *Communications in Mathematical Physics*, 376(1):287–322, 2020.
- H. He, G. Huang, and Y. Yuan. Asymmetric valleys: Beyond sharp and flat local minima. *Advances in neural information processing systems*, 32, 2019.
- S. Jastrzebski, M. Szymczak, S. Fort, D. Arpit, J. Tabor, K. Cho, and K. Geras. The break-even point on optimization trajectories of deep neural networks. *arXiv preprint arXiv:2002.09572*, 2020.
- S. Jastrzebski, Z. Kenton, N. Ballas, A. Fischer, Y. Bengio, and A. Storkey. On the relation between the sharpest directions of dnn loss and the SGD step length. *arXiv preprint arXiv:1807.05031*, 2018.
- Y. Jiang, B. Neyshabur, H. Mobahi, D. Krishnan, and S. Bengio. Fantastic generalization measures and where to find them. *arXiv preprint arXiv:1912.02178*, 2019.
- K. Jordan, Y. Jin, V. Boza, J. You, F. Cesista, L. Newhouse, and J. Bernstein. Muon: An optimizer for hidden layers in neural networks, 2024. URL <https://kellerjordan.github.io/posts/muon/>.
- N. S. Keskar, D. Mudigere, J. Nocedal, M. Smelyanskiy, and P. T. P. Tang. On large-batch training for deep learning: Generalization gap and sharp minima. *arXiv preprint arXiv:1609.04836*, 2016.
- D. P. Kingma and J. Ba. Adam: A method for stochastic optimization. *arXiv preprint arXiv:1412.6980*, 2014.
- F. Kunstner, R. Yadav, A. Milligan, M. Schmidt, and A. Bietti. Heavy-tailed class imbalance and why adam outperforms gradient descent on language models. *arXiv preprint arXiv:2402.19449*, 2024.
- G. Lavezzi, K. Guye, and M. Ciarcià. Nonlinear programming solvers for unconstrained and constrained optimization problems: a benchmark analysis. *arXiv preprint arXiv:2204.05297*, 2022.
- Y. LeCun, L. Bottou, G. B. Orr, and K.-R. Müller. Efficient backprop. In *Neural networks: Tricks of the trade*, pages 9–50. Springer, 2002.
- M. Li, M. Soltanolkotabi, and S. Oymak. Gradient descent with early stopping is provably robust to label noise for overparameterized neural networks. In *International conference on artificial intelligence and statistics*, pages 4313–4324. PMLR, 2020a.

- X. Li, Q. Gu, Y. Zhou, T. Chen, and A. Banerjee. Hessian based analysis of sgd for deep nets: Dynamics and generalization. In *Proceedings of the 2020 SIAM International Conference on Data Mining*, pages 190–198. SIAM, 2020b.
- Z. Liao and M. W. Mahoney. Hessian eigenspectra of more realistic nonlinear models. *Advances in Neural Information Processing Systems*, 34:20104–20117, 2021.
- J. Lindeberg. Eine neue herleitung des exponentialgesetzes in der wahrscheinlichkeitsrechnung. *Mathematische Zeitschrift*, 15(1):211 – 225, 1922.
- A. Liu, B. Feng, B. Xue, B. Wang, B. Wu, C. Lu, C. Zhao, C. Deng, C. Zhang, C. Ruan, et al. Deepseek-v3 technical report. *arXiv preprint arXiv:2412.19437*, 2024.
- H. Liu, Z. Li, D. Hall, P. Liang, and T. Ma. Sophia: A scalable stochastic second-order optimizer for language model pre-training. *arXiv preprint arXiv:2305.14342*, 2023.
- J. Liu, J. Su, X. Yao, Z. Jiang, G. Lai, Y. Du, Y. Qin, W. Xu, E. Lu, J. Yan, et al. Muon is scalable for llm training. *arXiv preprint arXiv:2502.16982*, 2025.
- K. Lyu, Z. Li, and S. Arora. Understanding the generalization benefit of normalization layers: Sharpness reduction. *Advances in Neural Information Processing Systems*, 35:34689–34708, 2022.
- L. Maes, T. H. Zhang, A. Jolicoeur-Martineau, I. Mitliagkas, D. Scieur, S. Lacoste-Julien, and C. Guille-Escuret. Understanding adam requires better rotation dependent assumptions. *arXiv preprint arXiv:2410.19964*, 2024.
- V. Malinovskii, A. Panferov, I. Ilin, H. Guo, P. Richtárik, and D. Alistarh. Pushing the limits of large language model quantization via the linearity theorem. *arXiv preprint arXiv:2411.17525*, 2024.
- J. Martens and R. Grosse. Optimizing neural networks with kronecker-factored approximate curvature. In *International conference on machine learning*, pages 2408–2417. PMLR, 2015.
- V. A. Marčenko and L. A. Pastur. Distribution of eigenvalues for some set of random matrices. *Mathematics of the USSR-Sbornik*, 1(4):457, 1967.
- J. Mingo and R. Speicher. *Free Probability and Random Matrices*. Springer, 2017.
- W. Ormaniec, F. Dangel, and S. P. Singh. What does it mean to be a transformer? insights from a theoretical hessian analysis. *arXiv preprint arXiv:2410.10986*, 2024.
- V. Pappayan. The full spectrum of deepnet Hessians at scale: Dynamics with sgd training and sample size. *arXiv preprint arXiv:1811.07062*, 2018.
- V. Pappayan. Measurements of three-level hierarchical structure in the outliers in the spectrum of deepnet Hessians. *arXiv preprint arXiv:1901.08244*, 2019.
- V. Pappayan. Traces of class/cross-class structure pervade deep learning spectra. *The Journal of Machine Learning Research*, 21(1):10197–10260, 2020.
- N. Park and S. Kim. How do vision transformers work? *arXiv preprint arXiv:2202.06709*, 2022.
- L. Pastur. On random matrices arising in deep neural networks: Gaussian case. *Pure and Applied Functional Analysis*, 5(6):1395 – 1424, 2020.
- L. Pastur. Eigenvalue distribution of large random matrices arising in deep neural networks: Orthogonal case. *Journal of Mathematical Physics*, 63(6), 2022.
- L. Pastur and V. Slavin. On random matrices arising in deep neural networks: General i.i.d. case. *Random Matrices: Theory and Application*, 12(1), 2023.

- B. A. Pearlmutter. Fast exact multiplication by the hessian. *Neural computation*, 6(1):147–160, 1994.
- J. Pennington and Y. Bahri. Geometry of neural network loss surfaces via random matrix theory. In *International conference on machine learning*, pages 2798–2806. PMLR, 2017.
- Z. Qu, W. Gao, O. Hinder, Y. Ye, and Z. Zhou. Optimal diagonal preconditioning: Theory and practice. *arXiv preprint arXiv:2209.00809*, 2022.
- N. Roux, P.-A. Manzagol, and Y. Bengio. Topmoumoute online natural gradient algorithm. *Advances in neural information processing systems*, 20, 2007.
- L. Sagun, L. Bottou, and Y. LeCun. Eigenvalues of the hessian in deep learning: Singularity and beyond. *arXiv preprint arXiv:1611.07476*, 2016.
- L. Sagun, U. Evci, V. U. Guney, Y. Dauphin, and L. Bottou. Empirical analysis of the hessian of over-parametrized neural networks. *arXiv preprint arXiv:1706.04454*, 2017.
- A. R. Sankar, Y. Khasbage, R. Vigneswaran, and V. N. Balasubramanian. A deeper look at the hessian eigenspectrum of deep neural networks and its applications to regularization. In *Proceedings of the AAAI Conference on Artificial Intelligence*, volume 35, pages 9481–9488, 2021.
- S. P. Singh, G. Bachmann, and T. Hofmann. Analytic insights into structure and rank of neural network hessian maps. *Advances in Neural Information Processing Systems*, 34:23914–23927, 2021.
- R. Sun and Y. Ye. Worst-case complexity of cyclic coordinate descent:  $O(n^2)$  gap with randomized version. *Mathematical Programming*, 185:487–520, 2021.
- M. Talagrand. *Spin Glasses: A Challenge for Mathematicians. Cavity and Mean Field Models*. Springer, 2003.
- T. Tao. *Topics in random matrix theory*, volume 132. American Mathematical Soc., 2012.
- G. Team, P. Georgiev, V. I. Lei, R. Burnell, L. Bai, A. Gulati, G. Tanzer, D. Vincent, Z. Pan, S. Wang, et al. Gemini 1.5: Unlocking multimodal understanding across millions of tokens of context. *arXiv preprint arXiv:2403.05530*, 2024.
- H. Touvron, L. Martin, K. Stone, P. Albert, A. Almahairi, Y. Babaei, N. Bashlykov, S. Batra, P. Bhargava, S. Bhosale, et al. Llama 2: Open foundation and fine-tuned chat models. *arXiv preprint arXiv:2307.09288*, 2023.
- J. Wang, M. Wang, Z. Zhou, J. Yan, L. Wu, et al. The sharpness disparity principle in transformers for accelerating language model pre-training. *arXiv preprint arXiv:2502.19002*, 2025.
- Z. Wang, Z. Li, and J. Li. Analyzing sharpness along gd trajectory: Progressive sharpening and edge of stability. *Advances in Neural Information Processing Systems*, 35:9983–9994, 2022.
- M. Wei and D. J. Schwab. How noise affects the hessian spectrum in overparameterized neural networks. *arXiv preprint arXiv:1910.00195*, 2019.
- E. P. Wigner. On the distribution of the roots of certain symmetric matrices. *Annals of Mathematics*, 67(2): 325–327, 1958.
- L. Wu, Z. Zhu, et al. Towards understanding generalization of deep learning: Perspective of loss landscapes. *arXiv preprint arXiv:1706.10239*, 2017.
- Y. Wu, X. Zhu, C. Wu, A. Wang, and R. Ge. Dissecting hessian: Understanding common structure of hessian in neural networks. *arXiv preprint arXiv:2010.04261*, 2020.
- J. Yao, S. Zheng, and Z. Bai. *Large sample covariance matrices and high-dimensional data analysis*. 2015.

- Z. Yao, A. Gholami, Q. Lei, K. Keutzer, and M. W. Mahoney. Hessian-based analysis of large batch training and robustness to adversaries. *Advances in Neural Information Processing Systems*, 31, 2018.
- Z. Yao, A. Gholami, K. Keutzer, and M. W. Mahoney. Pyhessian: Neural networks through the lens of the hessian. In *2020 IEEE international conference on big data (Big data)*, pages 581–590. IEEE, 2020.
- G. Zhang, L. Li, Z. Nado, J. Martens, S. Sachdeva, G. Dahl, C. Shallue, and R. B. Grosse. Which algorithmic choices matter at which batch sizes? insights from a noisy quadratic model. *Advances in neural information processing systems*, 32, 2019.
- H. Zhang, C. Xiong, J. Bradbury, and R. Socher. Block-diagonal hessian-free optimization for training neural networks. *arXiv preprint arXiv:1712.07296*, 2017.
- Y. Zhang, C. Chen, T. Ding, Z. Li, R. Sun, and Z.-Q. Luo. Why transformers need adam: A hessian perspective. *arXiv preprint arXiv:2402.16788*, 2024a.
- Y. Zhang, C. Chen, Z. Li, T. Ding, C. Wu, D. P. Kingma, Y. Ye, Z.-Q. Luo, and R. Sun. Adam-mini: Use fewer learning rates to gain more. *arXiv preprint arXiv:2406.16793*, 2024b.



## Table of Contents for the Appendix

<b>A</b>	<b>More Discussions</b>	<b>21</b>
<b>B</b>	<b>More Numerical Results</b>	<b>22</b>
B.1	Results from [Collobert, 2004]	22
B.2	More Numerical Results under Different $C$	22
B.3	Results on the Frobenious Norm of Hessian Blocks.	25
B.4	Ablation Studies	25
B.5	Experimental Details	27
<b>C</b>	<b>Proof of Theorem 1</b>	<b>29</b>
<b>D</b>	<b>Proof of Theorem 2</b>	<b>35</b>
D.1	Proof for the Hidden-layer Hessian with CE Loss	35
D.2	Proof for the Hidden-layer Hessian with MSE Loss	41
D.3	Proof for the Output-layer Hessian with CE Loss	43

## A More Discussions

**Discussions on the cross-layer Hessian  $H_{wv}$  under CE Loss.** We now provide an explanation on the initial block-circular structure of  $H_{wv}$  under CE loss (i.e., Figure 3 (a)) and why it vanishes along training (i.e., Figure 3 (b-f)). We find that this phenomenon can be seen by a direct Hessian calculation. The cross-layer Hessian

$$\frac{\partial^2 \ell_{\text{CE}}}{\partial w_i \partial v_j^\top} = \begin{bmatrix} 0 & \cdots & a_{1,i} & 0 & \cdots & 0 \\ \vdots & \ddots & \vdots & \vdots & \ddots & \vdots \\ 0 & \cdots & a_{d,i} & 0 & \cdots & 0 \end{bmatrix} \in \mathbb{R}^{d \times m} \quad (37)$$

is a matrix with one non-zero column at position  $i$  with  $a_{d',i} = -\frac{1}{N} \sum_{n=1}^N \sum_{c=1}^C (\delta_{y_n,c} - p_{n,c}) v_{c,i} \mathbb{I}(w_i^\top x_n \geq 0) x_{n,d'}, d' \in [d]$ . This explains the initial block-circulant structure. As the training goes,  $(\delta_{y_n,c} - p_{n,c}) \rightarrow 0$  and the block-circulant structure disappears.

**More discussions on our theory.** For completeness, we provide discuss more discussions on our theory, including some clarifications and future directions.

- **First**, our theory requires  $N$  and  $d$  proportionally grows to infinity, which is also known as “the proportional asymptotic regime”. We believe this regime is meaningful. First, the proportional asymptotic regime is standard in random matrix theory (e.g., see [Wigner, 1958, Tao, 2012]). Second, in the proportional asymptotic regime, we obtained new insights into the Hessian structure (e.g., the effect of large  $C$ ) and our insights matched a wide range of finite-dimensional experiments. We will try to extend our analysis to other regimes such as non-asymptotic or over-parameterized regime in the future.
- **Second**, our theory focuses on random initialization, and it does not cover the whole training process. Interestingly, we numerically find that the block-diagonal Hessian structure remains throughout the training process (see Figure 2 and 3). This suggests that block-diagonal structure continuously influences the behavior of optimizers, *not just at initialization*. It is possible to extend our theory to the whole training process, but it requires substantially new mathematical tools and we leave as a future direction.
- **Third**, our theory focuses on linear and 1-hidden-layer networks, and it currently does not cover deeper models. We believe our theory on linear and 1-hidden-layer networks is meaningful since it already provides new insights, e.g., the effect of large  $C$ . It is possible to extend the results to deeper models by recursively applying our decoupling methods, but substantial effort is needed. For deeper models, we conjecture the block-diagonal structure will be primarily driven by the number of output neurons in each layer (a.k.a., the “fan-out dimension”). It is also intriguing to explore other potential factors that will reshape the Hessian structure of deep models. We leave it as a future direction.
- **Forth**, our theory focuses on block-wise Frobenious norm instead of block-wise spectrum. We focus on Frobenious norm is it is more relevant to our current goal: justifying the Hessian structure. One future direction is to theoretically characterize the block-wise spectrum and provide guidance for optimizer design. Zhang et al. [2024a,b], Wang et al. [2025] did some initial attempts in this direction, but these works focused on numerical exploration and did not establish rigorous theory on characterizing block-wise spectrum. Based on our theory so far, it is possible to theoretically analyze the block-wise spectrum by more fine-grained analysis of the Steiltjes transform of the limit eigenvalue distribution, which we leave as a future direction.

## B More Numerical Results

Now we present the numerical results. We first re-state the experiments in [Collobert, 2004] and then present our numerical results. All experimental details of our results are explained in Appendix B.5.

### B.1 Results from [Collobert, 2004]

In Figure 5, we restate Figure 7.3 and 7.5 from [Collobert, 2004]. The authors reported block-diagonal Hessian structure for a 1-hidden-layer network with CE loss on a binary-classification dataset. Such structure disappeared when changing to MSE loss.

We make two comments here. First, for MSE loss in Figure 5 (b), it is not surprising to see non-block-diagonal structure since our theory states that such structure arises when  $C \rightarrow \infty$ , while  $C$  only equals to 2 here. Second, for CE loss in Figure 5 (a), the near-block-diagonal structure arises despite the small  $C$ . This is not covered in our theory since we focus on large  $C$ . Nevertheless, it does not contradict our theory, either. We leave the exploration of binary classification with CE loss as a future direction.

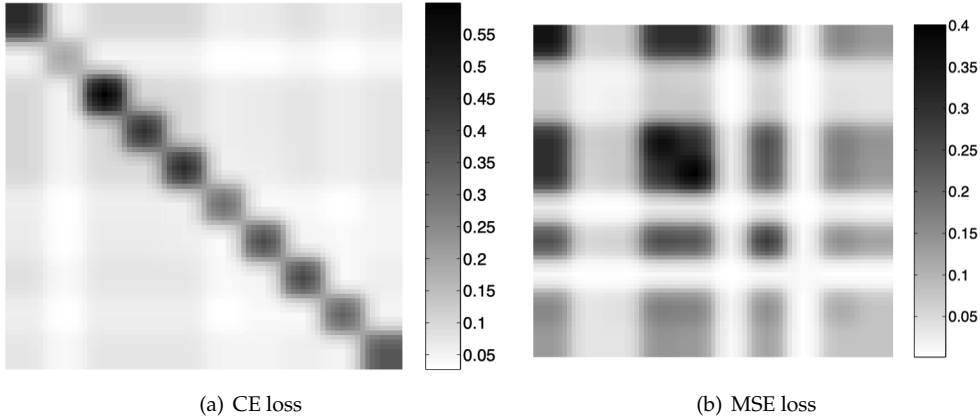


Figure 5: (a,b): Figure 7.3 and 7.5 from [Collobert, 2004]. . The Hessian matrices of a 1-hidden-layer network with 10 hidden neurons on the Forest binary-classification dataset. For CE loss, the Hessian is computed after 1 iteration. For MSE loss, the Hessian is computed after 10 iterations.

### B.2 More Numerical Results under Different $C$

We now present more numerical results under different  $C$  to support our theory. In Figure 4 in Section 7, we present the numerical results for **Case 2**. Now we present more results for **Case 1, 3, and 4**. We use the same random initialization and Gaussian synthetic dataset with  $C$  classes as in Section 7.

**Case 1: linear models with MSE loss.** In Figure 6, we present the Hessian of linear models under MSE loss. By the calculation of (3) in Section 4, the Hessian is strictly block-diagonal. The numerical results match the calculation.

**Case 3 and 4: 1-hidden-layer networks with MSE and CE loss.** In Figure 7 and 8, we consider 1-hidden-layer network at random initialization. We present the hidden-layer Hessian  $H_{ww}$  and output weights  $H_{vv}$  to see if they match our theoretical prediction. It can be seen that the block-diagonal structure becomes clearer as the number of classes  $C$  increases, which matches the theoretical prediction. These results hold for both MSE and CE loss.

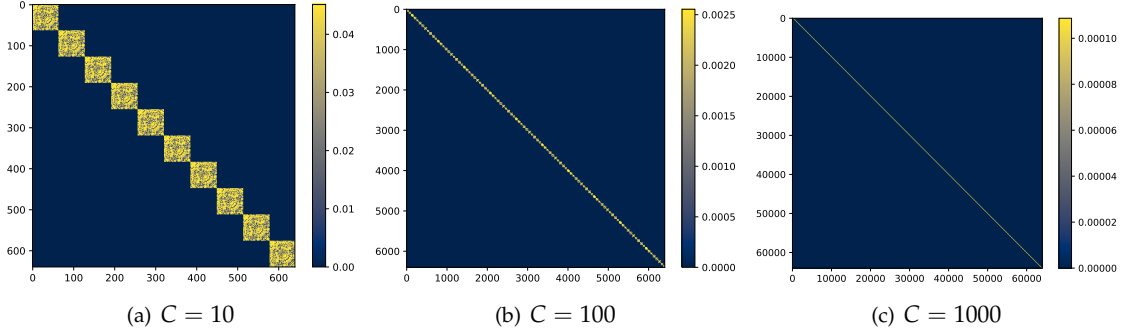


Figure 6: **(a-c):** The Hessian of **Case 1: linear models with MSE loss**. We use the same random initialization and Gaussian synthetic dataset with  $C$  classes as in Section 7. We observe that the block-diagonal Hessian structure arises for all  $C$ . This is because the off-diagonal blocks are strictly zero in this case (see (3)).

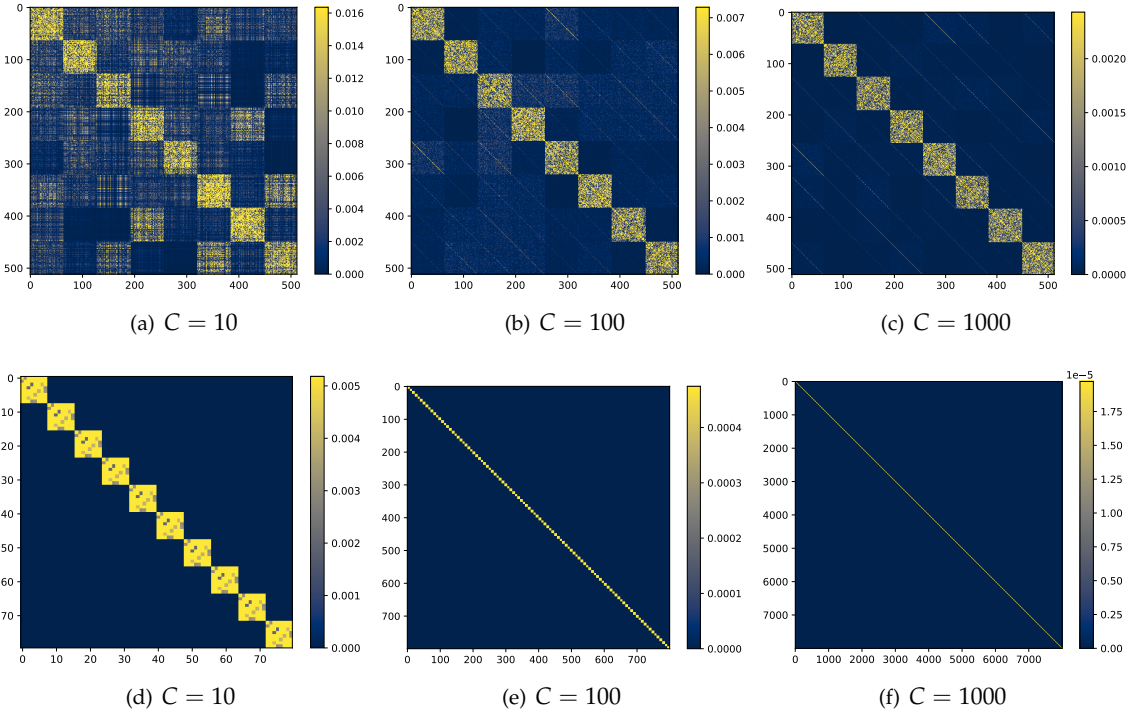


Figure 7: The Hessian in **Case 3: 1-hidden-layer network with MSE loss**. The network has 8 hidden neurons. We use the same random initialization and Gaussian synthetic dataset with  $C$  classes as in Section 7. **(a, b, c):** The hidden-layer Hessian  $H_{ww}$ . **(e, f, g):** The output-layer Hessian  $H_{vv}$ . We observe that the block-diagonal Hessian structure in  $H_{ww}$  becomes clearer as  $C$  increases.  $H_{vv}$  is always strictly block-diagonal, as expected by the calculations in (9).

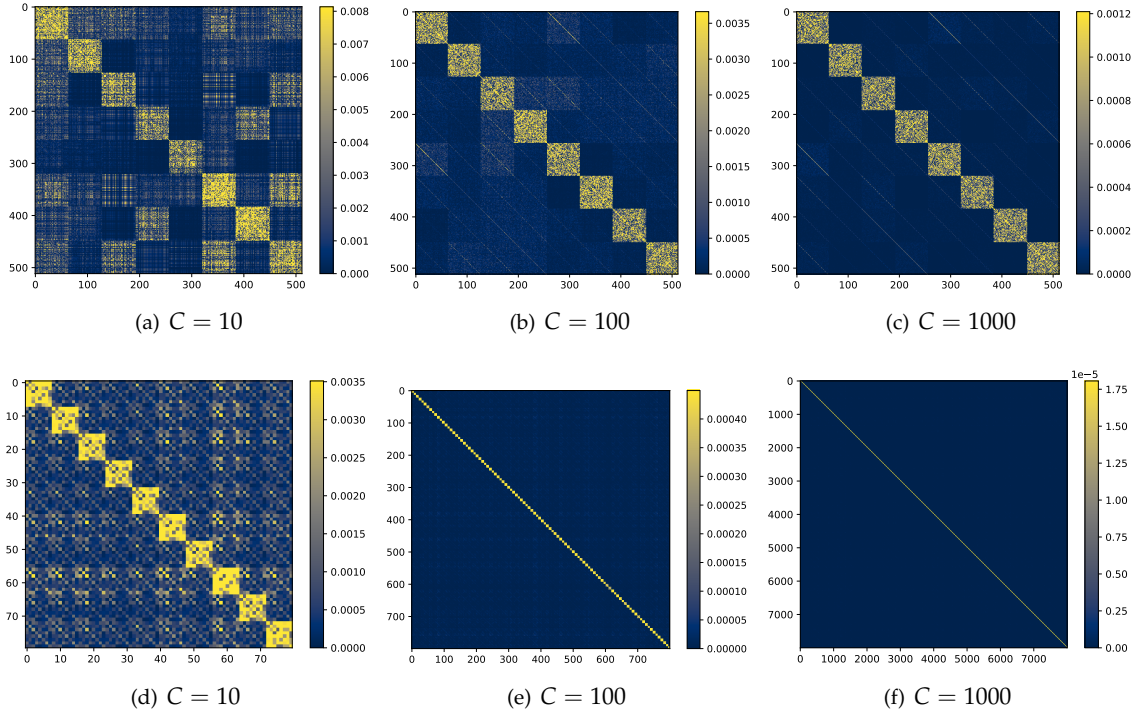


Figure 8: The Hessian in **Case 4: 1-hidden-layer network with CE loss**. The network has 8 hidden neurons. We use the same random initialization and Gaussian synthetic dataset with  $C$  classes as in Section 7. **(a, b, c)**: The hidden-layer Hessian  $H_{ww}$ . **(e, f, g)**: The output-layer Hessian  $H_{vv}$ . For both  $H_{ww}$  and  $H_{vv}$ , we observe that the block-diagonal Hessian structure becomes clearer as  $C$  increases.



### B.3 Results on the Frobenious Norm of Hessian Blocks.

Similar to Figure 4, which focuses on the linear model with CE loss, we now further conduct similar experiments on 1-hidden-layer networks with CE loss. We introduce the quantities as follows.

$$\tilde{H}_{11}^{\text{CE}} := \frac{1}{d} \left\| \frac{\partial^2 \ell_{\text{CE}}(W, V)}{\partial w_1 \partial w_1^\top} \right\|_F^2, \quad \tilde{H}_{12}^{\text{CE}} = \frac{C}{d} \left\| \frac{\partial^2 \ell_{\text{CE}}(W, V)}{\partial w_1 \partial w_2^\top} \right\|_F^2, \quad \tilde{r} = \frac{\left\| \frac{\partial^2 \ell_{\text{CE}}(W, V)}{\partial w_1 \partial w_2^\top} \right\|_F^2}{\left\| \frac{\partial^2 \ell_{\text{CE}}(W, V)}{\partial w_2 \partial w_2^\top} \right\|_F^2}$$

The results are shown in Figure 9. We find that the  $\tilde{H}_{11}^{\text{CE}}$  and  $\tilde{H}_{12}^{\text{CE}}$  approach the green lines, which are their theoretical limits in Theorem 2. Further,  $\tilde{r}$  decays to 0 with the same rate as we predicted in Theorem 2. These results support the results in Theorem 2.

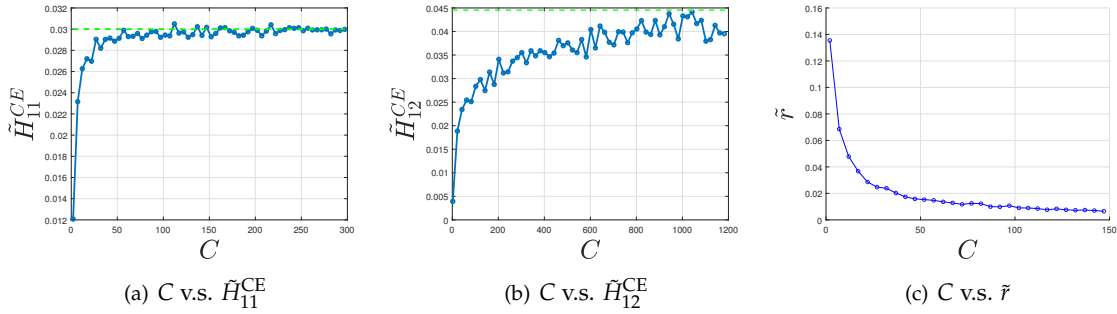


Figure 9: (a,b): The evolution of  $\tilde{H}_{11}^{\text{CE}}$  and  $\tilde{H}_{12}^{\text{CE}}$  as  $C$  increases. We find that the  $\tilde{H}_{11}^{\text{CE}}$  and  $\tilde{H}_{12}^{\text{CE}}$  approach the green lines, which are their theoretical limits in Theorem 2. (c):  $\tilde{r}$  decays to 0 with the same rate as we predicted in Theorem 2.

### B.4 Ablation Studies

We now conduct some ablation studies on other Factors contributing to the Hessian structure. Li et al. [2020a] argue that  $K$ -feature-clustered dataset will bring  $K$ -ranked Jacobian. We now investigate how this relates to the block-diagonal Hessian structure.

We construct the  $K$ -clustered dataset following the descriptions in [Li et al., 2020a]: “assume that the input  $x_n \in \mathbb{R}^d$  come from  $K$  clusters which are located on the unit Euclidean ball; assume our dataset consists of  $C \leq K$  classes where each class can be composed of multiple clusters.”. We attach the code for data generation below.

We present the results in Figure 10 and 11. We report two findings here: (1) When # classes  $C = 2$  is small, the Hessian has no block-diagonal structure, regardless of # clusters  $K$ . (2) When  $C = 500$  is large, the block-diagonal pattern appears regardless of # clusters  $K$ . This suggests that large  $C$  plays a more critical role than  $K$  in the Hessian structure.

```

1
2 def generate_cluster_data(n_total, n_classes, n_clusters, input_dim):
3     # Generate clustered synthetic data for specified dimensions
4     # used for ablation study
5     # n_total is the total number of samples
6     # n_classes is the number of classes (smaller than n_clusters)
7     # input_dim is the dimension of the data
8     # raise error if n_cluster is larger than n_classes
9     assert n_classes <= n_clusters, f"n_cluster = {n_classes} is not smaller than n_classes = {n_clusters}"
10
11     # n_samples_per_class is the number of samples per class
12     x = []

```

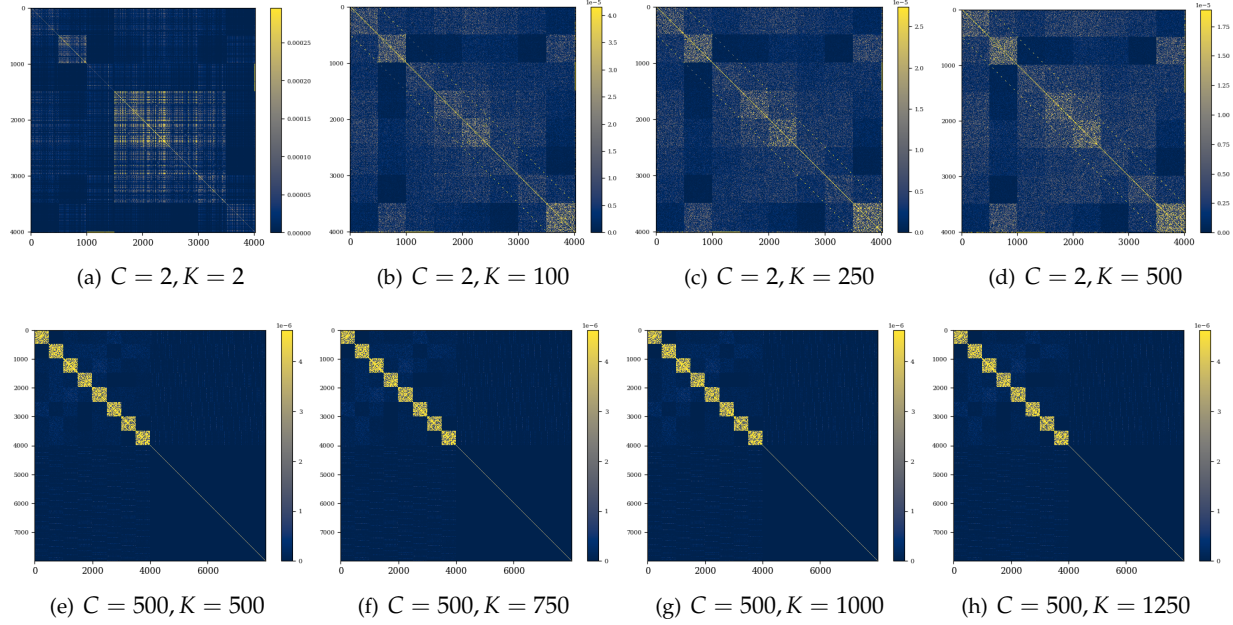


Figure 10: Ablation studies for the effect of # cluster  $K$  on the Hessian structure. We construct  $K$ -clustered dataset following the setup in [Li et al. 19]: “assume that the input  $x_n \in \mathbb{R}^d$  come from  $K$  clusters which are located on the unit Euclidean ball; assume our dataset consists of  $C \leq K$  classes where each class can be composed of multiple clusters.” We use MSE loss and random initialization. We find that: **(a-d)**: When  $C = 2$  is small, the Hessian has no clear structure, regardless of # clusters  $K$ . **(e-h)**: When  $C = 500$  is large, the block-diagonal pattern appears regardless of # clusters  $K$ . This suggests that large  $C$  plays a more critical role than  $K$  in the Hessian structure.

```

13  y = []
14  n_cluster_per_class = n_clusters // n_classes
15  n_samples_per_cluster = n_total // n_clusters
16  cluster_idx = 0
17  for class_idx in range(n_classes):
18
19      for _ in range(n_cluster_per_class):
20          cluster_idx += 1
21          if input_dim == 2:
22              center = np.array([np.cos(2 * np.pi * cluster_idx / n_clusters), np.sin(2 *
23  np.pi * (cluster_idx) / n_clusters)]) * 5 # Class centers on a circle
24          else:
25              #extend the 2D case to higher dimension
26              # Generate random points in higher dimensions and project onto hypersphere
27              center = np.random.randn(input_dim)
28              # Normalize to create a unit vector (point on unit hypersphere)
29              center = center / np.linalg.norm(center)
30
31      cluster_samples = np.random.randn(n_samples_per_cluster, input_dim) * 0.05 +
32  center # Add some noise
33  X.append(cluster_samples)
34  # assign label
35  y.extend([class_idx]*n_samples_per_cluster)
36
37  X = np.vstack(X) # Combine all class samples
38  y = np.array(y) # Convert labels to a NumPy array
39  return X, y

```

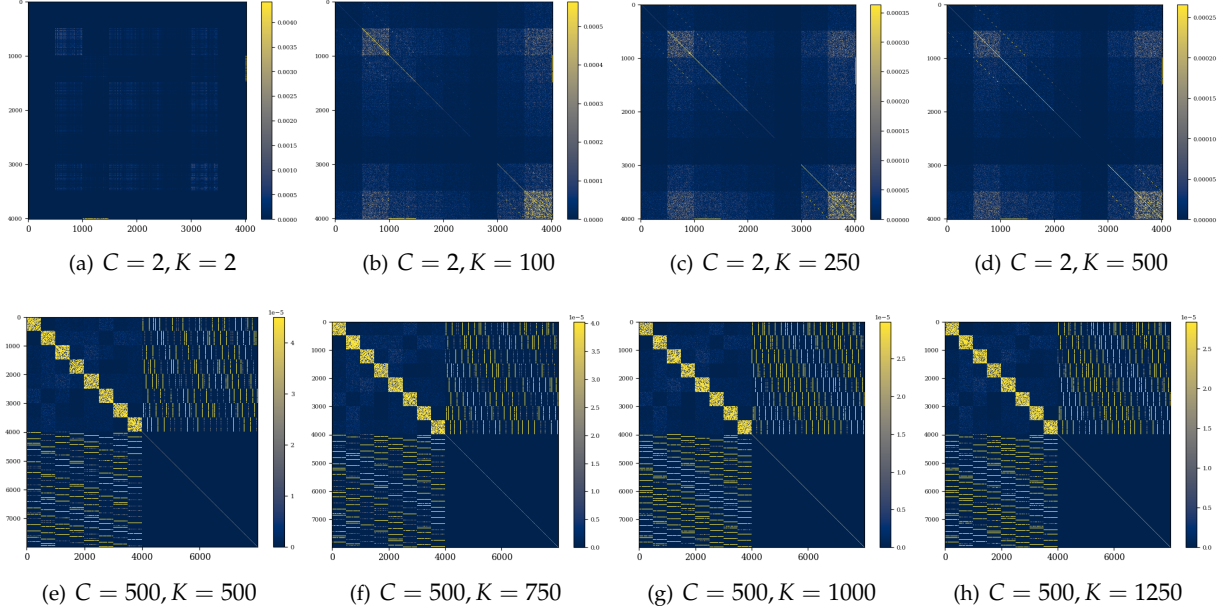


Figure 11: Same ablation studies as in Figure 10 except that we change to CE loss. We find that: **(a-d)**: When  $C = 2$  is small, the Hessian has no clear structure, regardless of # clusters  $K$ . **(e-h)**: When  $C = 500$  is large, the block-diagonal pattern appears in  $H_{ww}$  and  $H_{vv}$  regardless of # clusters  $K$ . This suggests that large  $C$  plays a more critical role than  $K$  in the Hessian structure.

## B.5 Experimental Details

Now we present the experimental details. All experiments are conducted on one NVIDIA V100 GPU.

**Implementation details for Figure 1.** We calculate Hessian on a randomly selected 128 images from CIFAR-100. We calculate Hessian via two backpropagation passes [Pearlmutter, 1994], our code is modified based on open-source Hessian-vector-product implementation<sup>3</sup>. We consider a 1-hidden-layer network with ReLU activation, 8 hidden neurons, and 100 output neurons at random initialization. For all Hessian matrices reported in the paper, we report the absolute value of each Hessian entry.

**Implementation details for Section 3.1 .** We first introduce the implementation details for the synthetic dataset used in both Section 3.1 and Appendix B. We build the dataset following Assumption 1 and we assign the label randomly. We attach the code for data generation here. In Section 3.1, we use `input_dim = 500, n_classes = 500, n_samples_per_class = 10`.

```

1 def generate_gaussian_data(n_samples_per_class, n_classes, input_dim):
2     X = []
3     y = []
4     for i in range(n_classes):
5         class_samples = np.random.randn(n_samples_per_class, input_dim)
6         X.append(class_samples)
7         y.extend([i] * n_samples_per_class) # not used
8
9     X = np.vstack(X)
10    y = np.array(y)
11    return X, y

```

<sup>3</sup><https://github.com/zyushun/hessian-spectrum>

Now we describe the model configurations in Section 3.1. We use 1-hidden-layer networks with 8 hidden neurons and ReLU activation. All the models are trained using Adam with  $\text{lr} = 1\text{e-}4$  with cosine annealing schedule with  $\text{lr\_min} = 0$ . We train the models until convergence. The loss curves are reported in Figure 12.

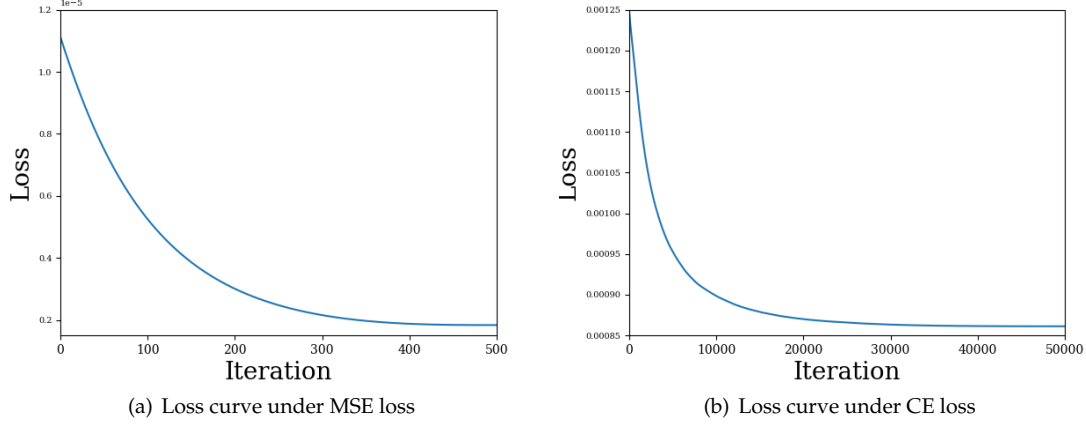


Figure 12: The loss curve of the models trained in Section 3.1. We train the models until convergence.

**Implementation details for Section 7 and Appendix B.** For these experiments, we use the same setups as in Section 3.1. We use  $\text{input\_dim} = 64$ ,  $\text{n\_samples\_per\_class} = 1$ , and the total number of samples  $N = C$ .

**Implementation details for Figure 4 and Figure 9.** For Figure 4, we consider  $N = 1000, d = 1000$ . For each  $C$ , we randomly sample 1000 realization of  $H_{11}, H_{12}$  and report their Frobenious norms. We use  $10^6$  repetitions in Monte-Carlo integrals. For Figure 9, we use  $N = 300, d = 300$ , and 200 repetitions for each  $C$ .

## C Proof of Theorem 1

Before delving into the proof, we first present the functions  $g_{ii}$ ,  $g_{ij}$  in Theorem 1. Let  $\mathbf{z}_C = (Z_1, \dots, Z_C) \sim \mathcal{N}_C(0, I_C)$ , define

$$h_1(\mathbf{z}_C) = \frac{e^{Z_1}}{\sum_{l=1}^C e^{Z_l}} \left( 1 - \frac{e^{Z_1}}{\sum_{l=1}^C e^{Z_l}} \right), \quad h_2(\mathbf{z}_C) = \frac{e^{Z_1+Z_2}}{\left( \sum_{l=1}^C e^{Z_l} \right)^2},$$

then

$$g_{ii}(\gamma, C) := \gamma \mathbf{E}[h_1(\mathbf{z}_C)^2] + (\mathbf{E}[h_1(\mathbf{z}_C)])^2, \quad g_{ij}(\gamma, C) := \gamma \mathbf{E}[h_2(\mathbf{z}_C)^2] + (\mathbf{E}[h_2(\mathbf{z}_C)])^2.$$

We now introduce some notations that will be used in the proof. Let  $\tilde{X}_N = (\tilde{x}_1, \dots, \tilde{x}_N) \in \mathbb{R}^{d \times N}$  be an independent copy of  $X_N \in \mathbb{R}^{d \times N}$ . Denote

$$\begin{aligned} p_i(x) &:= \frac{\exp(v_i^\top x)}{\sum_{c=1}^C \exp(v_c^\top x)}, \quad x \in \mathbb{R}^d, \\ \alpha_n &= p_i(x_n)(1 - p_i(x_n)), \quad \Lambda_n = \text{diag}(\alpha_1, \dots, \alpha_N), \\ \tilde{\alpha}_n &= p_i(\tilde{x}_n)(1 - p_i(\tilde{x}_n)), \quad \tilde{\Lambda}_n = \text{diag}(\tilde{\alpha}_1, \dots, \tilde{\alpha}_N), \\ \beta_n &= -p_i(x_n)p_j(x_n), \quad \Gamma_n = \text{diag}(\beta_1, \dots, \beta_N), \\ \tilde{\beta}_n &= -p_i(\tilde{x}_n)p_j(\tilde{x}_n), \quad \tilde{\Gamma}_n = \text{diag}(\tilde{\beta}_1, \dots, \tilde{\beta}_N). \end{aligned}$$

To ease notations, we write  $H_{ii} = \frac{\partial^2 \ell_{\text{CE}}(V)}{\partial v_i \partial v_i^\top} \in \mathbb{R}^{d \times d}$ ,  $H_{ij} = \frac{\partial^2 \ell_{\text{CE}}(V)}{\partial v_i \partial v_j^\top} \in \mathbb{R}^{d \times d}$ , then

$$H_{ii} = \frac{1}{N} X_N \Lambda_N X_N^\top, \quad H_{ij} = \frac{1}{N} X_N \Gamma_N X_N^\top.$$

Similarly, we define

$$\tilde{H}_{ii} = \frac{1}{N} X_N \tilde{\Lambda}_N X_N^\top, \quad \tilde{H}_{ij} = \frac{1}{N} X_N \tilde{\Gamma}_N X_N^\top.$$

Now we prove Theorem 1. The proof consists of two steps. First, we “decouple”  $X_N$ ,  $\Lambda_N$  and  $\Gamma_N$ . That is, we prove that  $H_{ii}$  and  $\tilde{H}_{ii}$  share the same Stieltjes transform as  $N$  and  $d$  grow proportionally to infinity. Similarly for  $H_{ij}$  and  $\tilde{H}_{ij}$ . Second, with the help of Theorem 3, we find the second moments of limit eigenvalue distribution of  $\tilde{H}_{ii}$  and  $\tilde{H}_{ij}$ . Recall that the second moment is the Frobenious norm, so the proof is concluded.

We now “decouple”  $X_N$ ,  $\Lambda_N$  and  $\Gamma_N$  using the following Lemma 1.

**Lemma 1.** For any  $z \in \mathbb{C}^+$ , as  $d, N \rightarrow \infty$ ,  $d/N \rightarrow \gamma \in (0, +\infty)$ , it holds almost surely that

$$s_{H_{ii}}(z) - s_{\tilde{H}_{ii}}(z) = O\left(N^{-\frac{1}{2}}\right), \quad (38)$$

$$s_{H_{ij}}(z) - s_{\tilde{H}_{ij}}(z) = O\left(N^{-\frac{1}{2}}\right). \quad (39)$$

*Proof.* Here, we only present the proof for  $s_{H_{ii}}$ . The proof for  $s_{H_{ij}}$  is done following the same procedure.

For  $t \in [0, 1]$ , let

$$X_N(t) = \sqrt{t} X_N + \sqrt{1-t} \tilde{X}_N.$$

Then  $X_N(t) = (x_1(t), \dots, x_N(t)) \in \mathbb{R}^{d \times N}$ , where

$$x_n(t) = \sqrt{t} x_n + \sqrt{1-t} \tilde{x}_n, \quad n \in [N].$$

Denote

$$\alpha_n(t) = p_i(x_n(t)) [1 - p_i(x_n(t))],$$

$$\Lambda_N(t) = \text{diag}(\alpha_1(t), \dots, \alpha_N(t)),$$

$$H_{ii}(t) = \frac{1}{N} X_N \Lambda_N(t) X_N^\top,$$

$$\mathcal{G}_N(z, t) = (H_{ii}(t) - z I_{d \times d})^{-1} \in \mathbb{R}^{d \times d},$$

By the definition of  $s_{H_{ii}}$ , it is easy to see that  $s_{H_{ii}} = \frac{1}{d} \text{tr}(\mathcal{G}_N(z, t))$ .

We first prove that  $s_{H_{ii}}(z), s_{\tilde{H}_{ii}}(z)$  concentrate around their mean. By treating  $s_{H_{ii}}(z), s_{\tilde{H}_{ii}}(z)$  as Lipchitz functions of the Gaussian vectors  $v_1, \dots, v_C, x_1, \dots, x_N$ , we have the following results from Talagrand's inequality,

$$\mathbf{P}(|s_{H_{ii}}(z) - \mathbf{E}[s_{H_{ii}}(z)]| \geq t) \leq c_1 e^{-p c_2 t^2},$$

$$\mathbf{P}(|s_{\tilde{H}_{ii}}(z) - \mathbf{E}[s_{\tilde{H}_{ii}}(z)]| \geq t) \leq \tilde{c}_1 e^{-\tilde{d} \tilde{c}_2 t^2},$$

where  $t > 0$  and constants  $c_1, c_2, \tilde{c}_1, \tilde{c}_2 > 0$ . Then from the Borel-Cantelli Lemma,

$$\begin{aligned} s_{H_{ii}}(z) - \mathbf{E}[s_{H_{ii}}(z)] &\xrightarrow{a.s.} 0, \\ s_{\tilde{H}_{ii}}(z) - \mathbf{E}[s_{\tilde{H}_{ii}}(z)] &\xrightarrow{a.s.} 0. \end{aligned} \tag{40}$$

Now we prove that

$$\delta_N(z) = \mathbf{E}[s_{H_{ii}}(z)] - \mathbf{E}[s_{\tilde{H}_{ii}}(z)] = O(N^{-\frac{1}{2}}). \tag{41}$$

Recall for any function  $A(t)$  valued in invertible matrices, we have

$$\frac{d}{dt} A^{-1}(t) = -A^{-1}(t) \frac{d}{dt} A(t) A^{-1}(t). \tag{42}$$

Then we have

$$\begin{aligned} \delta_N(z) &= \frac{1}{d} \mathbf{E}[\text{tr}(\mathcal{G}_N(z, 1) - \mathcal{G}_N(z, 0))] \\ &= \frac{1}{d} \int_0^1 \frac{d}{dt} \mathbf{E}[\text{tr}(\mathcal{G}_N(z, t))] dt \\ &= \frac{1}{d} \int_0^1 \frac{d}{dt} \mathbf{E}[\text{tr}((H_{ii}(t) - z I_{d \times d})^{-1})] dt \\ &\stackrel{(42)}{=} -\frac{1}{d} \int_0^1 \mathbf{E}\left[\text{tr}\left(\mathcal{G}_N(z, t)^2 \frac{d}{dt} H_{ii}(t)\right)\right] dt \\ &= -\frac{1}{dN} \int_0^1 \mathbf{E}\left[\text{tr}\left(X_N^\top \mathcal{G}_N(z, t)^2 X_N \frac{d}{dt} \Lambda_N(t)\right)\right] dt, \end{aligned} \tag{43}$$

Define

$$\Delta_N(z) = -\frac{1}{dN} \sum_{n=1}^N \int_0^1 \mathbf{E}\left[(X_N^\top \mathcal{G}_N(z, t) X_N)_{nn} \frac{d}{dt} \alpha_n(t)\right] dt,$$

then we have

$$\delta_N(z) \stackrel{(42)}{=} \frac{d}{dz} \Delta_N(z).$$

We now bound  $\delta_N(z)$  by bounding  $\Delta_N(z)$ . We first define  $D_\zeta = \{z | z \in \mathbb{C}^+, \Im z \geq \zeta > 0\}$ , where  $\Im z$  denotes the image part of  $z$ . Since all eigenvalues of  $H_{ii}(t) \in \mathbb{R}$ ,  $\Delta_N(z)$  is an analytic function in  $D_\zeta$ . Based on Cauchy's integral formula, for any  $z \in D_\zeta$  and arbitrary circle  $\gamma \in D_\zeta$  containing  $z$ , we have

$$\delta_N(z) = \frac{d}{dz} \Delta_N(z) = \frac{1}{2\pi i} \oint_\gamma \frac{\Delta_N(s)}{(s-z)^2} ds.$$

Then we have:



$$\delta_N(z) \leq \frac{\text{length}(\gamma)}{2\pi} \max_{s \in \gamma} \frac{1}{(s-z)^2} \max_{s \in \gamma} |\Delta_N(s)| \leq \text{Const.} \max_{z \in D_\zeta} |\Delta_N(z)|,$$

where Const. is some positive constant. Now we aim to prove the following equation:

$$\max_{z \in D_\zeta} |\Delta_N(z)| = O(N^{-\frac{1}{2}}) \quad (44)$$

If this is true, then  $|\delta_N(z)| = O(N^{-\frac{1}{2}})$  for all  $z \in D_\zeta$ . Let  $\zeta \rightarrow 0$ , we will get  $|\delta_N(z)| = O(N^{-\frac{1}{2}})$ , which converges to 0 (pointwise) as  $N \rightarrow \infty$ . In the following analysis, we aim to prove (44). We first rewrite  $\Delta_N(z)$  as follows.

$$\Delta_N(z) = -\frac{1}{2dN} \sum_{n=1}^N \sum_{l=1}^C \sum_{s=1}^d \int_0^1 \mathbf{E} \left[ x_n^\top \mathcal{G}_N(z, t) x_n B_{ln}(t) V_{ls} \left( \frac{X_{sn}}{\sqrt{t}} - \frac{\tilde{X}_{sn}}{\sqrt{1-t}} \right) \right] dt, \quad (45)$$

where

$$B_{ln}(t) = \left(1 - 2p_i(x_n(t))\right) p_i(x_n(t)) \left(\delta_{il} - p_l(x_n(t))\right),$$

and  $X_{sn}$  is the abbreviation for the  $(s, n)$ -th entry in  $X_N$ . Similar abbreviation also applies to  $\tilde{X}_{sn}$ . We define  $\delta_{il} = 1$  if  $i = l$  and  $\delta_{il} = 0$  if otherwise. Note that trivial upper bound of (45) does not vanish with  $N$ . To better evaluate the expectation in (45), we will use Stein's Lemma

$$\mathbf{E}[Zf(Z)] = \mathbf{E}[f'(Z)] \quad (46)$$

for  $Z \sim \mathcal{N}(0, 1)$  and differentiable function  $f : \mathbb{R} \rightarrow \mathbb{C}$  with sub-exponential decay at infinity. Then we have

$$\Delta_N(z) = -\frac{1}{2dN} \sum_{n=1}^N \sum_{l=1}^C \sum_{s=1}^d \int_0^1 \left( \frac{1}{\sqrt{t}} \mathbf{E} \left[ \frac{\partial F_N(n, l, z, t)}{\partial X_{sn}} V_{ls} \right] - \frac{1}{\sqrt{1-t}} \mathbf{E} \left[ \frac{\partial F_N(n, l, z, t)}{\partial \tilde{X}_{sn}} V_{ls} \right] \right) dt, \quad (47)$$

$$F_N(n, l, z, t) = x_n^\top \mathcal{G}_N(z, t) x_n B_{ln}(t),$$

Write  $\mathcal{G}_N = \mathcal{G}_N(z, t)$  for short, then

$$\begin{aligned} & \frac{1}{\sqrt{1-t}} \mathbf{E} \left[ \frac{\partial F_N(n, l, z, t)}{\partial \tilde{X}_{sn}} V_{ls} \right] - \frac{1}{\sqrt{t}} \mathbf{E} \left[ \frac{\partial F_N(n, l, z, t)}{\partial X_{sn}} V_{ls} \right] \\ &= \frac{2}{\sqrt{t}} \mathbf{E} \left[ \frac{\delta_{ns}}{N} B_{ln}(t) V_{ls} \alpha_n(t) (\mathcal{G}_N x_n)_n (\mathcal{G}_N x_n)^\top x_n - B_{ln}(t) V_{ls} (\mathcal{G}_N x_n)_s \right]. \end{aligned} \quad (48)$$

Hence  $\Delta_N(z) = \Delta_{N,1}(z) - \Delta_{N,2}(z)$ , where

$$\begin{aligned} \Delta_{N,1}(z) &= \frac{1}{dN^2} \sum_{l=1}^C \sum_{n=1}^{\min(d, N)} \int_0^1 \mathbf{E} \left[ B_{ln}(t) V_{ln} \alpha_n(t) (\mathcal{G}_N x_n)_n (\mathcal{G}_N x_n)^\top x_n \right] \frac{dt}{\sqrt{t}}, \\ \Delta_{N,2}(z) &= \frac{1}{dN} \sum_{n=1}^N \sum_{l=1}^C \sum_{s=1}^d \int_0^1 \mathbf{E} [B_{ln}(t) V_{ls} (\mathcal{G}_N x_n)_s] \frac{dt}{\sqrt{t}}. \end{aligned} \quad (49)$$

From Hölder's inequality,

$$\begin{aligned} \mathbf{E}[|V_{ln} (\mathcal{G}_N x_n)_n (\mathcal{G}_N x_n)^\top x_n|] &\leq \left( \mathbf{E}[V_{ln}^4] \right)^{\frac{1}{4}} \left( \mathbf{E}[(\mathcal{G}_N x_n)_n^2] \right)^{\frac{1}{2}} \left( \mathbf{E}[(\mathcal{G}_N x_n)^\top x_n]^4 \right)^{\frac{1}{4}}, \\ \mathbf{E}[|V_{ls} (\mathcal{G}_N x_n)_s|] &\leq \left( \mathbf{E}[V_{ls}^2] \right)^{\frac{1}{2}} \left( \mathbf{E}[(\mathcal{G}_N x_n)_s^2] \right)^{\frac{1}{2}}. \end{aligned}$$

Recall that

$$|B_{ln}(t)| \leq \frac{1}{9}, \quad |\alpha_n(t)| \leq \frac{1}{4}, \quad V_{ls} \sim \mathcal{N}(0, \frac{1}{d}),$$

$$\|\mathcal{G}_N\| \leq \min_{z \in D_\zeta} \left| \frac{1}{\lambda_{H_{ii}} - z} \right| \leq \min_{z \in D_\zeta} \frac{1}{\Im(z)} \leq \frac{1}{\zeta},$$

$$\mathbf{E}[(\mathcal{G}_N x_n)_s^2] = \frac{1}{d} \mathbf{E}[\|\mathcal{G}_N x_n\|^2] \leq \mathbf{E}[\|\mathcal{G}_N\|^2] \leq \frac{1}{\zeta},$$

we have

$$|\Delta_{N,1}(z)| \leq \frac{3^{1/4} C (\mathbf{E}[\|x_n\|^8])^{1/4}}{18N^2 d^{1/2} \zeta^2}, \quad |\Delta_{N,2}(z)| \leq \frac{2C}{9d^{1/2} \zeta}.$$

As  $d, N \rightarrow \infty$ ,  $d/N \rightarrow \gamma > 0$ , we have the following equations for any  $z \in D_\zeta$

$$|\Delta_{N,1}(z)| = O(N^{-3/2}), \quad |\Delta_{N,2}(z)| = O(N^{-1/2}).$$

Set  $\zeta \rightarrow 0$ , then we have (44) and hence (41), together with (40) implying

$$s_{H_{ii}}(z) - s_{\tilde{H}_{ii}}(z) = O(N^{-1/2}) \quad a.s., \forall z \in \mathbb{C}^+.$$

The proof for  $s_{H_{ij}}$  is done following the same procedure.  $\square$

Now we can apply Theorem 3 to characterize the limiting eigenvalue distribution of  $\tilde{H}_{ii}, \tilde{H}_{ij}$ , which are identical to the distributions of  $H_{ii}, H_{ij}$ .

**Proposition 1.** Fix  $C \geq 2$ , as  $d, N \rightarrow \infty$ ,  $\frac{d}{N} \rightarrow \gamma \in (0, +\infty)$ , we have

1.  $\mu_{H_{ii}}$  converges almost surely to a deterministic measure  $\mu_{11}^H$ , and its Stieltjes transform  $s_{\mu_{11}^H}(z)$  is uniquely specified by the functional equation

$$s(z) = \frac{1}{\int_{\mathbb{R}^C} \frac{h_1(\mathbf{t}) \varphi_C(\mathbf{t})}{1 + \gamma s(z) h_1(\mathbf{t})} d\mathbf{t}_1 \cdots d\mathbf{t}_C - z}, \quad \forall z \in \mathbb{C}^+. \quad (50)$$

Here  $\mathbf{t} = (t_1, \dots, t_C)$ , and

$$h_1(\mathbf{t}) = \frac{e^{t_1}}{\sum_{l=1}^C e^{t_l}} \left( 1 - \frac{e^{t_1}}{\sum_{l=1}^C e^{t_l}} \right),$$

$$\varphi_C(\mathbf{t}) = (2\pi)^{-\frac{C}{2}} e^{-\frac{1}{2} \sum_{l=1}^C t_l^2}.$$

2. For  $i \neq j$ ,  $\mu_{H_{ij}}$  converges weakly almost surely to a deterministic measure  $\mu_{12}$ , and its Stieltjes transform  $s_{\mu_{12}}(z)$  is uniquely specified by the functional equation

$$s(z) = \frac{1}{\int_{\mathbb{R}^C} \frac{h_2(\mathbf{t}) \varphi_C(\mathbf{t})}{1 + \gamma s(z) h_2(\mathbf{t})} d\mathbf{t}_1 \cdots d\mathbf{t}_C - z}, \quad \forall z \in \mathbb{C}^+. \quad (51)$$

Here

$$h_2(\mathbf{t}) = \frac{e^{t_1+t_2}}{\left( \sum_{l=1}^C e^{t_l} \right)^2}.$$

*Proof.* From Lemma 1, it suffices to prove the convergence of  $\mu_{\tilde{H}_{ii}}, \mu_{\tilde{H}_{ij}}$  to the limiting measure specified by (50), (51) respectively. For the case of  $\tilde{H}_{ii}$ , let

$$Y_{n,i}^{(N)} = p_i(\tilde{x}_n) = \frac{\exp(v_i^\top \tilde{x}_n)}{\sum_{l=1}^C \exp(v_l^\top \tilde{x}_n)},$$

then  $\tilde{a}_n = Y_{n,i}^{(N)} (1 - Y_{n,i}^{(N)})$ . Recall that  $\tilde{H}_{ii} = \frac{1}{N} X_N \tilde{\Lambda}_N X_N^\top$ ,  $\tilde{\Lambda}_N = \text{diag}(\tilde{a}_1, \dots, \tilde{a}_N)$ . Then  $\tilde{\Lambda}_N$  is independent of  $X_N$ , and the eigenvalue distribution of  $\tilde{\Lambda}_N$  is the counting measure  $\nu_N = \frac{1}{N} \sum_{n=1}^N \delta_{\tilde{a}_n}$ . Note that  $(\tilde{a}_n)_{n=1}^N$

are identically distributed but dependent, therefore we need to prove that  $\nu_N$  converges almost surely to a deterministic measure before applying Theorem 3.

From the strong law of large number, it holds almost surely that

$$\begin{aligned} \lim_{d \rightarrow \infty} \|w_c\|^2 &= 1 \quad \forall c \in [C], \\ \lim_{d \rightarrow \infty} w_c^\top w_{c'} &= 0 \quad \forall c, c' \in [C], c \neq c'. \end{aligned} \quad (52)$$

Now we restrict the probability space to a subspace that (52) holds. Note that this restriction does not change validity of the proof since (52) holds almost surely. Let  $\mathcal{F}_V$  be the  $\sigma$ -algebra generated by  $\{V_{ij}\}_{i \in [C], j \in \mathbb{N}^+}$ , then from CLT, the conditional distribution of

$$(v_1^\top \tilde{x}_1, \dots, v_C^\top \tilde{x}_1)$$

given  $\mathcal{F}_V$  converges weakly to  $\mathcal{N}_C(0, I_{C \times C})$ . Let  $\nu$  be the deterministic probability measure such that for any interval  $\Delta \subset \mathbb{R}$ ,

$$\nu(\Delta) = \mathbf{P} \left( \frac{e^{Z_1}}{\sum_{l=1}^C e^{Z_l}} \left( 1 - \frac{e^{Z_1}}{\sum_{l=1}^C e^{Z_l}} \right) \in \Delta \right), \quad (53)$$

where  $(Z_l)_{l=1}^C$  are i.i.d.  $\mathcal{N}(0, 1)$ . Let  $f(x)$  be a bounded continuous function on  $\mathbb{R}$ , from the conditional independence of  $(\tilde{\alpha}_n)_{n=1}^N$  given  $\mathcal{F}_V$ , as  $N \rightarrow \infty$ ,

$$\begin{aligned} & \int_{\mathbb{R}} f(x) \nu_N(dx) - \int_{\mathbb{R}} f(x) \nu(dx) \\ &= \left( \frac{1}{N} \sum_{n=1}^N f(\tilde{\alpha}_n) - \mathbf{E}[f(\tilde{\alpha}_1) | \mathcal{F}_V] \right) + \left( \mathbf{E}[f(\tilde{\alpha}_1) | \mathcal{F}_V] - \int_{\mathbb{R}} f(x) \nu(dx) \right) \\ & \rightarrow 0, \quad a.s.. \end{aligned} \quad (54)$$

Here the first term converges a.s to 0 because of the strong law of large number. And the second term converges to 0 from Portmanteau theorem. Then  $\nu_N$  converges weakly almost surely to  $\nu$ .

Now let  $\tilde{T}_N = \frac{N}{d} \tilde{H}_{ii}$ . Then  $\tilde{T}_N = \frac{1}{d} X_N \tilde{\Lambda}_N X_N^\top$ , and the eigenvalue distribution of  $\tilde{\Lambda}_N$  converges weakly almost surely to  $\nu$ . From Theorem 3,  $s_{\tilde{T}_N}$  converges weakly almost surely to the unique solution of

$$s(z) = \frac{1}{\frac{1}{\gamma} \int_{\mathbb{R}} \frac{t\nu(dt)}{1+ts(z)} - z}, \quad \forall z \in \mathbb{C}^+. \quad (55)$$

From (53),

$$\int_{\mathbb{R}} \frac{t\nu(dt)}{1+ts(z)} = \int_{\mathbb{R}^C} \frac{h_1(\mathbf{t}) \varphi_C(\mathbf{t})}{1+s(z)h_1(\mathbf{t})} dt_1 \cdots dt_C.$$

Note that  $s_{\tilde{T}_N}(z) = \frac{d}{N} s_{\tilde{H}_{ii}}\left(\frac{d}{N}z\right)$  and  $d/N \rightarrow \gamma$ . Then with a change of variable  $z' = \gamma z$  in (55), it implies that  $s_{\tilde{H}_{ii}}$  converges weakly almost surely to the unique solution of (50). Then we finish the proof for the  $H_{ii}$  case.

The proof for  $H_{ij}$  case is in the same procedure. The variables  $(\tilde{\beta}_n)_{n=1}^N$  are identically distributed, and  $\tilde{\beta}_n = -Y_{n,i}^{(N)} Y_{n,j}^{(N)}$ . Define the counting measure  $\eta_N = \frac{1}{N} \sum_{n=1}^N \delta_{\tilde{\beta}_n}$ , then  $\eta_N$  converges weakly almost surely to a deterministic probability measure  $\nu$ , where for any interval  $\Delta \subset \mathbb{R}$ ,

$$\eta(\Delta) = \mathbf{P} \left( \frac{e^{Z_1}}{\sum_{l=1}^C e^{Z_l}} \frac{e^{Z_2}}{\sum_{l=1}^C e^{Z_l}} \in \Delta \right).$$

Let  $\tilde{S}_N = \frac{N}{d} \tilde{H}_{ij}$ , then from Theorem 3,  $s_{\tilde{S}_N}$  converges weakly almost surely to the unique solution of

$$s(z) = \frac{1}{\frac{1}{\gamma} \int_{\mathbb{R}} \frac{t\eta(dt)}{1+ts(z)} - z}, \quad \forall z \in \mathbb{C}^+.$$

We have

$$\int_{\mathbb{R}} \frac{t\eta(dt)}{1+ts(z)} = \int_{\mathbb{R}^C} \frac{h_2(\mathbf{t})\varphi_C(\mathbf{t})}{1+s(z)h_2(\mathbf{t})} dt_1 \cdots dt_C. \quad (56)$$

Then from  $s_{\tilde{S}_N}(z) = \frac{d}{N} s_{\tilde{H}_{ij}}\left(\frac{d}{N}z\right)$ ,  $d/N \rightarrow \gamma$ , and a change of variable  $z' = \gamma z$  in (56), it implies that  $s_{\tilde{H}_{ij}}$  converges weakly almost surely to the unique solution of (51). This concludes the whole proof.  $\square$

The next proposition is to extract the second moment of the limiting eigenvalue distribution from the implicit equations (50) and (51). This leads to Theorem 1.

**Proposition 2.** Suppose that as  $d, N \rightarrow \infty$ ,  $\frac{d}{N} \rightarrow \gamma \in (0, +\infty)$ . Then for  $i \neq j$ , it holds almost surely that

$$\lim_{d, N \rightarrow \infty} \frac{\|H_{ii}\|_{\mathbb{F}}^2}{d} = \gamma \int_{\mathbb{R}^C} h_1(\mathbf{t})^2 \varphi_C(\mathbf{t}) dt_1 \cdots dt_C + \left( \int_{\mathbb{R}^C} h_1(\mathbf{t}) \varphi_C(\mathbf{t}) dt_1 \cdots dt_C \right)^2, \quad (57)$$

$$\lim_{d, N \rightarrow \infty} \frac{\|H_{ij}\|_{\mathbb{F}}^2}{d} = \gamma \int_{\mathbb{R}^C} h_2(\mathbf{t})^2 \varphi_C(\mathbf{t}) dt_1 \cdots dt_C + \left( \int_{\mathbb{R}^C} h_2(\mathbf{t}) \varphi_C(\mathbf{t}) dt_1 \cdots dt_C \right)^2, \quad (58)$$

$$\lim_{C \rightarrow \infty} \lim_{d, N \rightarrow \infty} \frac{C^2 \|H_{ii}\|_{\mathbb{F}}^2}{d} = \gamma e + 1, \quad (59)$$

$$\lim_{C \rightarrow \infty} \lim_{d, N \rightarrow \infty} \frac{C^4 \|H_{ij}\|_{\mathbb{F}}^2}{d} = \gamma e^2 + 1. \quad (60)$$

*Proof.* Recall that as  $z \rightarrow \infty$  in  $\mathbb{C}^+$ ,

$$s_{\mu}(z) = -\frac{1}{z} - \frac{1}{z^2} \int_{\mathbb{R}} x \mu(dx) - \frac{1}{z^3} \int_{\mathbb{R}} x^2 \mu(dx) + O\left(\frac{1}{z^4}\right).$$

Then in (50) as  $z \rightarrow \infty$ ,

$$\begin{aligned} s_{\mu_{11}^H}(z) &= \frac{1}{\int_{\mathbb{R}^C} \frac{h_1(\mathbf{t})\varphi_C(\mathbf{t})}{1+\gamma s_{\mu_{11}^H}(z)h_1(\mathbf{t})} dt_1 \cdots dt_C - z} \\ &= \frac{1}{\int_{\mathbb{R}^C} \frac{h_1(\mathbf{t})\varphi_C(\mathbf{t})}{1-\gamma h_1(\mathbf{t})z^{-1}+O(z^{-2})} dt_1 \cdots dt_C - z} \\ &= \frac{1}{\int_{\mathbb{R}^C} h_1(\mathbf{t})\varphi_C(\mathbf{t}) \left(1 + \gamma h_1(\mathbf{t})z^{-1} + O(z^{-2})\right) dt_1 \cdots dt_C - z} \\ &= -\frac{1}{z} - \frac{1}{z^2} \int_{\mathbb{R}^C} h_1(\mathbf{t})\varphi_C(\mathbf{t}) dt_1 \cdots dt_C \\ &\quad - \frac{1}{z^3} \left[ \gamma \int_{\mathbb{R}^C} h_1(\mathbf{t})^2 \varphi_C(\mathbf{t}) dt_1 \cdots dt_C + \left( \int_{\mathbb{R}^C} h_1(\mathbf{t}) \varphi_C(\mathbf{t}) dt_1 \cdots dt_C \right)^2 \right] + O\left(\frac{1}{z^4}\right). \end{aligned} \quad (61)$$

Hence

$$\int_{\mathbb{R}} x^2 \mu_{11}^H(dx) = \gamma \int_{\mathbb{R}^C} h_1(\mathbf{t})^2 \varphi_C(\mathbf{t}) dt_1 \cdots dt_C + \left( \int_{\mathbb{R}^C} h_1(\mathbf{t}) \varphi_C(\mathbf{t}) dt_1 \cdots dt_C \right)^2.$$

Then we obtain (16) since from Proposition 1,

$$\lim_{d, N \rightarrow \infty} \frac{\|H_{ii}\|_{\mathbb{F}}^2}{d} = \lim_{d, N \rightarrow \infty} \int_{\mathbb{R}} x^2 \mu_{H_{ii}}(dx) = \int_{\mathbb{R}} x^2 \mu_{11}^H(dx) \quad a.s..$$

The proof of (17) follows the same procedure, i.e., expanding  $s(z)$  as  $z \rightarrow \infty$  in (51). Now let  $\mathbf{q}_C = (q_1, \dots, q_C) \sim \mathcal{N}_C(0, I_{C \times C})$ . From the strong law of large number, as  $C \rightarrow \infty$ ,

$$\frac{e^{q_1} + \dots + e^{q_C}}{C} \xrightarrow{a.s.} \mathbf{E}[e^{q_1}] = \sqrt{e}.$$

Then from Slutsky's theorem,

$$C\sqrt{e} \cdot h_1(\mathbf{q}_C) = \frac{C\sqrt{e} \cdot e^{q_1}}{e^{q_1} + \dots + e^{q_C}} \left(1 - \frac{e^{q_1}}{e^{q_1} + \dots + e^{q_C}}\right) \xrightarrow{d} \text{Lognormal}(0, 1),$$

$$C^2 e \cdot h_2(\mathbf{q}_C) = \frac{C\sqrt{e} \cdot e^{q_1}}{e^{q_1} + \dots + e^{q_C}} \cdot \frac{C\sqrt{e} \cdot e^{q_2}}{e^{q_1} + \dots + e^{q_C}} \xrightarrow{d} \text{Lognormal}(0, 1) \otimes \text{Lognormal}(0, 1).$$

Here  $\otimes$  denotes the multiplicative convolution. That is,  $\text{Lognormal}(0, 1) \otimes \text{Lognormal}(0, 1)$  is the distribution of  $\xi_1 \xi_2$  where  $\xi_1, \xi_2$  are iid  $\text{Lognormal}(0, 1)$ . Then from  $\mathbf{E}[\xi] = \sqrt{e}$ ,  $\mathbf{E}[\xi^2] = e^2$ , we have

$$\begin{aligned} \lim_{C \rightarrow \infty} C \int_{\mathbb{R}^C} h_1(\mathbf{t}) \varphi_C(\mathbf{t}) dt_1 \dots dt_C &= \lim_{C \rightarrow \infty} \mathbf{E}[Ch_1(\mathbf{q}_C)] = 1, \\ \lim_{C \rightarrow \infty} C^2 \int_{\mathbb{R}^C} h_1(\mathbf{t})^2 \varphi_C(\mathbf{t}) dt_1 \dots dt_C &= \lim_{C \rightarrow \infty} \mathbf{E}[(Ch_1(\mathbf{q}_C))^2] = e, \\ \lim_{C \rightarrow \infty} C^2 \int_{\mathbb{R}^C} h_2(\mathbf{t}) \varphi_C(\mathbf{t}) dt_1 \dots dt_C &= \lim_{C \rightarrow \infty} \mathbf{E}[C^2 h_2(\mathbf{q}_C)] = 1, \\ \lim_{C \rightarrow \infty} C^4 \int_{\mathbb{R}^C} h_2(\mathbf{t})^2 \varphi_C(\mathbf{t}) dt_1 \dots dt_C &= \lim_{C \rightarrow \infty} \mathbf{E}[(C^2 h_2(\mathbf{q}_C))^2] = e^2. \end{aligned}$$

Then, (18) and (19) follows from (16) and (17) by taking  $C \rightarrow \infty$ , respectively.  $\square$

## D Proof of Theorem 2

Before delving into the proof, we first present the constant terms in Theorem 2. We remark that these constants are bounded as long as  $m \geq 2$ .

$$\begin{aligned} a_{11} &= \frac{1}{2\pi} \int_0^{+\infty} \int_0^{+\infty} xy \exp\left(\frac{xy}{m} - \frac{x^2}{2} - \frac{y^2}{2}\right) dx dy, \\ a_{12} &= \frac{1}{2\pi} \int_0^{+\infty} \int_0^{+\infty} x^2 y^2 \exp\left(\frac{xy}{m} - \frac{x^2}{2} - \frac{y^2}{2}\right) dx dy, \\ a_{21} &= \frac{1}{2\pi} \int_0^{+\infty} \int_0^{+\infty} xy \exp\left(\frac{2xy}{m} - \frac{x^2}{2} - \frac{y^2}{2}\right) dx dy, \\ a_{22} &= \frac{1}{2\pi} \int_0^{+\infty} \int_0^{+\infty} x^2 y^2 \exp\left(\frac{2xy}{m} - \frac{x^2}{2} - \frac{y^2}{2}\right) dx dy, \\ b_1 &= \frac{3}{4} + \frac{1}{8\pi} \int_0^{+\infty} \int_0^{+\infty} \exp\left(\frac{xy}{m} - \frac{x^2}{2} - \frac{y^2}{2}\right) dx dy, \\ b_2 &= \frac{3}{4} + \frac{1}{8\pi} \int_0^{+\infty} \int_0^{+\infty} \exp\left(\frac{2xy}{m} - \frac{x^2}{2} - \frac{y^2}{2}\right) dx dy. \end{aligned} \tag{62}$$

The functions  $h_{ii}$ ,  $h_{ij}$ ,  $u_{ii}$ ,  $u_{ij}$ ,  $q_{ii}$ ,  $q_{ij}$  are given by the right hand side of (86), (87), (95), (96), (98), (99), respectively.

### D.1 Proof for the Hidden-layer Hessian with CE Loss

Our proof uses the following strategy. Firstly we consider the case that  $V \in \mathbb{R}^{C \times m}$  is deterministic. In this case, the techniques in the proof of Theorem 1 is available. Then for the target case that entries of  $V$  are i.i.d. Gaussian, we use

$$\mathbf{E} \left[ \left\| \frac{\partial^2 \ell_{\text{CE}}(W, V)}{\partial w_i \partial w_j^\top} \right\|_F^2 \right] = \mathbf{E} \left[ \mathbf{E} \left[ \left\| \frac{\partial^2 \ell_{\text{CE}}(W, V)}{\partial w_i \partial w_j^\top} \right\|_F^2 \mid V \right] \right]$$

and apply the deterministic case results in the conditional expectation.

Now for short of notations we write  $G_{ii} = \frac{\partial^2 \ell_{\text{CE}}(W, V)}{\partial w_i \partial w_i^\top}$ ,  $G_{ij} = \frac{\partial^2 \ell_{\text{CE}}(W, V)}{\partial w_i \partial w_j^\top}$ . Then

$$\begin{aligned} G_{ii} &= \frac{1}{N} \sum_{n=1}^N \mathbf{1}(w_i^\top x_n > 0) \left[ \sum_{k=1}^C q_k(x_n) V_{ki}^2 - \left( \sum_{k=1}^C q_k(x_n) V_{ki} \right)^2 \right] x_n x_n^\top, \\ G_{ij} &= \frac{1}{N} \sum_{n=1}^N \mathbf{1}(w_i^\top x_n > 0) \mathbf{1}(w_j^\top x_n > 0) \left[ \sum_{k=1}^C q_k(x_n) V_{ki} V_{kj} - \left( \sum_{k=1}^C q_k(x_n) V_{ki} \right) \left( \sum_{k=1}^C q_k(x_n) V_{kj} \right) \right] x_n x_n^\top, \end{aligned} \quad (63)$$

where

$$q_k(x_n) = \frac{\exp(\sigma(Wx_n)^\top v_k)}{\sum_{l=1}^C \exp(\sigma(Wx_n)^\top v_l)}.$$

Let  $\tilde{X}_N = (\tilde{x}_1, \dots, \tilde{x}_N) \in \mathbb{R}^{d \times N}$  be an independent copy of  $X_N$ . Define

$$\begin{aligned} \tilde{G}_{ii} &= \frac{1}{N} \sum_{n=1}^N \mathbf{1}(w_i^\top \tilde{x}_n > 0) \left[ \sum_{k=1}^C q_k(\tilde{x}_n) V_{ki}^2 - \left( \sum_{k=1}^C q_k(\tilde{x}_n) V_{ki} \right)^2 \right] x_n x_n^\top, \\ \tilde{G}_{ij} &= \frac{1}{N} \sum_{n=1}^N \mathbf{1}(w_i^\top \tilde{x}_n > 0) \mathbf{1}(w_j^\top \tilde{x}_n > 0) \left[ \sum_{k=1}^C q_k(\tilde{x}_n) V_{ki} V_{kj} - \left( \sum_{k=1}^C q_k(\tilde{x}_n) V_{ki} \right) \left( \sum_{k=1}^C q_k(\tilde{x}_n) V_{kj} \right) \right] x_n x_n^\top. \end{aligned} \quad (64)$$

**Lemma 2.** Suppose that  $C \geq 2$ ,  $m \geq 3$  are fixed,  $V \in \mathbb{R}^{C \times m}$  is deterministic. For any  $z \in \mathbb{C}^+$ , as  $d, N \rightarrow \infty$ ,  $d/N \rightarrow \gamma \in (0, +\infty)$ , it holds almost surely that

$$s_{G_{ii}}(z) - s_{\tilde{G}_{ii}}(z) = O\left(N^{-\frac{1}{2}}\right), \quad (65)$$

$$s_{G_{ij}}(z) - s_{\tilde{G}_{ij}}(z) = O\left(N^{-\frac{1}{2}}\right). \quad (66)$$

*Proof.* Here, we only present the proof for  $s_{G_{ii}}$ . The proof for  $s_{G_{ij}}$  is done following the same procedure.

For  $t \in [0, 1]$ , let

$$X_N(t) = \sqrt{t} X_N + \sqrt{1-t} \tilde{X}_N.$$

Then  $X_N(t) = (x_1(t), \dots, x_N(t)) \in \mathbb{R}^{d \times N}$ , where

$$x_n(t) = \sqrt{t} x_n + \sqrt{1-t} \tilde{x}_n, \quad n \in [N].$$

Denote

$$\theta_n(t) = \mathbf{1}(w_i^\top x_n(t) > 0) \left[ \sum_{k=1}^C q_k(x_n(t)) V_{ki}^2 - \left( \sum_{k=1}^C q_k(x_n(t)) V_{ki} \right)^2 \right],$$

$$\Theta_N(t) = \text{diag}(\theta_1(t), \dots, \theta_N(t)),$$

$$G_{ii}(t) = \frac{1}{N} X_N \Theta_N(t) X_N^\top,$$

$$\mathcal{G}_N(z, t) = (G_{ii}(t) - z)^{-1}.$$

By treating  $s_{H_{ii}}(z), s_{\tilde{H}_{ii}}(z)$  as Lipchitz functions of the Gaussian vectors  $w_1, \dots, w_m, x_1, \dots, x_N$ , from Talagrand's inequality,

$$\mathbf{P}(|s_{G_{ii}}(z) - \mathbf{E}[s_{G_{ii}}(z)]| \geq t) \leq c_1 e^{-p c_2 t^2},$$

$$\mathbf{P}(|s_{\tilde{G}_{ii}}(z) - \mathbf{E}[s_{\tilde{G}_{ii}}(z)]| \geq t) \leq \tilde{c}_1 e^{-\tilde{d} \tilde{c}_2 t^2},$$



for  $t > 0$  and constants  $c_1, c_2, \tilde{c}_1, \tilde{c}_2 > 0$ . Then from the Borel-Cantelli Lemma,

$$\begin{aligned} s_{G_{ii}}(z) - \mathbf{E}[s_{G_{ii}}(z)] &\xrightarrow{a.s.} 0, \\ s_{\tilde{G}_{ii}}(z) - \mathbf{E}[s_{\tilde{G}_{ii}}(z)] &\xrightarrow{a.s.} 0. \end{aligned} \quad (67)$$

Now we prove that

$$\delta_N(z) = \mathbf{E}[s_{H_{ii}}(z)] - \mathbf{E}[s_{\tilde{H}_{ii}}(z)] = O\left(N^{-\frac{1}{2}}\right). \quad (68)$$

Following (43), we have

$$\Delta_N(z) = -\frac{1}{dN} \int_0^1 \mathbf{E} \left[ \text{tr} \left( X_N^\top \mathcal{G}_N(z, t)^2 X_N \frac{d}{dt} \Theta_N(t) \right) \right] dt. \quad (69)$$

Then  $\delta_N(z) = \frac{d}{dz} \Delta_N(z)$ , where

$$\Delta_N(z) = -\frac{1}{dN} \sum_{n=1}^N \int_0^1 \mathbf{E} \left[ (X_N^\top \mathcal{G}_N(z, t) X_N)_{nn} \frac{d}{dt} \theta_n(t) \right] dt. \quad (70)$$

Similarly to the proof of Theorem 1, it suffices to prove that for any open set  $O \subset \mathbb{C}^+$  such that  $\zeta = \inf_{z \in O} |\Im z| > 0$ ,

$$\max_{z \in O} |\Delta_N^{(1)}(z)| = O\left(N^{-\frac{1}{2}}\right). \quad (71)$$

We have

$$\begin{aligned} \frac{d}{dt} q_k(x_n(t)) &= \frac{1}{2} \sum_{l=1}^C \sum_{h=1}^m q_k(x_n(t)) [\delta_{kl} - q_l(x_n(t))] \mathbf{1}(w_h^\top x_n(t) > 0) V_{lh} w_h^\top \left( \frac{x_n}{\sqrt{t}} - \frac{\tilde{x}_n}{\sqrt{1-t}} \right), \\ \frac{d}{dt} \theta_n(t) &= \mathbf{1}(w_i^\top x_n(t) > 0) \sum_{k=1}^C \left( V_{ki}^2 - 2V_{ki} \sum_{k'=1}^C q_{k'}(x_n(t)) V_{k'i} \right) \frac{d}{dt} q_k(x_n(t)). \end{aligned}$$

Therefore

$$\Delta_N(z) = -\frac{1}{2dN} \sum_{n=1}^N \sum_{k=1}^C \sum_{l=1}^C \sum_{h=1}^m \sum_{s=1}^d \int_0^1 \mathbf{E} \left[ x_n^\top \mathcal{G}_N(z, t) x_n Q_{klhn}(t) W_{hs} \left( \frac{X_{sn}}{\sqrt{t}} - \frac{\tilde{X}_{sn}}{\sqrt{1-t}} \right) \right] dt, \quad (72)$$

where

$$Q_{klhn}(t) = \left( V_{ki}^2 - 2V_{ki} \sum_{k'=1}^C q_{k'}(x_n(t)) V_{k'i} \right) q_k(x_n(t)) [\delta_{kl} - q_l(x_n(t))] \mathbf{1}(w_h^\top x_n(t) > 0) V_{lh}.$$

From Stein's Lemma (46),

$$\Delta_N(z) = -\frac{1}{2dN} \sum_{n=1}^N \sum_{k=1}^C \sum_{l=1}^C \sum_{h=1}^m \sum_{s=1}^d \int_0^1 \left( \frac{1}{\sqrt{t}} \mathbf{E} \left[ \frac{\partial A_N^{(k,l,h,n)}(z, t)}{\partial X_{sn}} W_{hs} \right] - \frac{1}{\sqrt{1-t}} \mathbf{E} \left[ \frac{\partial A_N^{(k,l,h,n)}(z, t)}{\partial \tilde{X}_{sn}} W_{hs} \right] \right) dt, \quad (73)$$

where

$$A_N^{(k,l,h,n)}(z, t) = x_n^\top \mathcal{G}_N(z, t) x_n Q_{klhn}(t).$$

Then

$$\begin{aligned} &\frac{1}{\sqrt{t}} \mathbf{E} \left[ \frac{\partial A_N^{(k,l,h,n)}(z, t)}{\partial X_{sn}} W_{hs} \right] - \frac{1}{\sqrt{1-t}} \mathbf{E} \left[ \frac{\partial A_N^{(k,l,h,n)}(z, t)}{\partial \tilde{X}_{sn}} W_{hs} \right] \\ &= \frac{2}{\sqrt{t}} \mathbf{E} \left[ Q_{klhn}(t) W_{hs} \left( (\mathcal{G}_N x_n)_s - \frac{\delta_{ns}}{N} \theta_n(t) (\mathcal{G}_N x_n)_n (\mathcal{G}_N x_n)^\top x_n \right) \right]. \end{aligned} \quad (74)$$

Hence  $\Delta_N(z) = \Delta_{N,1}(z) - \Delta_{N,2}(z)$ , where

$$\begin{aligned}\Delta_{N,1}(z) &= \frac{1}{dN^2} \sum_{k=1}^C \sum_{l=1}^C \sum_{h=1}^m \sum_{n=1}^{\min(d,N)} \int_0^1 \mathbf{E} \left[ Q_{klhn}(t) \theta_n(t) W_{hn}(\mathcal{G}_N x_n)_n (\mathcal{G}_N x_n)^\top x_n \right] \frac{dt}{\sqrt{t}}, \\ \Delta_{N,2}(z) &= \frac{1}{dN} \sum_{n=1}^N \sum_{k=1}^C \sum_{l=1}^C \sum_{h=1}^m \sum_{s=1}^d \int_0^1 \mathbf{E} [Q_{klhn}(t) W_{hs}(\mathcal{G}_N x_n)_s] \frac{dt}{\sqrt{t}}.\end{aligned}\tag{75}$$

Let  $M_V = \max_{k \in [C], i \in [m]} |V_{ki}|$ . From Hölder's inequality,

$$\begin{aligned}\mathbf{E}[|W_{hn}(\mathcal{G}_N x_n)_n (\mathcal{G}_N x_n)^\top x_n|] &\leq \left( \mathbf{E}[W_{hn}^4] \right)^{\frac{1}{4}} \left( \mathbf{E}[(\mathcal{G}_N x_n)_n^2] \right)^{\frac{1}{2}} \left( \mathbf{E}[((\mathcal{G}_N x_n)^\top x_n)^4] \right)^{\frac{1}{4}}, \\ \mathbf{E}[|W_{hs}(\mathcal{G}_N x_n)_s|] &\leq \left( \mathbf{E}[W_{hs}^2] \right)^{\frac{1}{2}} \left( \mathbf{E}[(\mathcal{G}_N x_n)_s^2] \right)^{\frac{1}{2}},\end{aligned}$$

together with

$$|Q_{klhn}(t)| \leq 3M_v^4, \quad |\theta_n(t)| \leq 2M_v^2, \quad \|\mathcal{G}_N\| \leq \frac{1}{\zeta}, \quad W_{hs} \sim N(0, \frac{1}{d}), \quad \mathbf{E}[(\mathcal{G}_N x_n)_s^2] = \frac{1}{d} \mathbf{E}[\|\mathcal{G}_N x_n\|^2] \leq \frac{1}{\zeta},$$

we have

$$|\Delta_{n,1}(z)| \leq \frac{3^{\frac{1}{4}} 12 C^2 m M_V^5 (\mathbf{E}[\|x_n\|^8])^{\frac{1}{4}}}{\zeta^2 d^{\frac{3}{2}} N}, \quad |\Delta_{n,2}(z)| \leq \frac{6m C^2 M_V^3}{\zeta d^{\frac{1}{2}}}.$$

Then as  $d, N \rightarrow \infty$ ,  $d/N \rightarrow \gamma \in (0, +\infty)$ ,

$$|\Delta_{N,1}(z)| = O\left(N^{-\frac{3}{2}}\right), \quad |\Delta_{N,2}(z)| = O\left(N^{-\frac{1}{2}}\right).$$

Then we have (71) and then (65). The proof in the case of  $G_{ij}$  is similar and is omitted.  $\square$

**Proposition 3.** Suppose that  $C \geq 2$ ,  $m \geq 3$  are fixed,  $V \in \mathbb{R}^{C \times m}$  is deterministic. As  $d, N \rightarrow \infty$ ,  $\frac{d}{N} \rightarrow \gamma \in (0, +\infty)$ , we have

1.  $\mu_{G_{ii}}$  converges weakly almost surely to a deterministic measure  $\mu_{11}^G$ , where  $s_{\mu_{11}^G}(z)$  is uniquely specified by the functional equation

$$s(z) = \frac{1}{\int_{\mathbb{R}} \frac{tv_1(dt)}{1+\gamma s(z)t} dt - z}, \quad \forall z \in \mathbb{C}^+.\tag{76}$$

Here  $v_1$  is defined as follows. Let  $\mathbf{z} = (z_1, \dots, z_m) \sim \mathcal{N}_m(0, I_m)$ , define random variables

$$r_k = \frac{\exp(\sigma(\mathbf{z})^\top v_k)}{\sum_{l=1}^C \exp(\sigma(\mathbf{z})^\top v_l)}, \quad k \in [C],$$

$$\zeta_C(V) = \mathbf{1}(z_1 > 0) \left[ \sum_{k=1}^C r_k V_{k1}^2 - \left( \sum_{k=1}^C r_k V_{k1} \right)^2 \right].$$

Then  $v_1$  is given by that for all intervals  $\Delta \subset \mathbb{R}$ ,  $v_1(\Delta) = \mathbf{P}(\zeta_C(V) \in \Delta)$ .

2. For  $i \neq j$ ,  $\mu_{G_{ij}}$  converges weakly almost surely to a deterministic measure  $\mu_{12}^G$ , where  $s_{\mu_{12}^G}(z)$  is uniquely specified by the functional equation

$$s(z) = \frac{1}{\int_{\mathbb{R}} \frac{tv_2(dt)}{1+\gamma s(z)t} dt - z}, \quad \forall z \in \mathbb{C}^+.\tag{77}$$

Here  $v_2$  is defined as follows. Let  $\mathbf{z} = (z_1, \dots, z_m) \sim \mathcal{N}_m(0, I_m)$ , define random variables

$$\eta_C(V) = \mathbf{1}(z_1 > 0) \mathbf{1}(z_2 > 0) \left[ \sum_{k=1}^C r_k V_{k1} V_{k2} - \left( \sum_{k=1}^C r_k V_{k1} \right) \left( \sum_{k=1}^C r_k V_{k2} \right) \right].$$

Then  $v_2$  is given by that for all intervals  $\Delta \subset \mathbb{R}$ ,  $v_2(\Delta) = \mathbf{P}(\eta_C(V) \in \Delta)$ .

*Proof.* We give a proof for the  $G_{ii}$  case, the  $G_{ij}$  case is in the same procedure. From Lemma 2, it suffices to prove the convergence of  $\mu_{\tilde{H}_{ii}}$  to the limiting measure specified by (3). Let

$$\tilde{\theta}_n = \mathbf{1}(w_i^\top \tilde{x}_n > 0) \left[ \sum_{k=1}^C q_k(\tilde{x}_n) V_{ki}^2 - \left( \sum_{k=1}^C q_k(\tilde{x}_n) V_{ki} \right)^2 \right],$$

$$\tilde{\Theta}_N = \text{diag}\{\theta_1, \dots, \theta_N\},$$

then  $\tilde{H}_{ii} = \frac{1}{N} X_N \tilde{\Theta}_N X_N^\top$ , and  $\tilde{\Theta}_N$  is independent of  $X_N$ . The eigenvalue distribution of  $\tilde{\Theta}_N$  is the counting measure  $\tau_N = \frac{1}{N} \sum_{n=1}^N \delta_{\tilde{\theta}_n}$ . Since  $m$  is fixed, from the strong law of large number, it holds almost surely that

$$\lim_{d \rightarrow \infty} \|w_h\|^2 = 1 \quad \forall h \in [m],$$

$$\lim_{d \rightarrow \infty} w_h^\top w_{h'} = 0 \quad \forall h, h' \in [m], h \neq h'.$$
(78)

Without loss of generality we can restrict the probability space to a subspace that (78) holds. Let  $\mathcal{F}_W$  be the  $\sigma$ -algebra generated by  $\{W_{hs}\}_{h \in [m], s \in \mathbb{N}^+}$ , then from CLT, the conditional distribution of

$$(w_1^\top \tilde{x}_1, \dots, w_m^\top \tilde{x}_1)$$

given  $\mathcal{F}_W$  converges weakly to  $\mathcal{N}_m(0, I_m)$ . Since  $V$  is deterministic,  $(\tilde{\theta}_n)_{n=1}^N$  are independent conditioning on  $\mathcal{F}_W$ . Then for any  $f \in C_b(\mathbb{R})$ , as  $N \rightarrow \infty$ ,

$$\begin{aligned} & \int_{\mathbb{R}} f(x) \tau_N(dx) - \int_{\mathbb{R}} f(x) \nu_1(dx) \\ &= \left( \frac{1}{N} \sum_{n=1}^N f(\tilde{\theta}_n) - \mathbf{E}[f(\tilde{\theta}_1) | \mathcal{F}_W] \right) + \left( \mathbf{E}[f(\tilde{\theta}_1) | \mathcal{F}_W] - \int_{\mathbb{R}} f(x) \nu_1(dx) \right) \\ & \rightarrow 0, \quad a.s. \end{aligned}$$
(79)

Therefore  $\tau_N$  converges weakly almost surely to  $\nu_1$ .

Now let  $\tilde{T}_N = \frac{N}{d} \tilde{G}_{ii}$ . Then  $\tilde{T}_N = \frac{1}{d} X_N \tilde{\Theta}_N X_N^\top$ , and the eigenvalue distribution of  $\tilde{\Theta}_N$  converges weakly almost surely to  $\nu_1$ . From Theorem 3,  $s_{\tilde{T}_N}$  converges weakly almost surely to the unique solution of

$$s(z) = \frac{1}{\frac{1}{\gamma} \int_{\mathbb{R}} \frac{t \nu_1(dt)}{1+ts(z)} - z}, \quad \forall z \in \mathbb{C}^+.$$
(80)

Then with a change of variable  $z' = \gamma z$  in (80), it implies that  $s_{\tilde{G}_{ii}}$  converges weakly almost surely to the unique solution of (76).  $\square$

The next proposition is exactly (21) in Theorem 2.

**Proposition 4.** Suppose that  $m \geq 3$  is fixed, and  $V \in \mathbb{R}^{C \times m}$  has i.i.d.  $\mathcal{N}(0, \frac{1}{m})$  entries. If as  $d, N \rightarrow \infty$ ,  $\frac{d}{N} \rightarrow \gamma \in (0, +\infty)$ , then for  $i \neq j$ ,

$$\begin{aligned} \lim_{C \rightarrow \infty} \lim_{d, N \rightarrow \infty} \frac{\mathbf{E}[\|G_{ii}\|_F^2]}{d} &= \frac{2\gamma + 1}{4m^2}, \\ \lim_{C \rightarrow \infty} \lim_{d, N \rightarrow \infty} \frac{\mathbf{CE}[\|G_{ij}\|_F^2]}{d} &= \frac{\gamma(m-1)^2}{2^m(m-2)^3m} \left( \sqrt{\frac{m}{m-2}} + 1 \right)^{m-2}. \end{aligned}$$
(81)

*Proof.* Let  $\bar{V}$  be a deterministic realization of  $V$ . By expanding (76) and (77) at  $z = \infty$ , we have almost surely

$$\lim_{d, N \rightarrow \infty} \frac{\|G_{ii}\|_F^2}{d} = \int_{\mathbb{R}} x^2 \mu_{11}^G(dx) = \gamma \mathbf{E}[\xi_C(\bar{V})^2] + (\mathbf{E}[\xi_C(\bar{V})])^2,$$
(82)

$$\lim_{d, N \rightarrow \infty} \frac{\|G_{ij}\|_F^2}{d} = \int_{\mathbb{R}} x^2 \mu_{12}^G(dx) = \gamma \mathbf{E}[\eta_C(\bar{V})^2] + (\mathbf{E}[\eta_C(\bar{V})])^2. \quad (83)$$

Then we have

$$\lim_{d, N \rightarrow \infty} \frac{\mathbf{E}[\|G_{ii}\|_F^2 | V]}{d} = \gamma \mathbf{E}[\xi_C(V)^2 | V] + (\mathbf{E}[\xi_C(V) | V])^2, \quad (84)$$

$$\lim_{d, N \rightarrow \infty} \frac{\mathbf{E}[\|G_{ij}\|_F^2 | V]}{d} = \gamma \mathbf{E}[\eta_C(V)^2 | V] + (\mathbf{E}[\eta_C(V) | V])^2. \quad (85)$$

Taking expectation both sides we have

$$\lim_{d, N \rightarrow \infty} \frac{\mathbf{E}[\|G_{ii}\|_F^2]}{d} = \gamma \mathbf{E}[\xi_C(V)^2] + (\mathbf{E}[\xi_C(V)])^2, \quad (86)$$

$$\lim_{d, N \rightarrow \infty} \frac{\mathbf{E}[\|G_{ij}\|_F^2]}{d} = \gamma \mathbf{E}[\eta_C(V)^2] + (\mathbf{E}[\eta_C(V)])^2. \quad (87)$$

Write for short that  $\xi_C = \xi_C(V)$ ,  $\eta_C = \eta_C(V)$ . By the strong law of large number, as  $C \rightarrow \infty$ ,

$$\begin{aligned} \mathbf{E} \left[ \sum_{k=1}^C r_k V_{k1}^2 \mid \mathbf{z} \right] &= \mathbf{E} \left[ \frac{\frac{1}{C} \sum_{k=1}^C \exp(\sigma(\mathbf{z})^\top v_k) V_{k1}^2}{\frac{1}{C} \sum_{k=1}^C \exp(\sigma(\mathbf{z})^\top v_k)} \mid \mathbf{z} \right] \rightarrow \frac{\mathbf{E}[\exp(\sigma(\mathbf{z})^\top v_k) V_{k1}^2 \mid \mathbf{z}]}{\mathbf{E}[\exp(\sigma(\mathbf{z})^\top v_k) \mid \mathbf{z}]} = \frac{\sigma(z_1)^2}{m^2} + \frac{1}{m}, \\ \mathbf{E} \left[ \left( \sum_{k=1}^C r_k V_{k1} \right)^2 \mid \mathbf{z} \right] &= \mathbf{E} \left[ \left( \frac{\frac{1}{C} \sum_{k=1}^C \exp(\sigma(\mathbf{z})^\top v_k) V_{k1}}{\frac{1}{C} \sum_{k=1}^C \exp(\sigma(\mathbf{z})^\top v_k)} \right)^2 \mid \mathbf{z} \right] \rightarrow \left( \frac{\mathbf{E}[\exp(\sigma(\mathbf{z})^\top v_k) V_{k1} \mid \mathbf{z}]}{\mathbf{E}[\exp(\sigma(\mathbf{z})^\top v_k) \mid \mathbf{z}]} \right)^2 = \frac{\sigma(z_1)^2}{m^2}. \end{aligned}$$

Therefore

$$\mathbf{E}[\xi_C] = \mathbf{E}[\mathbf{E}[\xi_C | \mathbf{z}]] = \mathbf{E} \left[ \frac{\mathbf{1}(z_1 > 0)}{m} \right] = \frac{1}{2m}.$$

Similarly,

$$\mathbf{E}[\xi_C^2] = \mathbf{E}[\mathbf{E}[\xi_C^2 | \mathbf{z}]] = \mathbf{E} \left[ \frac{\mathbf{1}(z_1 > 0)}{m^2} \right] = \frac{1}{2m^2}.$$

Therefore

$$\lim_{C \rightarrow \infty} \lim_{d, N \rightarrow \infty} \frac{\|H_{ii}\|_F^2}{d} = \frac{2\gamma + 1}{4m^2}.$$

For the case of  $G_{ij}$ , by repeating all arguments above, we have

$$\begin{aligned} \eta_C &= \mathbf{1}(z_1 > 0) \mathbf{1}(z_2 > 0) \left[ \sum_{k=1}^C r_k V_{k1} V_{k2} - \left( \sum_{k=1}^C r_k V_{k1} \right) \left( \sum_{k=1}^C r_k V_{k2} \right) \right] \\ &= \mathbf{1}(z_1 > 0) \mathbf{1}(z_2 > 0) \sum_{k=1}^C \sum_{l=1}^C r_k r_l V_{k1} (V_{k2} - V_{l2}) \\ &= \frac{1}{2} \cdot \mathbf{1}(z_1 > 0) \mathbf{1}(z_2 > 0) \sum_{k=1}^C \sum_{l=1}^C r_k r_l (V_{k1} - V_{l1}) (V_{k2} - V_{l2}) \\ &= \frac{1}{2} \cdot \mathbf{1}(z_1 > 0) \mathbf{1}(z_2 > 0) \frac{\sum_{k=1}^C \sum_{l=1}^C \exp(\sigma(\mathbf{z})^\top v_k) \exp(\sigma(\mathbf{z})^\top v_l) (V_{k1} - V_{l1}) (V_{k2} - V_{l2})}{\left[ \sum_{k=1}^C \exp(\sigma(\mathbf{z})^\top v_k) \right]^2}. \end{aligned} \quad (88)$$

Let

$$h(k, l) = \exp(\sigma(\mathbf{z})^\top v_k) \exp(\sigma(\mathbf{z})^\top v_l) (V_{k1} - V_{l1}) (V_{k2} - V_{l2}).$$

Then for  $k \neq k' \neq l \neq l'$ ,

$$\mathbf{E}[h(k, l) \mid \mathbf{z}] = 0, \quad \mathbf{E}[h(k, l)^2 \mid \mathbf{z}] < \infty, \quad \mathbf{E}[h(k, l) h(k', l') \mid \mathbf{z}] = 0,$$

$$\mathbf{E}[h(k, l)h(k, l') \mid \mathbf{z}] = \left( \frac{\sigma(z_1)^2 \sigma(z_2)^2}{m^4} + \frac{\sigma(z_1)^2 + \sigma(z_2)^2}{m^3} + \frac{1}{m^2} \right) \exp \left( \frac{3}{m} \|\sigma(\mathbf{z})\|^2 \right).$$

Then as  $C \rightarrow \infty$ ,

$$\begin{aligned} \mathbf{E}[\sqrt{C}\eta_C] &= \mathbf{E}[\mathbf{E}[\sqrt{C}\eta_C \mid \mathbf{z}]] \\ &= \mathbf{E} \left[ \frac{1}{2} \mathbf{1}(z_1 > 0) \mathbf{1}(z_2 > 0) \mathbf{E} \left[ \frac{\frac{1}{C^{3/2}} \sum_{k=1}^C \sum_{l=1}^C h(k, l)}{\left[ \frac{1}{C} \sum_{k=1}^C \exp(\sigma(\mathbf{z})^\top v_k) \right]^2} \middle| \mathbf{z} \right] \right] \\ &= \mathbf{E} \left[ \frac{1}{2} \mathbf{1}(z_1 > 0) \mathbf{1}(z_2 > 0) \frac{\frac{1}{C^{3/2}} \sum_{k=1}^C \sum_{l=1}^C \mathbf{E} [h(k, l) \mid \mathbf{z}]}{\mathbf{E} \left[ \exp(\sigma(\mathbf{z})^\top v_k) \mid \mathbf{z} \right]^2} \right] + o(1) \\ &= o(1), \end{aligned} \tag{89}$$

$$\begin{aligned} \mathbf{E}[C\eta_C^2] &= \mathbf{E}[\mathbf{E}[C\eta_C^2 \mid \mathbf{z}]] \\ &= \mathbf{E} \left[ \frac{1}{4} \mathbf{1}(z_1 > 0) \mathbf{1}(z_2 > 0) \mathbf{E} \left[ \frac{\frac{1}{C^3} \left[ \sum_{k=1}^C \sum_{l=1}^C h(k, l) \right]^2}{\left[ \frac{1}{C} \sum_{k=1}^C \exp(\sigma(\mathbf{z})^\top v_k) \right]^4} \middle| \mathbf{z} \right] \right] \\ &\rightarrow \mathbf{E} \left[ \frac{1}{4} \mathbf{1}(z_1 > 0) \mathbf{1}(z_2 > 0) \frac{4 \mathbf{E} [h(k, l)h(k, l') \mid \mathbf{z}]}{\mathbf{E} \left[ \exp(\sigma(\mathbf{z})^\top v_k) \mid \mathbf{z} \right]^4} \right] \\ &= \mathbf{E} \left[ \mathbf{1}(z_1 > 0) \mathbf{1}(z_2 > 0) \left( \frac{\sigma(z_1)^2 \sigma(z_2)^2}{m^4} + \frac{\sigma(z_1)^2 + \sigma(z_2)^2}{m^3} + \frac{1}{m^2} \right) \exp \left( \frac{1}{m} \|\sigma(\mathbf{z})\|^2 \right) \right] \\ &= \left( \mathbf{E} \left[ \left( \frac{\sigma(z_1)^2}{m^2} + \frac{1}{m} \right) \exp \left( \frac{\sigma(z_1)^2}{m} \right) \mathbf{1}(z_1 > 0) \right] \right)^2 \left( \mathbf{E} \left[ \exp \left( \frac{\sigma(z_1)^2}{m} \right) \right] \right)^{m-2} \\ &= \frac{(m-1)^2}{2^m(m-2)^3 m} \left( \sqrt{\frac{m}{m-2}} + 1 \right)^{m-2}. \end{aligned} \tag{90}$$

Then from (87) we finish the proof.  $\square$

## D.2 Proof for the Hidden-layer Hessian with MSE Loss

For short of notations we write  $K_{ii} = \frac{\partial^2 \ell_{\text{MSE}}(W, V)}{\partial w_i \partial w_i^\top}$ ,  $K_{ij} = \frac{\partial^2 \ell_{\text{MSE}}(W, V)}{\partial w_i \partial w_j^\top}$ . Then

$$K_{ii} = \left( \sum_{k=1}^C V_{ki}^2 \right) L_{ii}, \quad K_{ij} = \left( \sum_{k=1}^C V_{ki} V_{kj} \right) L_{ij},$$

where

$$L_{ii} = \frac{1}{N} \sum_{n=1}^N \mathbf{1}(w_i^\top x_n > 0) x_n x_n^\top, \quad L_{ij} = \frac{1}{N} \sum_{n=1}^N \mathbf{1}(w_i^\top x_n > 0) \mathbf{1}(w_j^\top x_n > 0) x_n x_n^\top.$$

The following decoupling lemma is motivated by [Hanin and Nica, 2020].

**Lemma 3.** *Under the assumptions in Theorem 2, we have:*

1. There exists random matrices  $\hat{X}_N, \hat{\Lambda}_N$  in the same probability space, such that  $\hat{X}_N \stackrel{d}{=} X_N$ ,  $\hat{\Lambda}_N$  is a  $N$ -dimensional diagonal matrix with entries i.i.d.  $\text{ber}(\frac{1}{2})$  random variables independent of  $\hat{X}_N$ , and  $L_{ii} \stackrel{d}{=} \frac{1}{N} \hat{X}_N \hat{\Lambda}_N \hat{X}_N'$ .
2. For  $i \neq j$ , there exists random matrices  $\hat{X}_N, \hat{\Lambda}_N$  in the same probability space, such that  $\hat{X}_N \stackrel{d}{=} X_N$ ,  $\hat{\Lambda}_N$  is a  $N$ -dimensional diagonal matrix with entries i.i.d.  $\text{ber}(\frac{1}{4})$  random variables independent of  $\hat{X}_N$ , and  $L_{ij} \stackrel{d}{=} \frac{1}{N} \hat{X}_N \hat{\Lambda}_N \hat{X}_N'$ .

*Proof.* Let  $\xi_1, \dots, \xi_p, \eta_1, \dots, \eta_N$  be i.i.d. Radamacher random variables. Let

$$\tilde{X}_N = \text{diag}(\xi) X_N \text{diag}(\eta), \quad \tilde{\Lambda}_N = \text{diag}(1(w'_i \tilde{x}_1 > 0), \dots, 1(w'_i \tilde{x}_N > 0)).$$

Here  $\tilde{x}_1, \dots, \tilde{x}_N$  are column vectors of  $\tilde{X}_N$ . Since entries of  $X_N$  are i.i.d. centered,  $\{\tilde{X}_N, \tilde{\Lambda}_N\} \stackrel{d}{=} \{X_N, \Lambda_N\}$ . Hence

$$\begin{aligned} G_{ii} &\stackrel{d}{=} \frac{1}{N} \tilde{X}_N \tilde{\Lambda}_N \tilde{X}_N = \frac{1}{N} \text{diag}(\xi) X_N \text{diag}(\eta) \tilde{\Lambda}_N \text{diag}(\eta) X_N \text{diag}(\xi) \\ &= \frac{1}{N} \text{diag}(\xi) X_N \tilde{\Lambda}_N X_N \text{diag}(\xi). \end{aligned} \quad (91)$$

Clearly  $\text{diag}(\xi) X_N \stackrel{d}{=} X_N$ , then it suffices to show that  $\tilde{\Lambda}_N$  is diagonal with i.i.d.  $\text{ber}(\frac{1}{2})$  entries independent of  $\{\xi, X_N\}$ . To see this, we have

$$\tilde{\Lambda}_N(n, n) = 1(w'_i \text{diag}(\xi) x_n \eta_n > 0), \quad 1 \leq n \leq N.$$

Then the required property follows from that  $(\eta_n)_n$  are i.i.d. valuing in  $\{1, -1\}$  with equal probability.

For  $G_{ij}(i \neq j)$ , the proof is the same, except that

$$\tilde{\Lambda}_N(n, n) = 1(w'_i \text{diag}(\xi) x_n \eta_n > 0) \cdot 1(w'_j \text{diag}(\xi) x_n \eta_n > 0), \quad 1 \leq n \leq N$$

are i.i.d.  $\text{ber}(\frac{1}{4})$ . □

A probability measure  $\mu$  is said to have the Marchenko-Pastur distribution with parameter  $y > 0$  and  $\sigma^2 > 0$ , denoted as  $\text{MP}(y, \sigma^2)$ , if

$$\mu(dx) = (1 - y^{-1})1(y > 1)\delta_0(dx) + \frac{\sqrt{(\lambda_+ - x)(x - \lambda_-)}}{2\pi\sigma^2 y x} 1_{(\lambda_-, \lambda_+)}(x) dx, \quad \lambda_+ = \sigma^2(1 + \sqrt{y})^2, \quad \lambda_- = \sigma^2(1 - \sqrt{y})^2.$$

The Stieltjes transform of  $\text{MP}(y, \sigma^2)$  is given by

$$s(z) = \frac{\sigma^2(1 - y) - z + \sqrt{(z - \sigma^2 - y\sigma^2)^2 - 4y\sigma^4}}{2yz\sigma^2},$$

or equivalently by the equation (writing  $s = s_\mu(z)$  for short)

$$yz\sigma^2 s^2 + (z - \sigma^2(1 - y))s + 1 = 0. \quad (92)$$

**Proposition 5.** As  $d, N \rightarrow \infty$ ,  $\frac{d}{N} \rightarrow \gamma \in (0, +\infty)$ , we have

1.  $\mu_{L_{ii}}$  converges weakly almost surely to  $\text{MP}(2\gamma, \frac{1}{2})$ .
2. For  $i \neq j$ ,  $\mu_{L_{ij}}$  converges weakly almost surely to  $\text{MP}(4\gamma, \frac{1}{4})$ .

*Proof.* From Lemma 3, we have  $L_{ii} \stackrel{d}{=} \frac{d}{N} T_N$ , where  $T_N = \frac{1}{d} \hat{X}_N \hat{\Lambda}_N \hat{X}_N'$ . From Theorem 3,  $\mu_{T_N}$  converges weakly almost surely to a deterministic measure  $\mu_T$ . And  $s_{\mu_T}(z)$  is specified by the equation

$$s(z) = \frac{1}{\frac{1}{\gamma} \int_{\mathbb{R}} \frac{tv_1(dt)}{1+ts(z)} - z}, \quad \forall z \in \mathbb{C}^+, \quad (93)$$



where  $v_1 = \frac{1}{2}\delta_0 + \frac{1}{2}\delta_1$ . The equation can be simplified as

$$zs^2 + \left(z - \frac{1}{2\gamma} + 1\right)s + 1 = 0.$$

This is exactly (92) with  $y = 2\gamma$ ,  $\sigma^2 = \frac{1}{2\gamma}$ . Then  $\mu_{T_N} \rightarrow MP(2\gamma, \frac{1}{2\gamma})$  and hence  $\mu_{L_{ii}} \rightarrow MP(2\gamma, \frac{1}{2})$ . The  $L_{ij}$  case in the same procedure, replacing  $v_1$  in (93) with  $v_2 = \frac{3}{4}\delta_0 + \frac{1}{4}\delta_1$ .  $\square$

**Proposition 6.** Suppose that  $m$  is fixed and as  $d, N \rightarrow \infty$ ,  $\frac{d}{N} \rightarrow \gamma \in (0, +\infty)$ . Then for  $i \neq j$ , we have

$$\begin{aligned} \lim_{C \rightarrow \infty} \lim_{d, N \rightarrow \infty} \frac{\mathbf{E} [\|H_{ii}\|_F^2]}{C^2 d} &= \frac{1 + 2\gamma}{4m^2}, \\ \lim_{C \rightarrow \infty} \lim_{d, N \rightarrow \infty} \frac{\mathbf{E} [\|H_{ij}\|_F^2]}{Cd} &= \frac{1 + 4\gamma}{16m^2}. \end{aligned} \quad (94)$$

*Proof.* From Proposition 5 we have

$$\frac{\|L_{ii}\|_F^2}{d} = \int_{\mathbb{R}} x^2 \mu_{L_{ii}}(dx) \rightarrow \int_{\mathbb{R}} x^2 \mu_{MP(2\gamma, \frac{1}{2})}(dx) = \frac{1 + 2\gamma}{4} \quad a.s. \quad (95)$$

For  $i \neq j$ ,

$$\frac{\|L_{ij}\|_F^2}{d} = \int_{\mathbb{R}} x^2 \mu_{L_{ij}}(dx) \rightarrow \int_{\mathbb{R}} x^2 \mu_{MP(4\gamma, \frac{1}{4})}(dx) = \frac{1 + 4\gamma}{16} \quad a.s. \quad (96)$$

Since entries of  $V$  are i.i.d.  $\mathcal{N}(0, \frac{1}{m})$  independent of  $\{L_{ii}, L_{ij}\}$ ,

$$\begin{aligned} \lim_{C \rightarrow \infty} \lim_{d, N \rightarrow \infty} \frac{\mathbf{E} [\|H_{ii}\|_F^2]}{C^2 d} &= \lim_{C \rightarrow \infty} \mathbf{E} \left[ \left( \frac{\sum_{k=1}^C V_{ki}^2}{C} \right)^2 \right] \lim_{d, N \rightarrow \infty} \mathbf{E} \left[ \frac{\|L_{ii}\|_F^2}{d} \right] = \frac{1 + 2\gamma}{4m^2}, \\ \lim_{C \rightarrow \infty} \lim_{d, N \rightarrow \infty} \frac{\mathbf{E} [\|H_{ij}\|_F^2]}{Cd} &= \lim_{C \rightarrow \infty} \mathbf{E} \left[ \left( \frac{\sum_{k=1}^C V_{ki} V_{kj}}{\sqrt{C}} \right)^2 \right] \lim_{d, N \rightarrow \infty} \mathbf{E} \left[ \frac{\|L_{ij}\|_F^2}{d} \right] = \frac{1 + 4\gamma}{16m^2}. \end{aligned}$$

$\square$

### D.3 Proof for the Output-layer Hessian with CE Loss

Denote that

$$G_{ii} := \frac{\partial^2 \ell_{\text{CE}}(W, V)}{\partial v_i \partial v_i^\top} = \frac{1}{N} \sum_{n=1}^N p_{n,i} (1 - p_{n,i}) \sigma(Wx_n) \sigma(Wx_n)^\top,$$

and for  $i \neq j$ ,

$$G_{ij} := \frac{\partial^2 \ell_{\text{CE}}(W, V)}{\partial v_i \partial v_j^\top} = \frac{1}{N} \sum_{n=1}^N p_{n,i} p_{n,j} \sigma(Wx_n) \sigma(Wx_n)^\top.$$

Let  $Z$  be a  $d \times N$  random matrix with entries i.i.d.  $N(0, 1)$  independent of  $V$ , and  $z_1, \dots, z_N$  are column vectors of  $Z$ . Define

$$\begin{aligned} \tilde{p}_{i,n} &= \frac{\exp(\sigma(z_n)^\top v_i)}{\sum_{c=1}^C \exp(\sigma(z_n)^\top v_c)}, \quad n \in [N], i \in [C], \\ \tilde{G}_{ii} &= \frac{1}{N} \sum_{n=1}^N \tilde{p}_{n,i} (1 - \tilde{p}_{n,i}) \sigma(z_n) \sigma(z_n)^\top, \\ \tilde{G}_{ij} &= \frac{1}{N} \sum_{n=1}^N \tilde{p}_{n,i} \tilde{p}_{n,j} \sigma(z_n) \sigma(z_n)^\top. \end{aligned}$$

Following the proof of Lemma 12 with the Lindeberg principle, one can show that for  $k, l \in [m]$ ,  $k \neq l$ ,

$$\lim_{d, N \rightarrow \infty} \left( \mathbf{E} \left[ G_{ii}(k, k)^2 \right] - \mathbf{E} \left[ \tilde{G}_{ii}(k, k)^2 \right] \right) = 0,$$

$$\lim_{d, N \rightarrow \infty} \left( \mathbf{E} \left[ G_{ii}(k, l)^2 \right] - \mathbf{E} \left[ \tilde{G}_{ii}(k, l)^2 \right] \right) = 0,$$

$$\lim_{d, N \rightarrow \infty} \left( \mathbf{E} \left[ G_{ij}(k, k)^2 \right] - \mathbf{E} \left[ \tilde{G}_{ij}(k, k)^2 \right] \right) = 0,$$

$$\lim_{d, N \rightarrow \infty} \left( \mathbf{E} \left[ G_{ij}(k, l)^2 \right] - \mathbf{E} \left[ \tilde{G}_{ij}(k, l)^2 \right] \right) = 0.$$

Then since  $m$  is fixed and

$$\mathbf{E} \left[ \|G_{ii}\|_{\mathbb{F}}^2 \right] = m \mathbf{E} \left[ G_{ii}(k, k)^2 \right] + m(m-1) \mathbf{E} \left[ G_{ii}(k, l)^2 \right], \quad (97)$$

$$\mathbf{E} \left[ \|G_{ij}\|_{\mathbb{F}}^2 \right] = m \mathbf{E} \left[ G_{ij}(k, k)^2 \right] + m(m-1) \mathbf{E} \left[ G_{ij}(k, l)^2 \right],$$

$$\mathbf{E} \left[ \|\tilde{G}_{ii}\|_{\mathbb{F}}^2 \right] = m \mathbf{E} \left[ \tilde{G}_{ii}(k, k)^2 \right] + m(m-1) \mathbf{E} \left[ \tilde{G}_{ii}(k, l)^2 \right], \quad (98)$$

$$\mathbf{E} \left[ \|\tilde{G}_{ij}\|_{\mathbb{F}}^2 \right] = m \mathbf{E} \left[ \tilde{G}_{ij}(k, k)^2 \right] + m(m-1) \mathbf{E} \left[ \tilde{G}_{ij}(k, l)^2 \right], \quad (99)$$

we have

$$\begin{aligned} \lim_{d, N \rightarrow \infty} \left( \mathbf{E} \left[ \|G_{ii}\|_{\mathbb{F}}^2 \right] - \mathbf{E} \left[ \|\tilde{G}_{ii}\|_{\mathbb{F}}^2 \right] \right) &= 0, \\ \lim_{d, N \rightarrow \infty} \left( \mathbf{E} \left[ \|G_{ij}\|_{\mathbb{F}}^2 \right] - \mathbf{E} \left[ \|\tilde{G}_{ij}\|_{\mathbb{F}}^2 \right] \right) &= 0. \end{aligned} \quad (100)$$

From

$$\begin{aligned} \tilde{G}_{ii}(k, k) &= \frac{1}{N} \sum_{n=1}^N \tilde{p}_{n,i} (1 - \tilde{p}_{n,i}) \sigma(z_{n,k})^2, \\ \tilde{G}_{ii}(k, l) &= \frac{1}{N} \sum_{n=1}^N \tilde{p}_{n,i} (1 - \tilde{p}_{n,i}) \sigma(z_{n,k}) \sigma(z_{n,l}), \\ \tilde{G}_{ij}(k, k) &= \frac{1}{N} \sum_{n=1}^N \tilde{p}_{n,i} \tilde{d}_{n,j} \sigma(z_{n,k})^2, \\ \tilde{G}_{ij}(k, l) &= \frac{1}{N} \sum_{n=1}^N \tilde{p}_{n,i} \tilde{p}_{n,j} \sigma(z_{n,k}) \sigma(z_{n,l}), \end{aligned} \quad (101)$$

we have

$$\begin{aligned} \lim_{p, N \rightarrow \infty} \mathbf{E} \left[ \tilde{G}_{ii}(k, k)^2 \right] &= \mathbf{E} \left[ \tilde{p}_{1,i} \tilde{p}_{2,i} (1 - \tilde{p}_{1,i}) (1 - \tilde{p}_{2,i}) \sigma(z_{1,k})^2 \sigma(z_{2,k})^2 \right], \\ \lim_{p, N \rightarrow \infty} \mathbf{E} \left[ \tilde{G}_{ii}(k, l)^2 \right] &= \mathbf{E} \left[ \tilde{p}_{1,i} \tilde{p}_{2,i} (1 - \tilde{p}_{1,i}) (1 - \tilde{p}_{2,i}) \sigma(z_{1,k}) \sigma(z_{1,l}) \sigma(z_{2,k}) \sigma(z_{2,l}) \right], \\ \lim_{p, N \rightarrow \infty} \mathbf{E} \left[ \tilde{G}_{ij}(k, k)^2 \right] &= \mathbf{E} \left[ \tilde{p}_{1,i} \tilde{p}_{2,i} \tilde{p}_{1,j} \tilde{p}_{2,j} \sigma(z_{1,k})^2 \sigma(z_{2,k})^2 \right], \\ \lim_{p, N \rightarrow \infty} \mathbf{E} \left[ \tilde{G}_{ij}(k, l)^2 \right] &= \mathbf{E} \left[ \tilde{p}_{1,i} \tilde{p}_{2,i} \tilde{p}_{1,j} \tilde{p}_{2,j} \sigma(z_{1,k}) \sigma(z_{1,l}) \sigma(z_{2,k}) \sigma(z_{2,l}) \right]. \end{aligned} \quad (102)$$

Therefore

$$\begin{aligned}
& \lim_{C \rightarrow \infty} \lim_{p, N \rightarrow \infty} C^2 \mathbf{E} \left[ \tilde{G}_{ii}(k, k)^2 \right] \\
&= \lim_{C \rightarrow \infty} \mathbf{E} \left[ \mathbf{E} \left[ \frac{\exp((\sigma(z_1) + \sigma(z_2))^\top v_i)}{\left( \frac{1}{C} \sum_{c=1}^C \exp(\sigma(z_1)^\top v_c) \right) \left( \frac{1}{C} \sum_{c=1}^C \exp(\sigma(z_2)^\top v_c) \right)} (1 - \tilde{p}_{1,i})(1 - \tilde{p}_{2,i}) \sigma(z_{1,k})^2 \sigma(z_{2,k})^2 \mid z_1, z_2 \right] \right] \\
&= \mathbf{E} \left[ \frac{\mathbf{E} \left[ \exp((\sigma(z_1) + \sigma(z_2))^\top v_i) \sigma(z_{1,k})^2 \sigma(z_{2,k})^2 \mid z_1, z_2 \right]}{\left( \mathbf{E} \left[ \exp(\sigma(z_1)^\top v_i) \mid z_1 \right] \right) \left( \mathbf{E} \left[ \exp(\sigma(z_2)^\top v_i) \mid z_2 \right] \right)} \right] \\
&= \mathbf{E} \left[ \frac{\exp\left(\frac{1}{2m} |\sigma(z_1) + \sigma(z_2)|^2\right) \sigma(z_{1,k})^2 \sigma(z_{2,k})^2}{\exp\left(\frac{1}{2m} (|\sigma(z_1)|^2 + |\sigma(z_2)|^2)\right)} \right] \\
&= \mathbf{E} \left[ \exp\left(\frac{1}{m} \sigma(z_{1,1}) \sigma(z_{1,2})\right) \sigma(z_{1,1})^2 \sigma(z_{1,2})^2 \right] \left( \mathbf{E} \left[ \exp\left(\frac{1}{m} \sigma(z_{1,1}) \sigma(z_{1,2})\right) \right] \right)^{m-1} \\
&= a_{12} b_1^{m-1},
\end{aligned} \tag{103}$$

$$\begin{aligned}
& \lim_{C \rightarrow \infty} \lim_{p, N \rightarrow \infty} C^2 \mathbf{E} \left[ \tilde{G}_{ii}(k, l)^2 \right] \\
&= \lim_{C \rightarrow \infty} \mathbf{E} \left[ \mathbf{E} \left[ \frac{\exp((\sigma(z_1) + \sigma(z_2))^\top v_i) (1 - \tilde{p}_{1,i})(1 - \tilde{p}_{2,i})}{\left( \frac{1}{C} \sum_{c=1}^C \exp(\sigma(z_1)^\top v_c) \right) \left( \frac{1}{C} \sum_{c=1}^C \exp(\sigma(z_2)^\top v_c) \right)} \sigma(z_{1,k}) \sigma(z_{2,k}) \sigma(z_{1,l}) \sigma(z_{2,l}) \mid z_1, z_2 \right] \right] \\
&= \mathbf{E} \left[ \frac{\mathbf{E} \left[ \exp((\sigma(z_1) + \sigma(z_2))^\top v_i) \sigma(z_{1,k}) \sigma(z_{2,k}) \sigma(z_{1,l}) \sigma(z_{2,l}) \mid z_1, z_2 \right]}{\left( \mathbf{E} \left[ \exp(\sigma(z_1)^\top v_i) \mid z_1 \right] \right) \left( \mathbf{E} \left[ \exp(\sigma(z_2)^\top v_i) \mid z_2 \right] \right)} \right] \\
&= \mathbf{E} \left[ \frac{\exp\left(\frac{1}{2m} |\sigma(z_1) + \sigma(z_2)|^2\right) \sigma(z_{1,k}) \sigma(z_{2,k}) \sigma(z_{1,l}) \sigma(z_{2,l})}{\exp\left(\frac{1}{2m} (|\sigma(z_1)|^2 + |\sigma(z_2)|^2)\right)} \right] \\
&= \mathbf{E} \left[ \exp\left(\frac{1}{m} \sigma(z_{1,1}) \sigma(z_{1,2})\right) \sigma(z_{1,1}) \sigma(z_{1,2}) \right]^2 \left( \mathbf{E} \left[ \exp\left(\frac{1}{m} \sigma(z_{1,1}) \sigma(z_{1,2})\right) \right] \right)^{m-2} \\
&= a_{11}^2 b_1^{m-2},
\end{aligned} \tag{104}$$

$$\begin{aligned}
& \lim_{C \rightarrow \infty} \lim_{p, N \rightarrow \infty} C^4 \mathbf{E} [\tilde{G}_{ij}(k, k)^2] \\
&= \lim_{C \rightarrow \infty} \mathbf{E} \left[ \mathbf{E} \left[ \frac{\exp((\sigma(z_1) + \sigma(z_2))^\top (v_i + v_j))}{\left(\frac{1}{C} \sum_{c=1}^C \exp(\sigma(z_1)^\top v_c)\right)^2 \left(\frac{1}{C} \sum_{c=1}^C \exp(\sigma(z_2)^\top v_c)\right)^2} \sigma(z_{1,k})^2 \sigma(z_{2,k})^2 \mid z_1, z_2 \right] \right] \\
&= \mathbf{E} \left[ \frac{\mathbf{E} \left[ \exp((\sigma(z_1) + \sigma(z_2))^\top (v_i + v_j)) \sigma(z_{1,k})^2 \sigma(z_{2,k})^2 \mid z_1, z_2 \right]}{\left( \mathbf{E} \left[ \exp(\sigma(z_1)^\top v_i) \mid z_1 \right] \right)^2 \left( \mathbf{E} \left[ \exp(\sigma(z_2)^\top v_i) \mid z_2 \right] \right)^2} \right] \\
&= \mathbf{E} \left[ \frac{\exp\left(\frac{1}{m} |\sigma(z_1) + \sigma(z_2)|^2\right) \sigma(z_{1,k})^2 \sigma(z_{2,k})^2}{\exp\left(\frac{1}{m} (|\sigma(z_1)|^2 + |\sigma(z_2)|^2)\right)} \right] \\
&= \mathbf{E} \left[ \exp\left(\frac{2}{m} \sigma(z_{1,1}) \sigma(z_{1,2})\right) \sigma(z_{1,1})^2 \sigma(z_{1,2})^2 \right] \left( \mathbf{E} \left[ \exp\left(\frac{2}{m} \sigma(z_{1,1}) \sigma(z_{1,2})\right) \right] \right)^{m-1} \\
&= a_{22} b_2^{m-1},
\end{aligned} \tag{105}$$

$$\begin{aligned}
& \lim_{C \rightarrow \infty} \lim_{p, N \rightarrow \infty} C^4 \mathbf{E} [\tilde{G}_{ij}(k, k)^2] \\
&= \lim_{C \rightarrow \infty} \mathbf{E} \left[ \mathbf{E} \left[ \frac{\exp((\sigma(z_1) + \sigma(z_2))^\top (v_i + v_j))}{\left(\frac{1}{C} \sum_{c=1}^C \exp(\sigma(z_1)^\top v_c)\right)^2 \left(\frac{1}{C} \sum_{c=1}^C \exp(\sigma(z_2)^\top v_c)\right)^2} \sigma(z_{1,k}) \sigma(z_{2,k}) \sigma(z_{1,l}) \sigma(z_{2,l}) \mid z_1, z_2 \right] \right] \\
&= \mathbf{E} \left[ \frac{\mathbf{E} \left[ \exp((\sigma(z_1) + \sigma(z_2))^\top (v_i + v_j)) \sigma(z_{1,k}) \sigma(z_{2,k}) \sigma(z_{1,l}) \sigma(z_{2,l}) \mid z_1, z_2 \right]}{\left( \mathbf{E} \left[ \exp(\sigma(z_1)^\top v_i) \mid z_1 \right] \right)^2 \left( \mathbf{E} \left[ \exp(\sigma(z_2)^\top v_i) \mid z_2 \right] \right)^2} \right] \\
&= \mathbf{E} \left[ \frac{\exp\left(\frac{1}{m} |\sigma(z_1) + \sigma(z_2)|^2\right) \sigma(z_{1,k}) \sigma(z_{2,k}) \sigma(z_{1,l}) \sigma(z_{2,l})}{\exp\left(\frac{1}{m} (|\sigma(z_1)|^2 + |\sigma(z_2)|^2)\right)} \right] \\
&= \mathbf{E} \left[ \exp\left(\frac{2}{m} \sigma(z_{1,1}) \sigma(z_{1,2})\right) \sigma(z_{1,1}) \sigma(z_{1,2}) \right]^2 \left( \mathbf{E} \left[ \exp\left(\frac{2}{m} \sigma(z_{1,1}) \sigma(z_{1,2})\right) \right] \right)^{m-2} \\
&= a_{21}^2 b_2^{m-2}.
\end{aligned} \tag{106}$$

Then from (98)-(100) and (103)-(106) we obtain (23).